Astbury Centre for Structural Molecular Biology

UNIVERSITY OF LEEDS

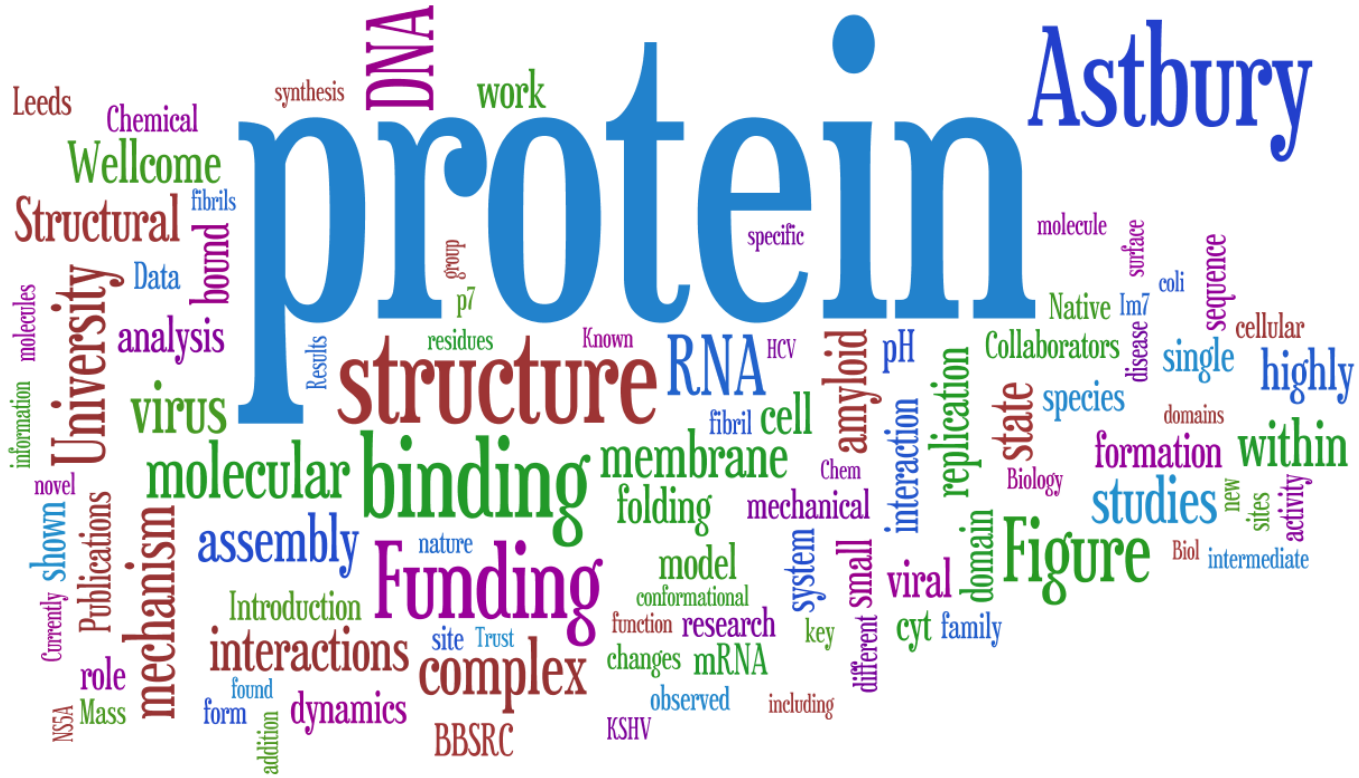

Annual Report 2008

Front cover illustration:

The 100 most commonly used words in this Astbury report converted into a "word cloud", where the cloud gives greater prominence to words that appear more frequently in the source text. This "Wordle" picture courtesy of www.wordle.net

Acknowledgement
The Astbury Centre for Structural Molecular Biology thanks its many sponsors for support of the work and its members for writing these reports. The report is edited by Alan Berry.

This report is also available electronically via http://www.astbury.leeds.ac.uk

Mission Statement

The Astbury Centre for Structural Molecular Biology will promote interdisciplinary research of the highest standard on the structure and function of biological molecules, biomolecular assemblies and complexes using physico-chemical, molecular biological and computational approaches.

Introduction

It is a tremendous pleasure to write the Introduction to the Annual Report on the activities of the Astbury Centre in 2008. I am hugely indebted to my predecessor, Peter Stockley, who stepped down as Director of the Centre at the end of 2008. It is a great privilege for me to follow Peter in serving as Director of our highly interdisciplinary research centre. Peter led many developments within the Centre during his tenure which have had a big impact on the science that has been possible, and the outstanding facilities that we enjoy. Peter oversaw the inaugural meeting of our Scientific Advisory Board in November 2008, an event that underlined the buoyancy and collegiality of the Centre at all levels. The meeting was coupled with the first Astbury Symposium which was attended by around 200 internal and external delegates.

This annual report provides a snapshot of the Astbury Centre's research portfolio in 2008. The report describes many scientific advances that have the potential to make a major impact on global society. You will find many examples that demonstrate that an interdisciplinary approach can make a tremendous impact on major problems in modern biology. The breadth of activity in the Centre is extremely broad, ranging from studies of molecular interactions within cells, through to the development of new physical and chemical methods for studying biological systems. Several of our members were recognised for their contributions to science this year, including through the Hites Award for an outstanding publication in *Journal of the American Society of Mass Spectrometry* (Ashcroft), the Royal Society of Chemistry (RSC) Corday–Morgan medal (Nelson), the annual award of the British Society of Rheology (Olmsted) and the Honess Lecture at the International Herpesvirus conference (Whitehouse).

Astbury Centre members continue to be very successful in raising external grant income, including many of our newly appointed staff who have succeeded in getting their first major grants funded. Peter Henderson has led a major €15M project – the European Drug Initiative for Channels and Transporters – that will target about eighty proteins that play a major role in disease. The project involves twenty-seven partners from twelve countries, including two Nobel Laureates; other researchers from the Centre include Steve Baldwin, Carola Hunte, Peter Johnson and Colin Fishwick. At the end of 2008, Astbury Centre members were applicants on grants totaling around £36M.

Postdoctoral researchers and postgraduate students continue to make major contributions to the activities of the Centre. Stuart Knowling has done a superb job leading the Astbury Society which has organised many enjoyable social and scientific events this year including the third Annual Astbury Lecture and associated Sports Day. A team of PhD students and postdoctoral researchers demonstrated the potential to apply scientific expertise to commercially-relevant problems. Stuart Kyle, a PhD student from the Centre, and his team, David Smith, Serena Russell, Romana Mughal and Alice Bartlett, won the Smith & Nephew Prize for Best Medical Technology in the finals of the prestigious Biotechnology Young Entrepeneurs Scheme. Their hypothetical company – BioInspire – focused on the identification of pathogenic organisms from their protein fingerprints. Many researchers have been externally recognized for the excellence of their work including Amanda Bolt, Anil Agarwal, Rebecca White and Dan Morton, who won prizes at RSC events, and Nik Daskalakis, who won a prize at a Biochemical Society meeting. Two PhD students won competitive awards to fund placements in leading laboratories in the US: Sarah Kinnings won a Research Mobility Programme award from the Worldwide Universities Network, and Jonathan Fuller won a CCPB travel award for an Early-Stage Researcher. In 2008, 33

postgraduate students were awarded a PhD degree, and 39 new PhD students initiated a research project with a supervisor from the Astbury Centre.

The Astbury Centre continues to host a vibrant and highly international seminar programme. The third Astbury Annual lecture was delivered by Professor Ulrich Hartl from the Max Planck Institute of Biochemistry. Professor Hartl provided a fascinating insight into how chaperones assist protein folding processes. In total, there were 17 seminars in 2008 which were presented by visitors from institutions in 8 different countries; three visitors were invited and hosted by postgraduate or postdoctoral members of the Centre.

We have formally welcomed four new members to the Astbury Centre in 2008: Peter Olmsted, Sarah Harris, John Barr and Carola Hunte. Simon Phillips became the first Director of the Research Complex at Harwell, but continues his links with the Astbury Centre as a Visiting Member. Tom McLeish moved to become the Pro-Vice Chancellor for Research at the University of Durham.

2009 marks the tenth anniversary of the establishment of the Astbury Centre for Structural Molecular Biology as a formal University Centre. The year promises to be exciting, and we are planning a major meeting in June 2009 to celebrate our first decade as an interdisciplinary research centre. In addition, we are planning a second residential research retreat and an open day for industry in the autumn.

The Centre produces a regular electronic Newsletter that describes our on-going activities. Details of how to receive an electronic copy of this Newsletter may be found on the Astbury Centre website. This annual report (as well as those from previous years) is also available as a PDF document that can be downloaded from our website.

Finally, I would like to thank our editor, Alan Berry, for leading the preparation of this Report, ably assisted by Donna Fletcher.

Adam Nelson
Director, Astbury Centre for Structural Molecular Biology
Leeds, April 2009

Contents

Contributions indexed by Astbury Centre Principal Investigator

Biomolecular mass spectrometry – simultaneous mass measurements & cross-sectional areas

Tom W. Knapman, David P. Smith, Victoria L. Morton, James R. Ault, John P. Hodkinson, James Muldoon, Lynsey N. Jones, Aneika Leney, Lucy A. Woods, Caroline Pritchard, Rebecca J. Rose, Joshua Berryman, Richard Malham, Sheena E. Radford, Peter G. Stockley, Nicola J. Stonehouse, Andrew J. Wilson, Peter F. J. Henderson, Sarah Harris, Amalia Aggeli and Alison E. Ashcroft.

Introduction

Detailed knowledge of the tertiary and quaternary structure of proteins and protein complexes is of immense importance in understanding their functionality. A relatively new technique, travelling wave ion mobility spectrometry coupled to electrospray ionisation mass spectrometry (ESI-TWIMS-MS), offers a unique opportunity to separate multi-component biomolecular entities on the basis of their physical shape and to measure the molecular mass and cross-sectional area (Ω) of individual components, in a single, rapid (≤ 2 mins) experiment, directly providing 3D-architectural information. Thus, this technique can separate ions of the same mass (e.g., protein conformers), or the same m/z ratio (e.g., oligomers).

Results

After calibration of the ESI-TWIMS-MS system by reference to standard ion mobility spectrometry, a series of 12 proteins of varying mass (2-45 kDa) was analysed by ESI-TWIMS-MS from solution conditions at pH 7 (Fig. 1). The cross-sectional areas measured [Ω(measured)] from these analyses compared favourably with cross-sectional areas estimated [Ω(calculated)] from the Protein Data Bank co-ordinates of these proteins using a new in-house, Monte Carlo-based computational method (the Leeds Method) (Fig. 1).

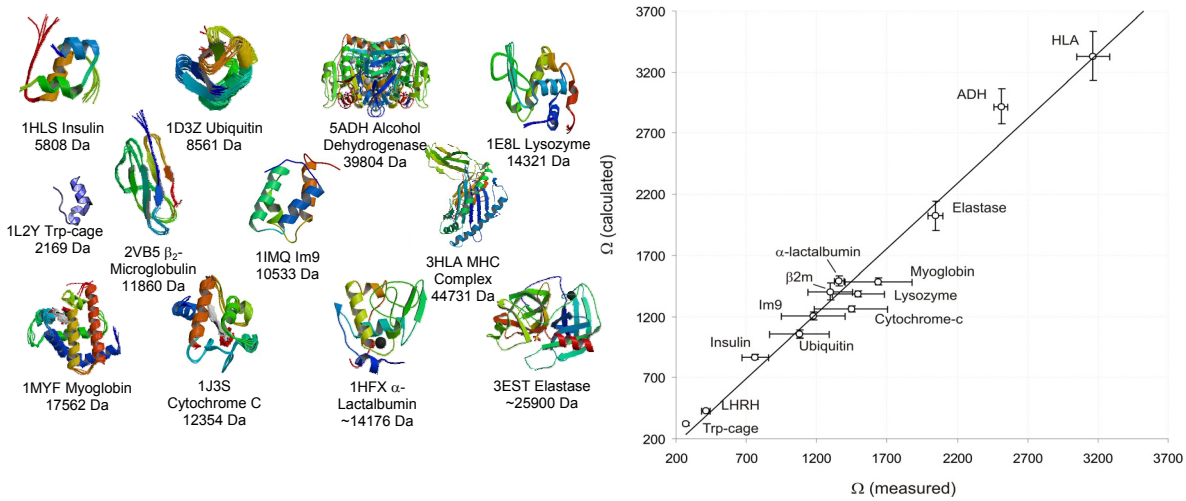

Figure 1. (left) Native proteins used to verify the ESI-TWIMS-MS calibration; (right) Ω(measured) by ESI-TWIMS-MS *vs*. Ω(calculated) from PDB co-ordinates using the Leeds Method.

Building on these evaluations, the separation of co-populated biomolecules followed by measurement of their individual Ωs and mass in a single experiment has been used to address a number of key biochemical enigmas, including the characterisation of protein conformers and oligomers observed during amyloid fibril formation and virus capsid assembly. One such example is a recent study of protein folding whereby mixtures of co-populated conformers have been separated and characterised (Fig. 2).

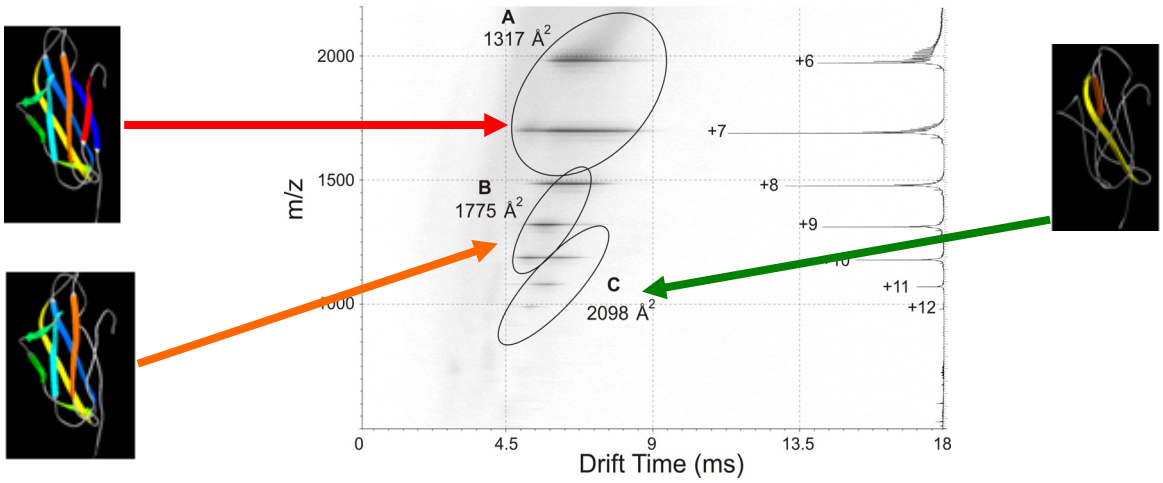

Figure 2. Cross-sectional areas (Ωs) (Å^2) calculated for three co-populated conformations of the amyloidogenic protein β_2-microglobulin at pH 2.6 by ESI-TWIMS-MS. The folded (A), partially unfolded (B) and acid-unfolded (C) conformers have TWIMS-measured Ωs of 1317 Å^2, 1775 Å^2, and 2098 Å^2 respectively. The driftscope plot shows drift time (mobility, msec) *vs. m/z vs*. intensity; the inset on the right hand side shows the summed *m/z* spectra over the entire experiment.

Publications

Rose, R.J., Welsh, T.S., Waksman, G., Ashcroft, A.E., Radford, S.E. & Paci, E. (2008) Donor-strand exchange in chaperone-assisted pilus assembly revealed in atomic detail by molecular dynamics. *J. Mol. Biol.,* **375**, 908-919.

Knapman, T.W., Aggeli, A. & Ashcroft, A.E. (2008) Critical concentrations of β-sheet peptide self-assembly quantified directly by nanoESI-MS. *Rapid Commun. Mass Spectr.,* **22**, 1611-4.

Morton, V.L., Stockley, P.G., Stonehouse, N.J. & Ashcroft, A.E. (2008) Insights into virus capsid assembly using non-covalent mass spectrometry. *Mass Spectrom. Rev.,* **27**, 575-595.

Rolfsson, O., Toropova, K., Morton, V.L., Francese, S., Basnak, G., Thompson, G. Homans, S.W., Ashcroft, A.E., Stonehouse, N.J. Ranson, N. & Stockley, P.G. (2008) RNA packing specificity and folding during assembly of the bacteriophage MS2. *Computational & Mathematical Methods in Medicine,* **9**, 339-349.

Rose, R.J., Paci, E., Costakes, G., Daviter, T., Hultgren, S., Remaut, H., Waksman, G. Ashcroft, A.E. & Radford, S.E. (2008) Kinetic control of donor-strand exchange determines specific assembly of subunits in pilus biogenesis. *Proc. Natl. Acad. Sci. USA,* **105**, 12873-8.

Verger, D., Rose, R.J., Paci, E., Costakes, G., Daviter, T., Hultgren, S. Remaut, H., Ashcroft, A.E., Radford, S.E. & Waksman, G. (2008) Structural determinants of polymerization reactivity of the Pilus subunit PapF. *Structure,* **16**, 1724-31.

Smith, D.P., Anderson, J., Plante, J. Ashcroft, A.E., Radford, S.E., Wilson, A.J. & Parker, M.J. (2008) Trifluoromethyldiazirine: an effective photo-induced cross-linking probe for exploring amyloid formation. *Chem. Comm.,* **44,** 5728-5730.

Hodkinson, J.P., Jahn, T.R., Radford, S.E. & Ashcroft, A.E. (2009) HDX-ESI-MS reveals enhanced conformational dynamics of the amyloidogenic protein β_2-microglobulin upon release from the MHC-1. *J. Amer. Soc. Mass Spectrom.,* **20**, 278-286.

Smith, D.P., Knapman, T.W., Malham, R.W., Berryman, J.T., Radford, S.E. & Ashcroft, A.E. (2008) Deciphering drift time measurements from travelling wave ion mobility spectrometry – MS studies, *European Journal of Mass Spectrometry*, doi: 10.1255/ejms.947, on-line.

Funding

This work was funded by the BBSRC, the EPSRC, the Wellcome Trust, Waters UK Ltd., and the Laboratory of the Government Chemist.

HDX-ESI-MS reveals enhanced conformational dynamics of the amyloidogenic protein β_2-microglobulin upon release from the MHC-1

John P. Hodkinson, David P. Smith, Lucy A. Woods,
Sheena E. Radford and Alison E. Ashcroft.

Introduction

The light chain of the major histocompatibility complex class 1 (MHC-1) (Figure 1), the protein β_2-microglobulin (β_2m), has amyloidogenic properties that only arise upon its dissociation from the MHC-1. Here hydrogen/deuterium exchange electrospray ionisation mass spectrometry (HDX-ESI-MS) has been used to compare the solution dynamics of β_2m in its MHC-1 bound state compared with those of β_2m as a free monomer. The capability of tandem mass spectrometry to dissociate the MHC-1 into its individual constituents in the gas phase following deuterium incorporation in solution has permitted the direct observation of the exchange properties of MHC-1 bound β_2m for the first time.

Figure 1. Ribbon diagram of the MHC-1 (PDB 2VLL) showing the heavy chain (α1, α2, α3; green ribbon) and the light chain (β_2m; red ribbon). The peptide binds in the cleft formed by the two helical regions (α1 and α2) of the heavy chain.

Results

ESI-MS is a powerful technique with which to monitor protein conformational dynamics using HDX. HDX-ESI-MS showed clearly that when β_2m is bound in the MHC-1, its H$\rightarrow$D exchange follows EX2 kinetics with an exchange rate of 0.002 ± 0.0003 min^{-1}, and indicates that ~20 protons remain protected from exchange after 17 days.

In comparison, when in an unbound state free from the MHC-1, β_2m exhibits very different characteristics exemplified by HDX mechanisms which encompass both EX1 and EX2 kinetics. The EX2 kinetics show a ten-fold increase in the exchange rate (0.023 ± 0.002 min^{-1}) compared with MHC-1 bound β_2m, and that ~10 highly protected protons exchange only via an EX1 mechanism. The EX1 data observed for unbound β_2m are consistent with unfolding of the protein's exchange-protected core, with a $t_{½}$ of 68 mins.

The comparison between MHC-1 bound and unbound β_2m highlights a remarkable change in the conformational dynamics of β_2m on its release from the MHC-1. When bound to the MHC-1, there is a significant damping of the conformational dynamics of β_2m, consistent with stable, macromolecular, protein complex architecture, whilst upon dissociation from the stabilising influence of the MHC-1, free β_2m becomes highly dynamic and undergoes unfolding transitions which result in an aggregation-competent protein.

These observations are of significance as partial, or more complete, unfolding is considered to be the key initiating step in protein aggregation processes which lead to disease-related fibril formation.

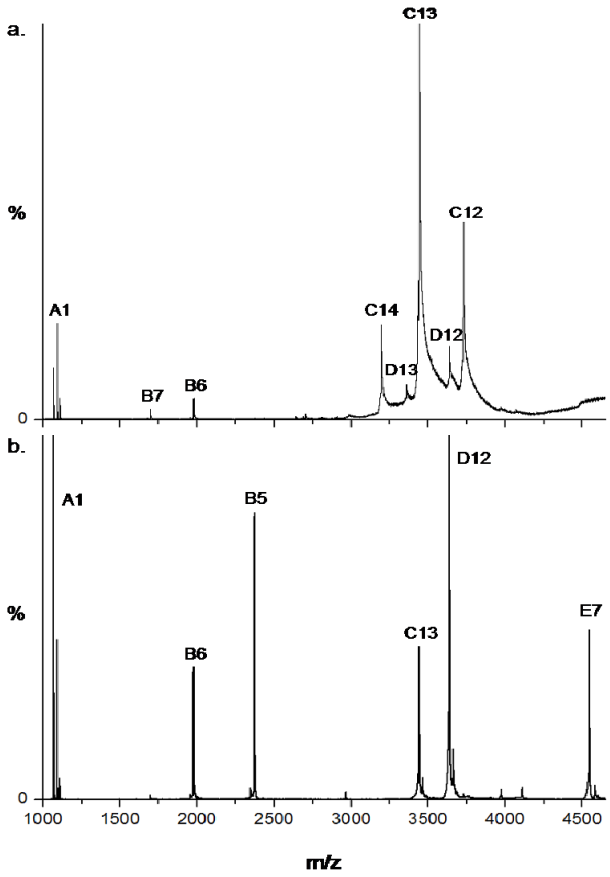

Figure 2.
(upper) ESI-MS m/z spectrum of the MHC-1 (pH 7.0), showing predominantly intact MHC-1 (C), together with traces of free β_2m (B), peptide (A) and MHC-1 without peptide (D);

(lower) ESI-MS/MS m/z spectrum showing dissociation of the intact MHC-1 (C; +13 charge state ions, m/z 3442) to yield: MHC-1 heavy chain (E), free β_2m (B), peptide (A) and MHC-1 without peptide (D).

The numbers adjacent to the letters relate to the charge states of those ions.

Collaborators

We thank Dr Brian M. Baker (Department of Chemistry & Biochemistry, University of Notre Dame, IN, USA) for providing the HLA/MHC-1 preparation protocol, clones and the peptide.

Publications

Rose, R.J., Welsh, T.S., Waksman, G., Ashcroft, A.E., Radford, S.E. & Paci, E. (2008) Donor-strand exchange in chaperone-assisted pilus assembly revealed in atomic detail by molecular dynamics. *J. Mol. Biol.,* **375**, 908-919.

Rose, R.J., Paci, E., Costakes, G., Daviter, T., Hultgren, S., Remaut, H., Waksman, G. Ashcroft, A.E. & Radford, S.E., (2008) Kinetic control of donor-strand exchange determines specific assembly of subunits in pilus biogenesis. *Proc. Natl. Acad. Sci. USA,* **105**, 12873-8.

Verger, D., Rose, R.J., Paci, E., Costakes, G., Daviter, T., Hultgren, S. Remaut, H., Ashcroft, A.E., Radford, S.E. & Waksman, G. (2008) Structural determinants of polymerization reactivity of the Pilus subunit PapF. *Structure,* **16**, 1724-31.

Smith, D.P., Anderson, J., Plante, J. Ashcroft, A.E., Radford, S.E., Wilson, A.J. & Parker, M.J. (2008) Trifluoromethyldiazirine: an effective photo-induced cross-linking probe for exploring amyloid formation. *Chem. Comm.,* **44,** 5728-5730.

Smith, D.P., Knapman, T.W., Malham, R.W., Berryman, J.T., Radford, S.E. & Ashcroft, A.E. (2008) Deciphering drift time measurements from travelling wave ion mobility spectrometry – MS studies, *European Journal of Mass Spectrometry*, doi: 10.1255/ejms.947, on-line.

Hodkinson, J.P., Jahn, T.R., Radford, S.E. & Ashcroft, A.E. (2009) HDX-ESI-MS reveals enhanced conformational dynamics of the amyloidogenic protein β_2-microglobulin upon release from the MHC-1. *J. Amer. Soc. Mass Spectrom.,* **20**, 278-286.

Funding

This work was funded by the BBSRC, the EPSRC, the Wellcome Trust, Waters UK Ltd., and the Laboratory of the Government Chemist.

Stoichiometry and specificity of RNA binding by the bunyavirus nucleocapsid protein

Bjorn-Patrick Mohl and John N. Barr

Introduction.

Bunyamwera virus (BUNV) is the prototypic member of both the *Orthobunyavirus* genus and the *Bunyaviridae* family of negative stranded RNA viruses. In common with all negative stranded RNA viruses, the BUNV genomic and anti-genomic strands are not naked RNAs, but instead are encapsidated along their entire lengths with the virus-encoded nucleocapsid (N) protein to form a ribonucleoprotein (RNP) complex. This association is critical for the negative strand RNA virus life cycle because only RNPs are active for productive RNA synthesis and RNA packaging. We are interested in understanding the molecular details of how N and RNA components associate within the bunyavirus RNP, and what governs the apparently selective encapsidation of viral replication products. Towards this goal, we recently devised a protocol that allowed generation of native BUNV N protein that maintained solubility under physiological conditions and allowed formation of crystals that yielded high-resolution X-ray diffraction data. Here we extend this work to show that this soluble N protein is able to oligomerise and bind RNA to form a highly uniform RNP complex, which exhibits characteristics common with the viral RNP. We used this model RNP to examine specificity of N/RNA binding. We specifically wanted to determine if the BUNV N protein required the presence of an obligatory signal on all bound RNAs.

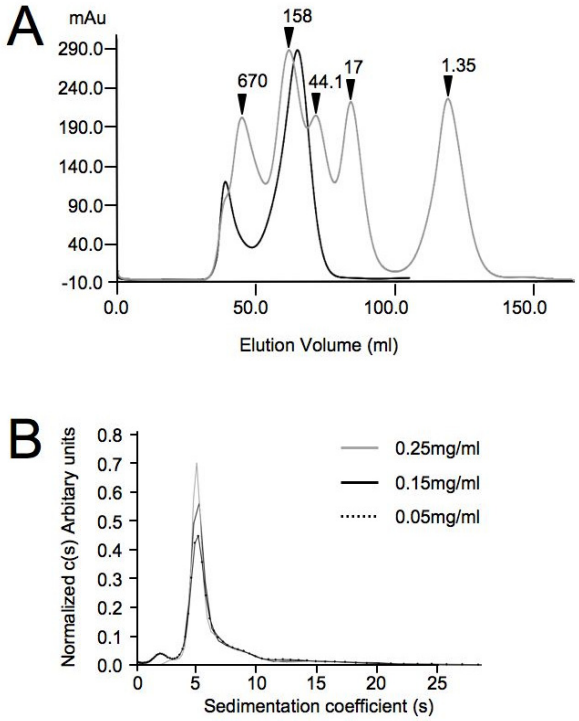

Figure 1. (A) Gel filtration and (B) analytical ultracentrifugation analysis of the BUNV N protein.

The BUNV N protein forms a tetramer.

To determine the molecular weight of the 26.9kDa BUNV N protein in solution, bacterially-expressed BUNV N protein was subjected to size exclusion chromatography (Fig. 1A), and analytical sedimentation centrifugation (Fig. 1B) using an Optima XL-I ultracentrifuge. The results showed high coincidence (109kDa/113kDa), and indicated that the N protein oligomerised to form a tetramer. Spectroscopic measurements indicated that the N protein was associated with RNA, likely from the bacterial host cells.

The N protein tetramer binds a 48nt-long RNA.
To determine the size of the RNA bound by the N tetramer, total RNA was harvested from the N-RNA complex by phenol and chloroform extractions, followed by ethanol precipitation. The size of the harvested RNA was determined using a 10% denaturing polyacrylamide gel, and compared to the mobility of low range RNA size markers (Fig. 2). The RNA appeared as a predominant 48 nt-long band (Fig. 2, lane 3), which indicated that the N/RNA stoichiometry is approximately 12nts per N monomer.

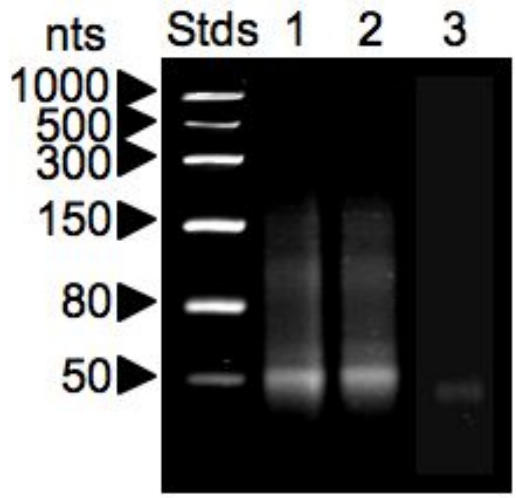

Figure 2. Polyacylamide gel electrophoresis of RNAs harvested from N protein tetramers. Lane 3 represents reduced loading of the harvested RNA compared to duplicate samples loaded in lanes 1 and 2.

The bound RNAs show no common sequence or structure.
We next wanted to clone and sequence the bound RNAs to determine whether they contained conserved features required for the N/RNA interaction. Extracted RNA was modified by first tailing the 3' ends using poly(A) polymerase and then ligating an adapter RNA to the 5' ends using T4 RNA ligase. The resulting RNAs were then used as templates for reverse transcriptase-directed RT-PCR. The amplified RT-PCR products were cloned and sequenced, and then analyzed using Vector NTi alignment software, and subjected to M-fold secondary structure prediction. This analysis showed that no common sequences or structures were present within bound RNAs. We conclude that the N/RNA interaction does not require an obligatory signal within the bound RNAs.

Publications

Mohl, B. P and Barr, J.N. (2009). Investigating the specificity and stoichiometry of RNA binding by the nucleocapsid protein of Bunyamwera virus. *RNA*. **15**, 391-9.

Funding.
Work in the Barr laboratory is funded by The Wellcome Trust, and is gratefully acknowledged.

Structural analysis of engineered *N*-acetyl-neuraminic acid lyase

Ivan Campeotto, Mandy Bolt, Tom Harman, Chi H. Trinh, Arwen Pearson, Adam Nelson, Simon E.V. Phillips and Alan Berry

Introduction:

Sialic acids play a pivotal role in mediating host-pathogen interactions and therefore drug analogues of sialic acid are exciting prospects as therapeutic agents. One example of clinical relevance is the inhibition of influenza virus attachment and particle release from infected cells targeted by the sialic acid derivatives Relenza® (GSK) and Tamiflu® (Roche). *De novo* chemical synthesis of sialic acid analogues is difficult owing to the number of chiral centers, and their production often relies on the use of the enzyme *N*-acetylneuraminic acid lyase (NAL) also called *N*-acetylneuraminic acid aldolase or sialic acid aldolase. NAL catalyzes the reversible condensation between *N*-acetyl-D-mannosamine and pyruvate to yield sialic acid (Fig.1) but the wild-type enzyme has restricted substrate specificity and limited substrate stereoselectivity.

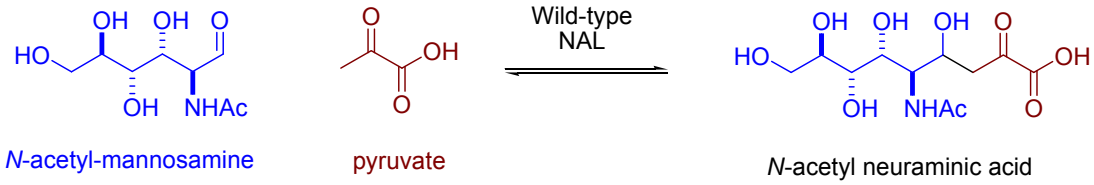

Fig.1 NAL wild-type reaction, showing the condensation between *N*-acetyl-D-mannosamine and pyruvate to yield sialic acid.

Using an approach which encompasses directed evolution and structure guided saturation mutagenesis, NAL variants have been made which have altered substrate specificity and stereoselectivity. The mutant E192N catalyses the aldol reaction between pyruvate and a dipropylamide substrate **1**, whereas the variants NAL-*R* (E192N/T167V/S208V) and NAL-*S* (E192N/T167G) catalyse the same reaction but with stereocontrol at C-4: an *R*-configured centre is the major stereoisomer when NAL-*R* is used, and an *S*-configured centre can be obtained by using the NAL-*S* mutant (Fig. 2). X-ray crystallographic studies of these proteins, with and without substrates, has been undertaken in order to offer an insight into the mechanism of substrate specificity and stereocontol in the NAL variants.

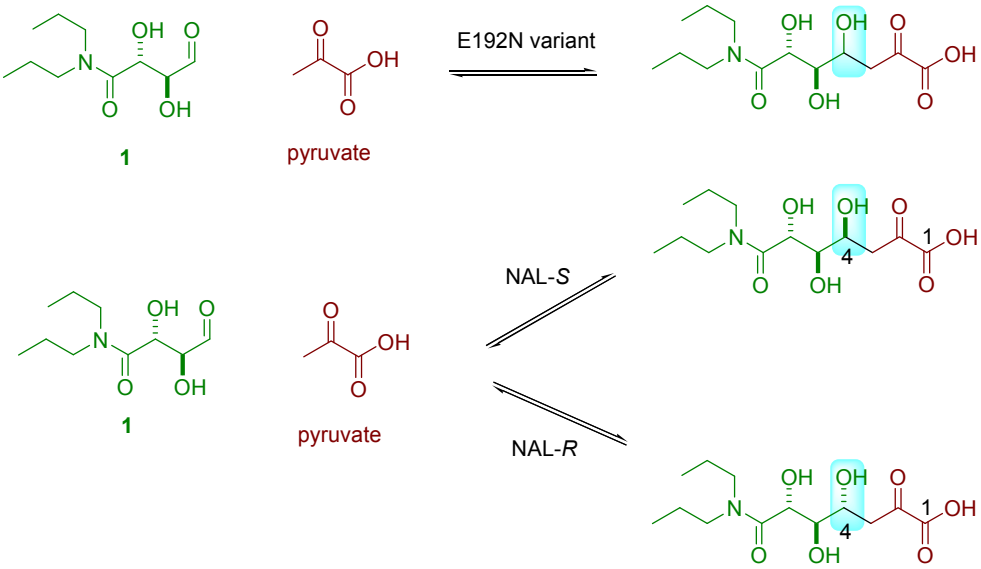

Figure 2. Reactions of NAL variants. The mutant E192N catalyses the aldol reaction between the dipropylamide substrate. **1**, and pyruvate. The variants NAL-*R* and NAL-*S* make *R* and *S* configured carbon centres at C-4 respectively.

Crystallographic studies on the wild type NAL and the mutant E192N:
NAL is a tetramer of four-identical subunits, each of which forms an $(\alpha/\beta)_8$-barrel fold. The active site is characteristically located at C-terminal end of the β-barrel.

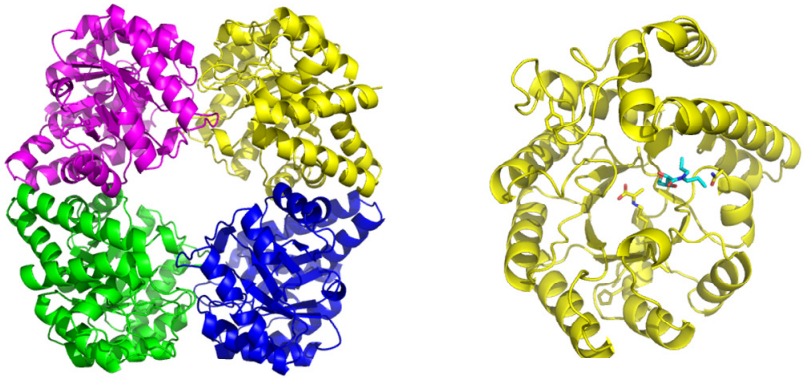

Figure 3. *E.coli* NAL overall X-ray structure of the tetramer (**a**) and the monomer (**b**) where the binding pocket with the ligands pyruvate (yellow) and inhibitor (cyan) are shown.

A number of crystal structures for the *E.coli* enzyme and variants have been solved:

- The crystal structure of the wild type NAL in the absence of, and in complex with, pyruvate were obtained at 1.65Å and 2.0Å resolution, respectively.
- The crystal structure of the mutant E192N was solved with and without pyruvate at 2.0Å and 1.9Å resolution, respectively.
- The crystal structure of the mutant E192N in complex with pyruvate and the inhibitor (2R,3R)-*N,N*-dipropyl-2-3-4-trihydroxybutyramide was solved at 2.1Å (Fig.4).

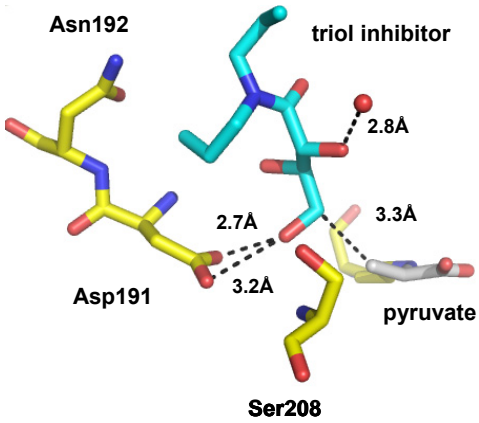

Figure 4 Ligands binding in the catalytic pocket of the NAL variant E192N.

These structures show the location of the substrate before the formation of the new C-C bond and hence probably mimics an entry or exit complex. They highlight the roles of the residues at positions 191 and 192 and provide insights into the origin of the broadened substrate specificity of E192N, due to a larger cavity than the wild type at the end of the catalytic pocket.

Crystallographic studies on the mutants NAL-*R* and NAL-*S*:
Four crystal structures of the NAL-*S* and NAL-*R*, both in the presence and absence of pyruvate have been solved at resolutions between 1.9Å and 2.3Å Analysis of these structures to understand the changes in stereochemistry brought about by the mutations are on-going but suggest a role for Tyr137, located in the catalytic pocket in close proximity to the pyruvate.

Publications:
Bolt, A., Berry, A., & Nelson, A. (2008) Directed evolution of aldolases for exploitation in synthetic organic chemistry. *Arch Biochem Biophys*, **474**, 318-330

Funding support:
This work has been sponsored by BBSRC and the Wellcome Trust.

Exploring proteins using force as a denaturant

Eleanore Hann, Jim Pullen, David Sadler, Sheena Radford and David Brockwell

Introduction

It is becoming increasingly apparent that many processes *in vivo* are facilitated by mechanically perturbing the structure of proteins and their complexes. In many seemingly diverse cellular events such as the remodelling of complexes, protein translocation and protein degradation, application of force exponentially increases the rate of protein unfolding thereby 'catalysing' the process. The aim of our research is to investigate the fundamental effects of force on model proteins and to investigate how these effects are utilised *in vivo*.

Currently research in the group covers three areas: (i) delineation of the mechanical unfolding transition state and rational engineering of the mechanical stability of the small, topologically simple protein L; (ii) direct measurement of the unbinding force and pathway of protein:ligand interactions and (iii) investigating how energy dependent bacterial proteases rapidly degrade substrate proteins with high thermodynamic and kinetic stability Here we report progress on studying the mechanical unfolding of protein L.

Visualising the transition state to unfolding by mutational analysis.

We have previously shown that protein L is significantly resistant to mechanical deformation. As this protein is not thought to have a mechanical function this observation concurs with the hypothesis that key determinants of protein mechanical strength are the type and arrangement of secondary structural elements relative to the extension points. Analysis of steered molecular dynamics simulations of the unfolding process revealed that the key step in unfolding was the shearing apart of two mechanical sub-units within this small protein (Fig. 1a).

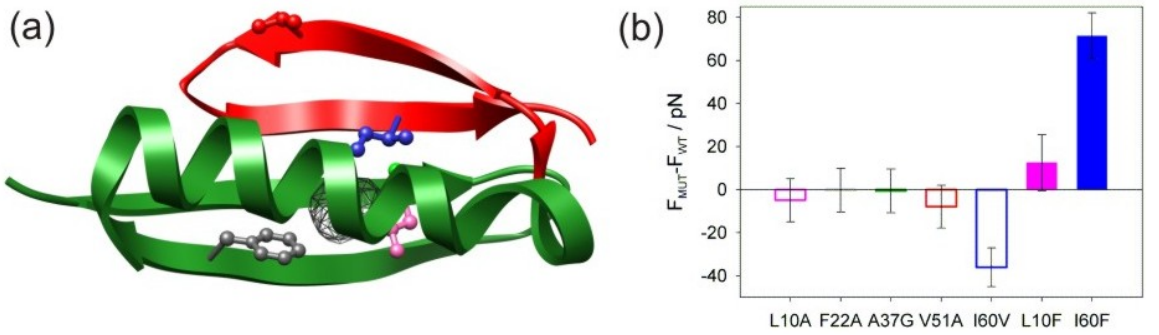

Figure 1: (a) Three dimensional structure of protein L. Side-chains of residues mutated in this study are shown as ball-and-stick representation (L10, pink; F22, grey; A37, green; V51, red and I60, blue). The main-chain of residues that form mechanical sub-unit 1 (residues 1-44, comprising strand I, the β-hairpin, strand II and the helix) and sub-unit 2 (residues 45- 64 comprising strand III, the second β-hairpin and strand IV) are coloured green and red, respectively. The cavity present in the hydrophobic core of WT protein L is shown as a meshed surface. (b) Core mutations can be used to modulate the mechanical strength of protein L. Bar chart showing the change in mechanical strength of different protein L variants relative to the WT protein.

To verify these observations, single conservative hydrophobic mutations were introduced into each secondary structural element within protein L and their effects on mechanical resistance quantified. Of the five variants constructed, four had mechanical phenotypes identical to wild-type. Deletion of a methylene group at position 60, however, significantly destabilised the protein by 36 pN (Fig. 1b) and moved the unfolding transition state closer to the unfolded state. These data suggest that the mechanical effects of hydrophobic side-chain deletions are critically dependent on the location of the deleted interactions relative to the mechanical interface. Residue 60 thus acts as 'lynchpin' that locks the native state into a mechanically strong structure.

Rational engineering of protein L mechanical strength

The finding that the extent of hydrophobic interactions across the mechanical interface plays a key role in determining the mechanical response of protein L suggests that an increase in interfacial contacts could increase protein mechanical strength. To test this hypothesis, a hydrophobic enhancement variant was constructed (I60F) that crossed the mechanical interface, filling a cavity present in the core of wild-type protein L (Fig. 1a). Remarkably, this single mutation increased the mechanical strength of protein L by 72 pN (Fig. 1b). Substitution of valine by phenylalanine thus increases the mechanical strength of protein L more than twofold (Fig. 2). These findings provide a generic method to rationally tune the mechanical strength of proteins and suggest a mechanism by which nature can evolve a varied mechanical response without a gross change of topology. Biophysical analyses of protein L variants I60V and I60F are underway.

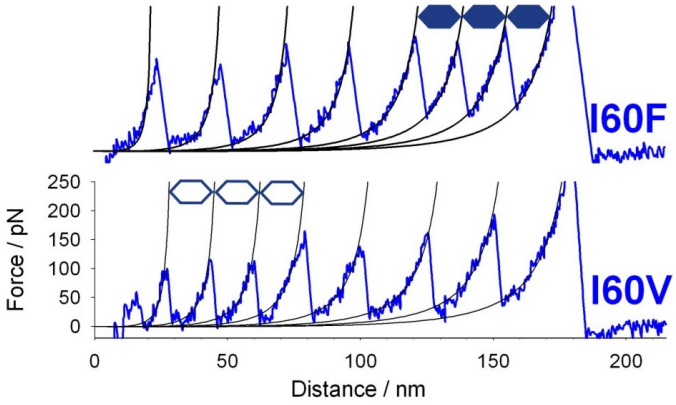

Figure 2: The mechanical strength of protein L can be enhanced two-fold. Sample force-extension profiles for a polymeric protein comprising of four I27 alternating with three protein L domains. Protein L unfolding events are identified by hexagons. Bottom: Removal of hydrophobic contacts across the unfolding interface (I60V) results in a mechanically weak phenotype where protein L domains typically unfold before I27. Top: increasing the hydrophobic contacts across the interface (I60F) results in a very strong mechanical phenotype where protein L typically unfolds after the I27 domains.

Collaborators

Emanuele Paci, School of Physics and Astronomy, University of Leeds.
Masaru Kawakami, School of Materials Science, Japan Advanced Institute of Science and Technology, Japan.

Publications

Taniguchi, Y., Brockwell, D. & Kawakami, M. (2008) The effect of temperature on the mechanical resistance of the native and intermediate states of I27. *Biophys. J.* **95**, 5296-5305.

Bhavin, K., Byrne K., Kawakami M., Brockwell, D., Smith D., Radford S. & McLeish, T. (2008) Internal friction of single polypeptide chains at high stretch. *Faraday Discuss.* **139**, 35-51.

Sadler, D., Petrik, E., Taniguchi, Y., Pullen, J., Kawakami, M, Radford, S & Brockwell, D., (2009) Identification of a mechanical rheostat in the hydrophobic core of protein L. Submitted

Funding

We thank Keith Ainley for technical support and the BBSRC, EPSRC and the University of Leeds for funding. DJB is an EPSRC funded White Rose Doctoral Training Centre lecturer.

Structural studies of the motor protein dynein

Anthony J. Roberts, Bara Malkova, Yusuke Kato, Hiroshi Imai and Stan A. Burgess

Introduction

Dynein is a family of minus-end directed microtubule motors that function in a wide diversity of cellular processes in eukaryotes including the trafficking of numerous cargoes (e.g. vesicles, mRNA, mitochondria), the positioning of the nucleus, Golgi apparatus and the mitotic spindle, as well as driving the propagated-bending waves of cilia and flagella. Dynein is one of three different families of molecular motors, the others being kinesin and the actin- based motor myosin, and by far the least well understood. Dynein is large (~ 520 kDa), with a motor domain ~ten times larger than that of the other microtubule-based motor kinesin and has an evolutionary origin within the AAA+ superfamily of mechanoenzymes, unlike kinesin and myosin.

We have shown recently by negative stain electron microscopy (EM) that dynein has a stalk-head-tail structure (Fig. 1A). The head is ring-like and contains six AAA+ domains. ATP hydrolysis primarily in AAA1 drives the conformational changes associated with the power stroke and those governing its binding to and release from, the microtubule track via a small domain at the end of the ~12nm long anti-parallel coiled coil of the stalk.

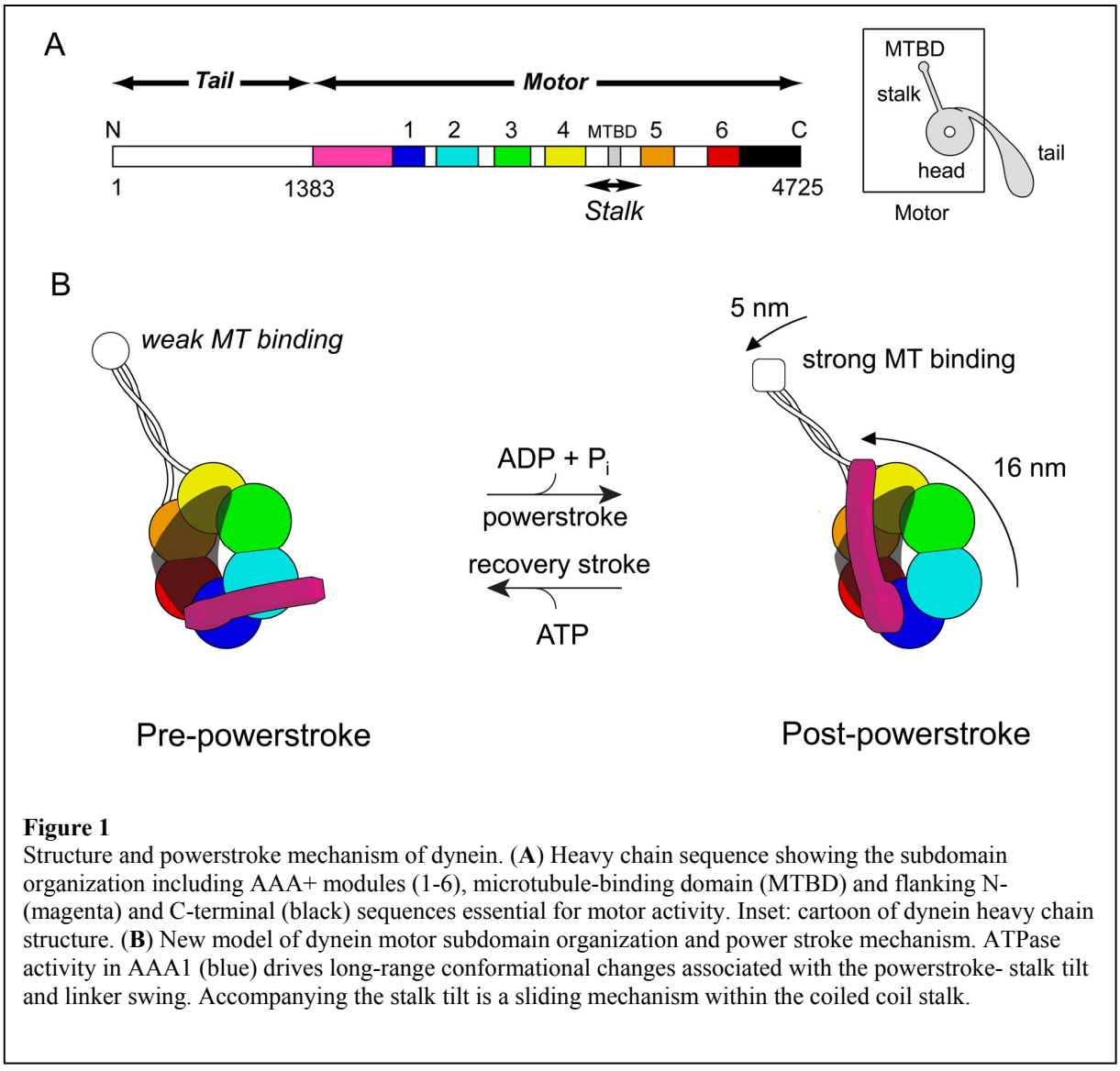

Figure 1
Structure and powerstroke mechanism of dynein. (**A**) Heavy chain sequence showing the subdomain organization including AAA+ modules (1-6), microtubule-binding domain (MTBD) and flanking N- (magenta) and C-terminal (black) sequences essential for motor activity. Inset: cartoon of dynein heavy chain structure. (**B**) New model of dynein motor subdomain organization and power stroke mechanism. ATPase activity in AAA1 (blue) drives long-range conformational changes associated with the powerstroke- stalk tilt and linker swing. Accompanying the stalk tilt is a sliding mechanism within the coiled coil stalk.

In collaboration with Prof. Kazuo Sutoh's group (University of Tokyo) we have mapped the locations of key sites within the motor domain using GFP-labeled fusion proteins and truncated motor domain constructs. We have identified four of the AAA+ modules within the ring, as well as the locations of flanking N- and C-terminal sequences (Fig. 1B) and shown that the ring comprises the AAA+ modules alone. We show that the N-terminal sequence defines an elongated lever which undergoes a nucleotide-driven swinging action of > 90° and that the stalk tilts by 15° (Fig. 1B). We also showed that sliding of the two α-helices in the stalk governs microtubule-binding and ATP hydrolysis by dynein.

Current research

Studies in my lab are focused on understanding the structure and mechanisms of the molecular motor dynein alongside continuing studies of myosin motors in collaboration with Prof. Peter Knight within the Astbury Centre.

We are pursuing the 3D structure of the dynein motor by cryo-EM- using both flagellar dyneins (in collaboration with Prof. Kazuhiro Oiwa's group, KARC, Kobe, Japan) and recombinant cytoplasmic dyneins (in collaboration with Prof. Sutoh and Dr. Kon, University of Tokyo), funded by BBSRC. We have obtained 3D density maps of the motor in both pre- and post-powerstroke conformations for the first time. These studies have led us to propose a new model for the structure and mechanism of dynein motors (Fig. 1B).

A new project funded by the Human Frontiers Science Program (HFSP) is to investigate the biochemical and biophysical properties of dimeric cytoplasmic dynein bound to microtubules as well as their structure(s) by cryo-EM. The collaborators in my team are Dr. Takahide Kon and Prof. Hideo Higuchi (University of Tokyo) and Dr. Andrej Vilfan (Ljubljana, Slovenia).

Finally, in collaboration with Dr. Tom Edwards (University of Leeds) and Dr. Dan Mulvihill (University of Kent), we are pursuing atomic resolution structures of subdomains of the motor. Expression trials of various sub-domains are currently underway.

Publications

Kotani, N., Sakakibara, H., Burgess, S.A., Kojima, H. & Oiwa, K. (2007) Mechanical properties of inner-arm dynein-F (dynein I1) studied with in vitro motility assays. *Biophys. J.* **93**, 886–894.

Burgess, S. A., Yu, S., Walker, M. L., Hawkins, R. J., Chalovich, J. M. & Knight, P. J. (2007) Structures of smooth muscle myosin and heavy meromyosin in the folded, shutdown state. *J. Mol. Biol*. **372**, 1165-1178.

Jung H.S., Burgess S.A., Billington, N., Colegrave, M., Patel, H., Chalovich, J.M., Chantler, P.D. & Knight, P.J. (2008) Conservation of the regulated structure of folded myosin 2 in species separated by at least 600 million years of independent evolution. *Proc. Natl. Acad. Sci USA*. **105**, 6022-6026.

Kon, T., Imamula, K., Roberts, A.J., Ohkura, R., Knight, P.J., Gibbons, I.R., Burgess, S.A., & Sutoh, K. (2009) Helix sliding in the stalk of dynein modulates ATPase and microtubule binding. *Nat. Struct. Mol. Biol*. **16**, 325-333.

Roberts, A.J., Numata, N., Walker, M.L., Malkova, B., Kon, T., Ohkura, R., Arisaka, F., Knight, P.J., Sutoh, K. & Burgess, S.A. (2008) AAA+ ring and linker swing mechanism in the dynein motor. *Cell* **136**, 485-495.

Funding

This work is funded by BBSRC, HFSP and The Wellcome Trust.

Hepatitis C virus (HCV) particle assembly as a therapeutic target

Toshana Foster, Lynsey Corless, Philip Tedbury, Elizabeth Atkins, Corine StGelais, Mark Verow, Carsten Zothner, David Rowlands, Mark Harris & Stephen Griffin

Hepatitis C virus (HCV) chronically infects 170-200 million individuals causing severe liver disease such as cirrhosis and hepatocellular carcinoma. Current therapy based on a combination of interferon α and ribavirin, is ineffective in 50% of cases due to innate viral resistance. Virus-specific therapies are forthcoming, yet their development has been slowed by an inability to grow the virus. Recently, however, an infectious culture system for HCV has become available, enabling investigation of the processes involved in virus assembly and entry.

In 2003 we demonstrated that the HCV p7 protein formed an oligomeric ion channel whose activity was blocked by the antiviral drug, amantadine. Now the HCV culture system has allowed us to investigate p7 as a drug target in the context of the complete virus life cycle and to explore the cellular processes involved in virion production.

Current projects:

1) **The role of p7 in the HCV life cycle.** p7 is critical for the production of infectious HCV. In collaboration with Prof. Steven Weinman (University of Kansas), we have shown that p7 acts as a proton channel in cells, consistent with our findings *in vitro*. Both specific mutations and p7 inhibitors prevent the efficient secretion of assembled HCV particles, implying a late role for its proton channel activity. We also have evidence that p7 may be incorporated into virions and play a role during virus entry (Fig. 1). p7 also interacts with the viral NS2 protein, which itself is also required for particle production. Targeting p7 for therapy, therefore, will hit HCV at multiple stages of its life cycle.

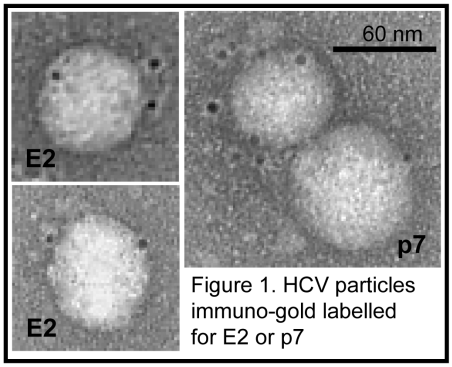

Figure 1. HCV particles immuno-gold labelled for E2 or p7

2) **The solution NMR structure of the p7 ion channel complex.**

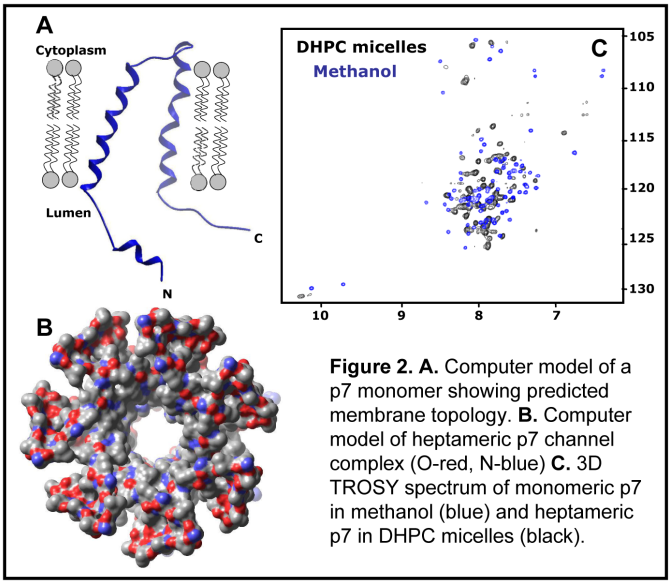

Figure 2. A. Computer model of a p7 monomer showing predicted membrane topology. **B.** Computer model of heptameric p7 channel complex (O-red, N-blue) **C.** 3D TROSY spectrum of monomeric p7 in methanol (blue) and heptameric p7 in DHPC micelles (black).

With Prof. Steven Homans (University of Leeds), we are close to solving the solution structure of the complete heptameric p7 ion channel complex in a membrane-mimetic environment. This will pave the way for rational drug design and mutagenic analyses (Fig. 2).

3) **Development of p7 inhibitors via high throughput screening and rational drug design.** We have developed a convenient liposome-based assay for p7 function. In collaboration with Drs Colin Fishwick & Richard Foster (University of Leeds Medicinal

Chemistry & Chemical Biology Group, MCCB) we are adopting both a rational and high throughput approach to identifying novel, high fidelity p7 inhibitors.

4) **Determinants of HCV resistance to p7 inhibitors.** We recently demonstrated that the sensitivity of HCV to p7 inhibitors varies for each virus strain. To define the genetic determinants associated with drug resistance, we have embarked upon a detailed mutagenic analysis of p7 to test sensitivity both *in vitro* and in cell culture.

5) **Cellular pathways involved in HCV particle assembly.** Many enveloped viruses, including HIV, hijack the host cell endosomal pathway to facilitate virion production. In collaboration with Dr Colin Crump (University of Cambridge), we have demonstrated that HCV also utilises this pathway by interacting with components of the ESCRT III complex. Preventing this interaction could provide an alternative means of targeting HCV assembly for therapy.

Publications:

Hughes M., Griffin S. & Harris M. (2009) Domain III of NS5A contributes to both RNA replication and assembly of hepatitis C virus particles. *J. Gen. Virol.* **6,** 1329 - 1334

Adair R., Patel A., Corless L., GriffinS., Rowlands D. J. & McCormick C. (2009) Expression of hepatitis C virus (HCV) structural proteins in *trans* facilitates encapsidation and transmission of HCV subgenomic RNA. *J. Gen. Virol.* **90,** 833-842.

Griffin S., StGelais C., Rowlands D. J. & Harris M. (2008) Genotype-dependent sensitivity of hepatitis C virus to inhibitors of the p7 ion channel. *Hepatology* **48,** 1779-1790.

Griffin S., Trowbridge R., Thommes P., Parry N., Rowlands D. J., Harris M. & Bright H. (2008) Chimeric GB virus B RNAs containing hepatitis C virus p7 are infectious *in vivo*. *Journal of Hepatology* **49,** 908-915.

Mankouri J., Griffin S. & Harris M. (2008) Hepatitis C virus NS5A protein re-directs trafficking of the epidermal growth factor receptor. *Traffic* **9,** 1497-1509

St Gelais C., Tuthill T., Clarke D. S., Rowlands D. J., Harris M. & Griffin S. (2007) Inhibition of hepatitis C virus p7 membrane channels in a liposome based assay system. *Antiviral Research* **76,** 48-58.

Collaborators:

University of Leeds: Prof. Steven Homans, Dr Colin Fishwick, Dr Richard Foster.
University of Kansas, USA: Prof. Steven Weinman
University of Cambridge: Dr Colin Crump

Funding:

SG holds an MRC New Investigator Award. EA and CStG received Pfizer-funded CASE studentship from the BBSRC. PT and TF were funded by the Wellcome Trust. p7 NMR studies were funded by the Royal Society.

Studies on the hepatitis C virus non-structural proteins NS2 and NS5A

Jamel Mankouri, Anna Nordle, Andrew Milward, Sarah Gretton, Philip Tedbury, Mair Hughes, Toshana Foster, Barnabas King, Lynsey Corless, Zsofia Igloi, Arwen Pearson, Steve Homans, Steve Griffin and Mark Harris

Hepatitis C virus (HCV) infects 170 million individuals and is a major cause of chronic liver disease, including fibrosis, cirrhosis and hepatocellular carcinoma. The virus has a single stranded positive sense RNA genome of 9.5kb that contains a long open reading frame encoding a single polyprotein of 3000 amino acids which is cleaved into 10 individual polypeptides by a combination of host cell and virus specific proteases. The molecular mechanisms of virus replication and pathogenesis remain to be elucidated, however, recently a clone of the virus that is able to replicate in cell culture has been identified and we are using this model extensively to understand how viral protein products function within the viral lifecycle.

A major focus of work is the NS5A protein, firstly in terms of perturbation of cellular signalling pathways - we have previously shown that NS5A perturbs two key mitogenic pathways within the cell; it inhibits the Ras-ERK MAP kinase pathway and stimulates PI3K signalling pathways, the latter promotes cell survival and activates the proto-oncogene β-catenin with implications for the link between HCV and hepatocellular carcinoma. We are currently funded by the MRC and Yorkshire Cancer Research to analyse these signalling events in more detail. Our data demonstrate that NS5A blocks Ras-Erk signalling by perturbing the endocytotic profile of the epidermal growth factor receptor. More recently we have shown that NS5A disrupts oxidative stress induced p38 MAPK signalling and prevents the activation of a pro-apoptotic potassium channel, Kv2.1.

We are also investigating the role of NS5A in virus replication. We are generating a series of NS5A mutants – particularly in PxxP motifs that interact with cellular SH3 domains – to characterise the role of these interactions in viral replication. These data have revealed genotype specific differences with regard to the requirement for specific proline residues. We have also focussed on domain III of NS5A - mutagenesis has revealed a role for serine residues in this domain in virus assembly but not RNA replication.

We are also addressing the role of NS5A phosphorylation in viral replication - we have used mass spectrometry to identify phosphorylation sites and are now analysing the phenotype of mutants in a critical serine that is the major phosphorylated residue in genotype 1b NS5A. Preliminary data suggest that a phosphomimetic mutation (to aspartate) disrupts RNA replication consistent with a regulatory role for NS5A phosphorylation.

Structural studies are ongoing - we are investigating the structure of domains II and III of NS5A by NMR, these experiments suggest that both domains are natively unfolded but we are investigating the possibility that interactions with SH3 domains (which bind to a proline rich linker sequence between the two domains) might induce the folding of these domains.

We are analysing a novel autoproteolytic event in the virus lifecycle – the cleavage between the NS2 and NS3 proteins. We have shown that this protease requires zinc and have identified a key cysteine residue that is required for cleavage, current work is addressing the role of NS2 in both viral RNA replication and assembly of new virus particles. Our data point to a pivotal role of NS2 in linking these two processes and furthermore suggest direct physical interactions between NS2 and the p7 ion channel protein.

Publications:

Hughes, M., Griffin, S. and Harris, M. (2009) Domain III of NS5A contributes to both RNA replication and assembly of hepatitis C virus particles. *J. Gen. Virol.,* in press

Mankouri, J., Griffin, S and Harris, M. (2008) The hepatitis C virus non structural protein NS5A alters the trafficking profile of the epidermal growth factor receptor. *Traffic*, **9**, 1497-1509

Mankouri, J., Milward, A., Pryde, K., Warter, L., Martin, A. & Harris, M. (2008) A comparative cell biological analysis reveals only limited functional homology between the NS5A proteins of hepatitis C virus and GB virus B *J. Gen. Virol.,* **89**, 1911-1920

Shelton, H & Harris, M. (2008) Hepatitis C virus NS5A protein binds the SH3 domain of the Fyn tyrosine kinase with high affinity: Mutagenic analysis of residues within the SH3 domain that contribute to the interaction. *Virol. J.* **5**, 24

Collaborators:

Kalle Saksela, University of Helsinki, Finland
John McLauchlan, MRC Virology Unit, Glasgow
Annette Martin, Institute Pasteur, Paris
Mair Hughes holds an Arrow Therapeutics CASE studentship (NS5A).

Funding:
This work is funded by the Wellcome Trust, MRC, Yorkshire Cancer Research and BBSRC.

Molecular mechanism of substrate translocation by a nucleoside-cation-symport-1 family transport protein

Nicholas G. Rutherford, Jonathan M. Hadden, John O'Reilly, Pikyee Ma, Simon G. Patching, Massoud Saidijam, Ryan J. Hope, Halina T. Norbertczak, Peter C.J. Roach and Peter J. F. Henderson

Introduction

The membrane transport protein for indolyl methyl- and benzyl-hydantoins found in *Microbacterium liqufaciens*, 'Mhp1', mediates the uptake of hydantoins as part of a metabolic salvage pathway for their conversion to amino acids. Mhp1 was originally studied for its potential in the commercial production of optically pure L- or D- amino acids for pharmaceutical feedstocks and for human nutrition. Its amino acid sequence places Mhp1 in the so-called nucleoside-cation-symport, 'NCS-1', sub-family 2.A.39 of the Major Facilitator Superfamily containing at least 800 homologues found in eubacteria, archaea, fungi and plants currently listed in UNIPROT. Known additional substrates for the NCS-1 sub-family include allantoin, uracil, cytosine (including the antifungal, 5-fluorocytosine), purines, thiamine, pyridoxal-based compounds, and nicotinamide riboside (see http://www.membranetransport.org/). In Leeds we have characterised the transport activity of Mhp1, amplified expression and purified the protein, and discovered novel assays based on fluorimetric measurements. Colleagues from Imperial College and the Diamond Light Source visited the Astbury Centre to learn these skills and set up crystallisation trials and determine the three-dimensional structure of the protein by X-ray crystallography.

Results

At Imperial and Diamond, So Iwata and his colleagues determined the three-dimensional structure of the Mhp1hydantoin transport protein in two different conformational states, an outward-facing 'open' and an outward-facing 'occluded' conformation with benzyl-hydantoin bound. The structure contains 12 transmembrane helices (TMs) with a core of two inverted repeats of TMs 1-5 and 6-10 (Fig. 1). The ligand can enter the outward-facing cavity inducing a conformational change of TM10 that closes the aperture of the cavity occluding the ligand.

The X-ray structure of theMhp1 protein additionally revealed an unexpected similarity to the leucine transport protein $LeuT_{Aa}$ of the neurotransmitter-sodium-symporter family, 'NSS', and to the galactose transport protein vSGLT of the solute-sodium-family, 'SSS, , despite the fact that the amino acid sequence of Mhp1 exhibits only an insignificant 15% identity to $LeuT_{Aa}$ and 16% to vSGLT, as calculated by the LALIGN algorithm (http://fasta.bioch.virginia.edu/fasta_www2/fasta_www.cgi?rm=lalign). Comparison of the two Mhp1 structures with those of $LeuT_{Aa}$ and vSGLT suggests a cycle of conformational changes that utilises the internal symmetry of the proteins to complete the process of substrate translocation. This similarity of the overall structure suggests that a wide range of proteins within these transporter families use the same molecular framework, and therefore a similar general mechanism for transport. Since a number of these are involved in human diseases and disorders such as depression, drug addiction, Parkinson's disease and epilepsy, it is extremely important to understand their molecular transport mechanism.

Conclusions

We conclude that a symmetrical structural rearrangement of Mhp1 alternating between forms opening to each side of the membrane is essential for its function. The coordinated and reciprocating conformational changes (RCC) observed on both sides of the membrane seem to be the key for the molecular mechanism of transport, and provide a structural basis for the widely-held view of an alternating access model deduced from kinetics data. This RCC

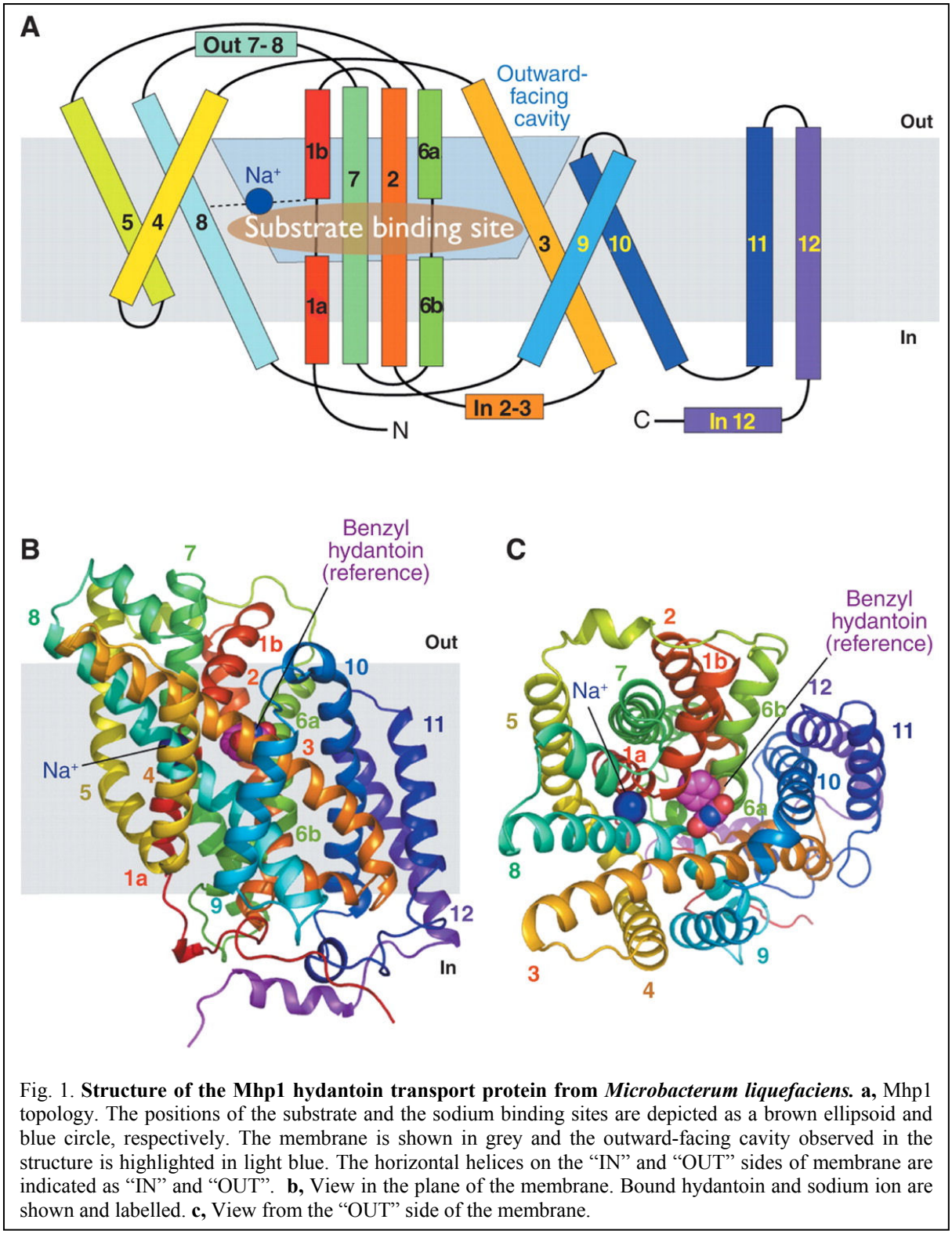

Fig. 1. **Structure of the Mhp1 hydantoin transport protein from *Microbacterum liquefaciens*. a,** Mhp1 topology. The positions of the substrate and the sodium binding sites are depicted as a brown ellipsoid and blue circle, respectively. The membrane is shown in grey and the outward-facing cavity observed in the structure is highlighted in light blue. The horizontal helices on the "IN" and "OUT" sides of membrane are indicated as "IN" and "OUT". **b,** View in the plane of the membrane. Bound hydantoin and sodium ion are shown and labelled. **c,** View from the "OUT" side of the membrane.

principle is likely to be shared by a very wide range of membrane transport proteins with a similar structural framework, and by related receptor proteins.

Collaborators

We thank Simone Weyand, Tatsuro Shimamura, Shunsuke Yajima, Shun'ichi Suzuki, Osman Mirza, Kuakarun Krusong, Elisabeth P. Carpenter, So Iwata and Alexander D. Cameron of the Membrane Protein Laboratory, Diamond Light Source, Chilton, Didcot, and the Biochemistry Department, South Kensington Campus, Imperial College London University for their help and input into this collaboration.

Funding and Acknowledgements
This research was funded primarily by the Biotechnology and Biological Sciences Research Council, grants B17935 and BB/C51725, with important contributions from Ajinomoto Inc., the European Membrane Protein consortium, EMeP, the Membrane Protein Structure Initiative, MPSI, and the Wellcome Trust. We are also grateful to Simon Phillips, Steve Baldwin, Kunihiko Watanabe and Momi Iwata for support or advice. Jeff Abramson kindly communicated coordinates for the vSGLT protein. JSPS and the Leverhulme Trust provided personal funding to A.C., S.Y. and P.J.F.H., respectively. S.W. was a recipient of an European Molecular Biology Organization, EMBO, long-term fellowship.

Publication

Weyand, S., Shimamura, T., Yajima, S., Suzuki, S., Osman Mirza, O., Krusong, K., Carpenter, E.P., Rutherford, N.G., Hadden, J.M., O'Reilly, J., Ma, P., Patching, S.G. Saidijam, M., Hope, R.J., Norbertczak, H.T., Roach, P.C.J., Iwata, S., Henderson, P.J.F. & Cameron, A.D. (2008) Molecular mechanism of substrate translocation by a nucleoside-cation-symport-1 family transport protein. *Science* **322**, 709-713.

Structure of the yeast cytochrome bc_1 complex with its bound substrate cytochrome *c*

Wei-Chun Kao and Carola Hunte

Introduction

Electron transfer processes are of great importance in many metabolic pathways of living organisms. They are essential for photosynthesis and cellular respiration, in which small diffusible redox proteins facilitate electron transport between large membrane-embedded enzymes. The intermolecular electron transfer involves transient interactions of the reaction partners. These interactions are of low affinity with equilibrium dissociation constants in the range of µM to mM. To promote high turnover and efficiency of the energy converting machinery, binding of the mobile electron carrier proteins has to be transient but also specific. Transient complexes are difficult to crystallize and their structures are poorly represented in the RCSB PDB database. In the mitochondrial respiratory chain, the soluble protein cytochrome *c* (cyt *c*) transports electrons from the cytochrome bc_1 complex (cyt bc_1) to cytochrome *c* oxidase. We determined crystal structures of yeast cyt bc_1 with bound cyt *c* providing the first structural information about this interaction critical for electron transfer.

The mitochondrial cyt bc_1 is a homodimeric multisubunit integral membrane protein complex with a molecular mass close to 500 kDa. The enzyme catalyzes the electron transfer from ubiquinol to cyt *c* coupled to the net translocation of protons across the membrane. A key feature of the mechanism is the large scale domain movement of the Rieske protein by 20 Å, which facilitates electron transfer from oxidation of ubiquinol at center P to subunit cyt c_1. Cyt *c* docks onto the latter subunit and takes up the electron. In 2002, the initial description of the interface resulted from the X-ray structure at 2.97-Å resolution of cyt bc_1 with bound cyt *c*, both proteins from the yeast *Saccharomyces cerevisiae* (PDB ID 1kyo). A single cyt *c* molecule is bound to the homodimeric complex. The interface of the complex is small. The heme moieties are centrally located in a mainly non-polar contact site with a cation-π interaction surrounded by complementary charged residues. These interactions appear to be the dominant features of transient electron transfer complexes, and are also observed for the interface of the yeast cyt *c* peroxidase: cyt *c* and the bacterial reaction center: cyt c_2 complexes.

X-ray structure of yeast cyt bc_1 with bound cyt *c* at 1.9-Å resolution.

We now determined the structure of isoform-1 cyt *c* bound to cyt bc_1 at 1.9-Å resolution in reduced state. The complex was crystallized at physiological ionic strength with bound antibody fragments, which provide space in the crystal lattice for cyt *c* (Fig. 1).

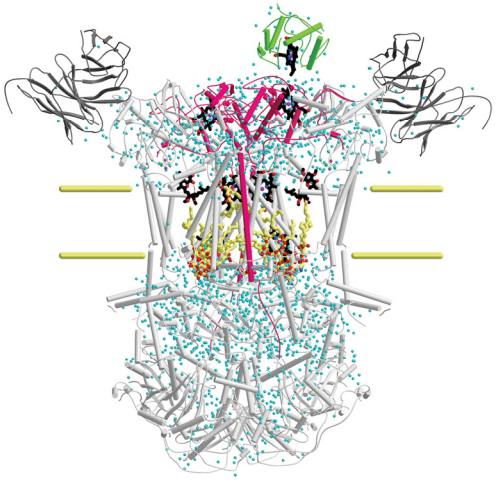

Figure 1 - In the 1.9-Å resolution structure, one molecule cyt *c* (green) binds to one of the two subunits cyt c_1 (pink) of the cyt bc_1 dimer (light grey). The protein was crystallized with antibody F*v* fragments (dark grey). Water molecules are shown in cyan. Lipid and detergent molecules are colored yellow with oxygen atoms in red. Carbon and oxygen atoms of heme groups and stigmatellin are in black and red, respectively. Yellow horizontal lines indicate the relative position of the membrane (PDB ID 3cx5).

Remarkably, the cyt bc_1 dimer is slightly asymmetric. Monovalent cyt *c* binding coincides with conformational changes of the Rieske head domain and subunit QCR6p. The structure allowed for the first time the analysis of interfacial water molecules. Also, the monovalent cyt *c* binding permitted a direct comparison of free and occupied docking site in the same crystal structure. Though the cyt c_1:cyc *c* interface is approximately 70% hydrophobic, it is not sealed to the bulk solvent and a relatively low surface complementarity provides space for hydration. Indeed, the interface is highly hydrated. Whereas the side chains of cyt c_1 residues are not affected by cyt *c* binding, their hydration pattern changes significantly. 10 additional water molecules, either displaced or newly bound, are present on the cyt c_1 surface when cyt *c* is bound with the major change in the hydrophobic region of the interface. This is correlated with highly ordered surface residues of cyt c_1 and disordered charged residues of cyt *c*. Pronounced hydration and a 'mobility mismatch' at the interface are favorable for transient binding.

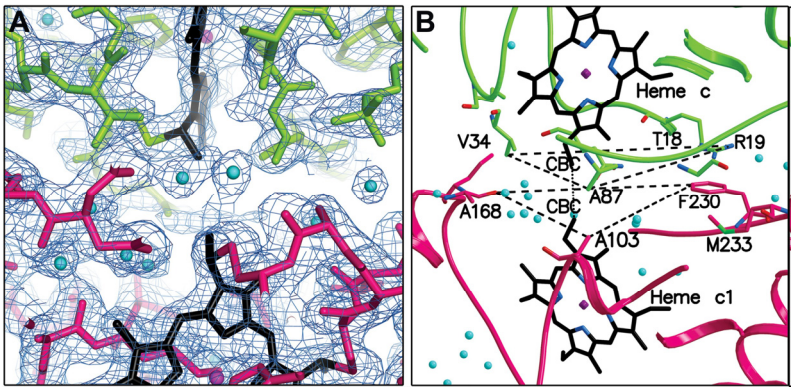

Fig. 2. The interface of cyt *c* (green) and cyt c_1 (pink) at high resolution (PDB ID 3cx5). Hemes: black; water molecules: cyan. *A*, $2F_oF_c$ electron density map at the interface, contoured at 1σ and drawn as a blue mesh. *B*, View of the core interface. The minimal core interface (dashed lines) is defined by the four labeled residue pairs including cation-π interaction F230/R19.

Comparison of the two isoform-1 cyt *c* containing structures with the third structure (PDB ID 3cxh) of the complex with bound isoform-2 cyt *c* (1,2) led to the definition of a core interface, which refers to four common interaction pairs including the cation-π interaction (Fig. 2). They encircle the heme groups and are surrounded by variable interactions. The core interface may be a feature to gain specificity for formation of the reactive complex.

The consistency in the binding interaction despite differences in primary sequence, redox-state and crystal contacts together with crystallization at physiological ionic strength clearly suggest that the structures show the native bound state of the electron transfer complex.

Publications

Solmaz, S.R. & Hunte, C. (2008) Structure of complex III with bound cytochrome *c* in reduced state and definition of a minimal core interface for electron transfer. *J. Biol. Chem.* **283**, 17542-17549.

Nyola, A. & Hunte C. (2008) A structural analysis of the transient interaction between cytochrome bc_1 complex and its substrate cytochrome *c*. *Biochem. Soc. Trans*. **36**, 981-985.

Collaborators

Dr. Sozanne Solmaz, Max Planck Institute of Biophysics, Frankfurt
Ajeeta Nyola, Max Planck Institute of Biophysics, Frankfurt

Funding

Funding by the German Research Foundation (DFG, SFB 472) and the Cluster of Excellence "Macromolecular Complexes" at the Goethe University Frankfurt (DFG Project EXC 115)" is acknowledged.

Poxvirus K7 protein adopts a Bcl-2 fold and interacts with Human DEAD box RNA helicase DDX3

Arnout P. Kalverda, Gary S. Thompson and Steve W. Homans

Poxviruses have evolved numerous strategies to evade host innate immunity. Vaccinia virus K7 is a 149 residue protein with previously unknown structure that is highly conserved in the orthopoxvirus family. K7 bears sequence and functional similarities to A52, which interacts with several cellular partners to suppress NF-κB activation and to stimulate the secretion of the anti inflammatory cytokine IL-10. In contrast to A52, K7 forms a complex with DEAD box RNA helicase DDX3. We determined the NMR solution structure of K7 to provide insight into the structural basis for poxvirus antagonism of innate immune signaling. The structure reveals an α-helical fold belonging to the Bcl-2 family despite an unrelated primary sequence. Chemical shift mapping studies on a ^{15}N labeled sample of the K7-DDX3 complex have allowed us to localise the binding site for DDX3 to a negatively charged face of K7. The K7 binding region on DDX3 has been mapped to a 20 residue N-terminal fragment of DDX3 that is part of an unstructured region ahead of the core RNA helicase domains. This interaction is responsible for the ability of K7 to inhibit interferon induction and indicates that the N-terminal region of DDX3 has a critical role in the immune signaling cascade leading to *ifnb* promoter induction and interferon release.

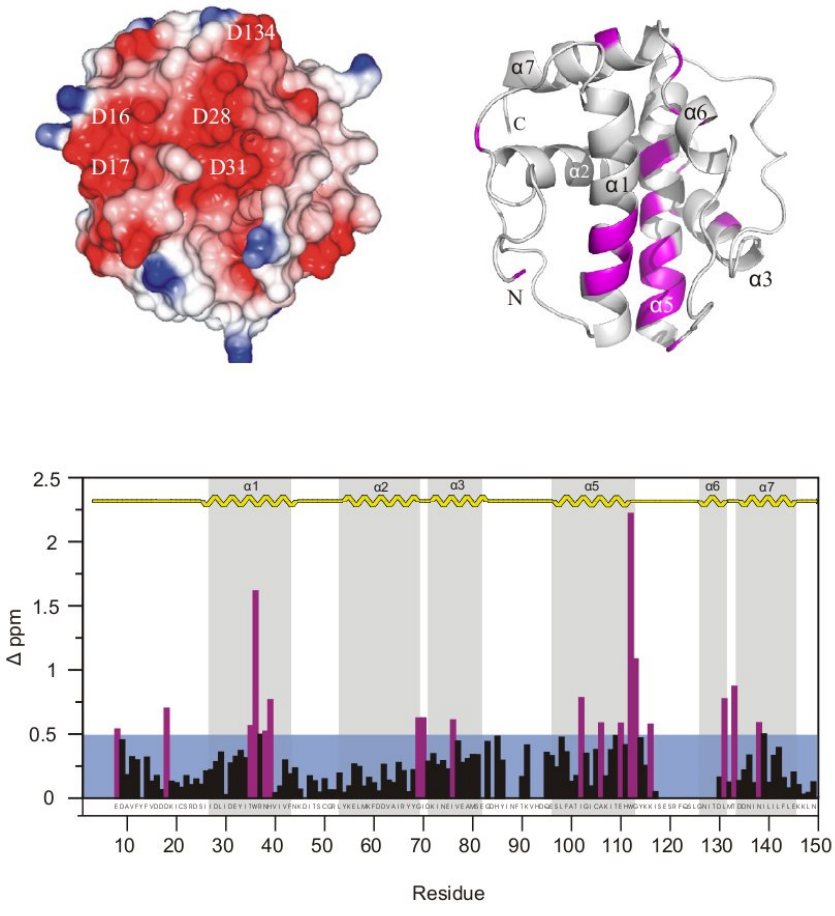

Identification of the DDX3 binding face of K7 by chemical shift mapping. Left, electrostatic surface map of K7 revealing the density of negatively charged residues on this face. Right, ribbon model of K7 with residues with a change in chemical shift of > 0.5 ppm coloured in magenta. Bottom, graph of chemical shift changes for all residues in K7.

Currently work is focused on assigning the backbone chemical shifts of the K7-DDX3 complex. An assignment of these spectra will provide data for investigating both the structure of the complex in solution and any changes in dynamics that occur on binding per residue basis.

Publications

Kalverda, A.P., Thompson, G.S., Vogel, A., Schröder, M., Bowie, A.G., Khan, A.R. & Homans S.W. (2009) Poxvirus K7 protein adopts a Bcl-2 fold: Biochemical mapping of its interactions with human DEAD box RNA helicase DDX3. *J. Mol. Biol.* **385**, 843-853.

Funding & Collaborators

We would like to acknowledge our collaborators Andre Vogel, Martina Schröder, Andrew G. Bowie, Amir R. Khan from the School of Biochemistry and Immunology, Trinity College Dublin, Ireland and funding by Science Foundation Ireland.

Thermodynamic characterisation of a hydrophilic ligand-protein interaction

Caitriona Dennis, Neil Syme, Agnieszka Bronowska and Steve Homans

Introduction

The molecular basis for protein-ligand recognition is governed by a series of intricate affinities that result in a highly specific overall interaction. Despite the universal nature of these interactions, our understanding of this molecular basis is, as yet, poorly understood and as a result, current methods for structure-based drug design are severely compromised. The limited ability to predict ligand affinity is largely due to the complexity of all the interactions that are occurring: the energetics and the dynamics of the interacting groups involving contributions from the ligand, the protein and solvent rearrangement. In order to gain a better understanding of ligand binding, it is necessary to decompose these interactions into enthalpic (structural) and entropic (dynamic) contributions. This binding process has been characterised in recent years using a model hydrophobic system, MUP (Mouse Urinary Protein) with various ligands. In this study, a model hydrophilic system, rRa-HBP2 (recombinant histamine binding protein) is used in the deconvolution of binding thermodynamics. This, in effect, provides a complete comparison of enthalpic and entropic contributions in two systems with classically distinct binding signatures.

Histamine-binding Protein

Histamine-binding protein 2 (HBP2) is a member of the lipocalin family isolated from the brown-ear tick *Rhipicephalus appendiculatus*. Ticks secrete HBP2 during feeding in order to sequester histamine and evade an immune response. Unlike MUP, which has one ligand-binding site, HBP2 contains two binding sites each lined with charged residues and they differ by their affinities for histamine. In this study, however, in order to simplify the thermodynamic analysis of ligand binding, one of these binding sites, the apparent low-affinity site was mutated (D24R) in order to sterically block ligand binding in this pocket.

X-ray analysis

In order to enable a structure-based interpretation of the thermodynamic measurements, crystal structures of HBP2-D24R – histamine complex apo HBP2-D24R and were solved (Figs. 1a and b).

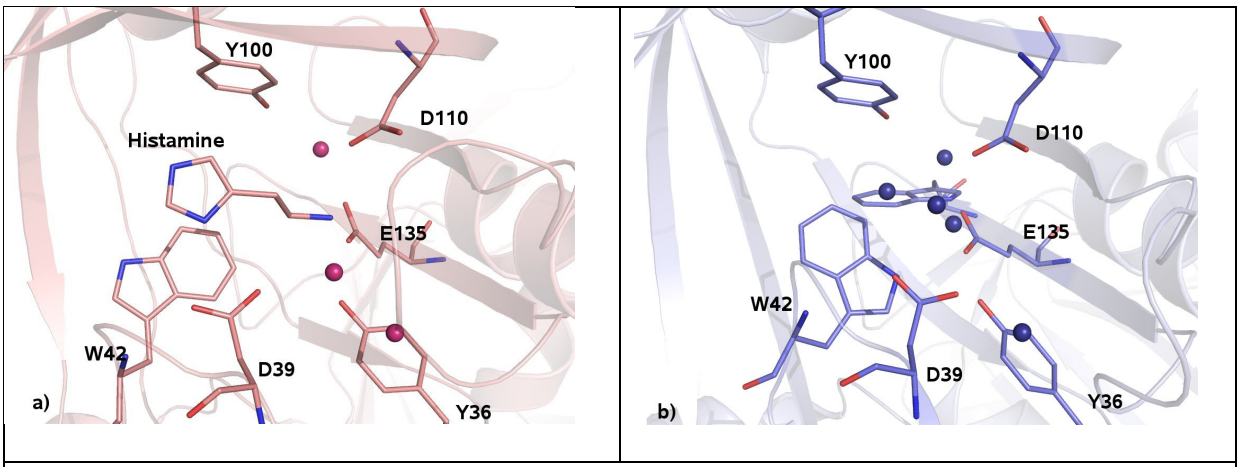

Figure 1. Close up of the binding pocket of HBP2-D24R. In **a)** Arrangement of the binding pocket with histamine bound. Residues responsible for binding are labeled and three ordered water molecules are present. **b)** The binding pocket in the apo form. Two extra water molecules are observed to bind in place of histamine.

It can be seen that histamine is bound in the pocket through an extensive network of hydrogen bonds and ionic interactions (Fig. 1a). In addition, a number of ordered water molecules rest within the pocket stabilised by hydrogen bond interactions. The apo structure shows 5 ordered water molecules in the binding pocket, 3 in similar positions to those observed in the complex and 2 in the place of histamine structure (Fig. 1b)

Global thermodynamics
Isothermal titration calorimetry (ITC) experiments were carried out to assess the global thermodynamics of histamine binding. It was revealed that histamine bound with nanomolar affinity in a 1:1 stoichiometry with a process largely enthalpy driven.

NMR relaxation studies
Using ^{15}N relaxation measurement to evaluate the entropic contribution of histamine binding to HBP2-D24R, changes in local entropy were observed within the binding pocket and dispersed over the whole protein. This, in effect, revealed an overall increased mobility of the protein backbone upon ligand binding, leading to a favourable entropic contribution to the free energy of binding.

Molecular dynamics
To examine contributions of changes in protein side-chain dynamics to overall binding dynamics, all-atom molecular dynamics simulations of apo HBP2-D24R and the complex with histamine with explicit inclusion of solvent water was carried out. As observed with the backbone data, an overall increase in entropy on ligand binding was observed. To complete, the whole thermodynamics of ligand binding, Conductor-Like Screening Model (COSMO) calculation was used to estimate the solvation dynamics of histamine.

Driving forces for ligand binding
In our HBP2 hydrophilic system, the dominant favourable entropic contribution to binding derives from ligand desolvation, a phenomenon observed in the MUP 'classical' hydrophobic system. In contrast, however, the overall entropic contribution to binding is unfavourable due to the unfavourable desolvation of the protein binding pocket. Instead, the overall unfavourable entropy of binding, which is essentially identical to that in MUP, is dominated by the interplay of ligand desolvation and the loss in ligand degrees of freedom.

Collaborators
Dr Guido Paesen, CEH Oxford

Funding
This work was funded by the BBSRC and The Wellcome Trust.

Role of protein interactomes in Alzheimer's disease

Isobel Morten, Harry King, Heledd Griffiths, Nicole Watt, Tony Turner and Nigel Hooper

Introduction

Alzheimer's disease (AD) is the commonest neurodegenerative disease of old age. Currently, there are no drugs available to halt or slow the progression of this devastating disease which is placing a huge burden on patients and carers. AD is characterised by the deposition in the brain of senile plaques that are composed of the amyloid-β peptide (Aβ) (Fig. 1). Through mechanisms that are poorly understood, Aβ oligomers, fibrils and/or aggregates are toxic to nerve cells. Aβ is derived from the larger transmembrane amyloid precursor protein (APP) through proteolytic cleavage by the β- and γ-secretases. The β-secretase (BACE1) cleaves within the APP sequence at the N-terminus of the Aβ peptide, with the γ-secretase complex cleaving the resulting membrane-bound stub at the C-terminus of the Aβ sequence. Inhibition of both the β- and γ-secretases is being considered as potential therapeutic approaches to combat AD.

The prion protein is probably best known for its role in the transmissible spongiform encephalopathies or prion diseases, such as Creutzfeldt-Jakob disease in humans and bovine spongiform encephalopathy in cattle. In these diseases the normal cellular for of the prion protein (PrP^{C}) undergoes a conformational conversion to the infectious form, PrP^{Sc}. PrP^{C} appears to have roles in the cellular resistance to oxidative stress, in cellular copper and zinc homeostasis and in cell signalling. In addition, we have shown that PrP^{C} inhibits the β-secretase cleavage of APP, lowering the amount of Aβ produced and, therefore, potentially protecting against AD (Fig. 1). In both cell models and mice, reduction of PrP^{C} levels resulted in an increase in Aβ production. BACE1 co-immunoprecipitated with PrP^{C} from cells and brain samples, suggesting a direct interaction between the two proteins. This inhibitory effect of PrP^{C} on the BACE1 cleavage of APP was lost when PrP^{C} contained insertion or point mutations associated with human prion diseases or when the protein was converted to the infectious form PrP^{Sc}, raising the possibility that Aβ contributes to prion disease pathogenesis.

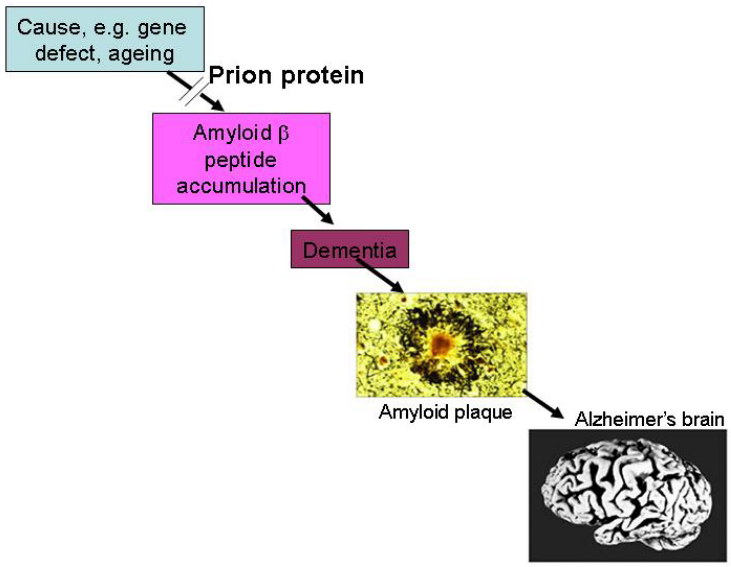

Figure 1. The role of the prion protein in Alzheimer's disease prevention.
In the amyloid cascade hypothesis of AD, a genetic mutation, ageing or some other environmental trigger causes an accumulation of the neurotoxic Aβ peptide that aggregates to form the characteristic amyloid plaques found post-mortem in the brains of AD patients. The normal cellular form of the prion protein, PrP^{C}, through inhibiting the production of the Aβ peptide, may prevent the development of AD.

These observations raise the following questions which we are actively pursuing: (i) Could mimicking the mechanism by which PrP^C inhibits Aβ peptide formation be a potential therapeutic treatment for AD? (ii) Could small reductions in PrP^C levels in individuals affect the proteolytic processing of APP in a subtle way over decades to affect long-term Aβ production that, in turn, would accelerate the onset of AD? (iii) Does Aβ contribute to the pathogenesis of prion diseases? (iv) Is depletion of PrP^C a sound approach for the treatment of prion diseases?

Several other proteins, in addition to PrP^C, have been reported to regulate the proteolytic processing of APP. For example, members of the reticulon family inhibit BACE1 activity, while the leucine-rich repeat transmembrane 3 (LRRTM3) protein increases its activity. Other proteins bind to APP and/or alter its subcellular trafficking to modulate its proteolytic processing, including Nogo-66 receptor, F-spondin, ApoER2, SORLA, the sorting nexin SNX33, and the GPI-anchored TAG-1. F-spondin, PrP^C and the neural cell adhesion molecule (NCAM) were recently identified to interact with APP *in vivo*, i.e. be components of the brain interactome of APP. From these studies, it is evident that APP processing and Aβ generation can be modulated by a diverse number of interacting proteins in various cellular compartments. This modulation could involve direct binding to BACE1 (and/or the α- or γ-secretases) or APP itself, thereby influencing enzyme activities or the susceptibility of APP to cleavage. Alternatively, the mode of action may be indirect, involving the segregation of the secretases and APP into either the same or different membrane domains or cellular compartments. The molecular and cellular mechanisms underlying the modulation of APP processing in this way clearly need to be understood in order to provide a complete knowledge of AD pathogenesis, yet in many of the above cases this information is lacking. The components of the APP and BACE1 interactomes could potentially be exploited therapeutically to modulate Aβ production.

Publications

Parkin, E.T., Watt, N.T., Hussain, I., Eckman, E.A., Eckman, C.B., Manson, J.C., Baybutt, H.N., Turner, A.J. & Hooper, N.M. (2007) Cellular prion protein regulates β-secretase cleavage of the Alzheimer's amyloid precursor protein. *Proc. Natl. Acad. Sci USA* **104**, 11062-11067.

Hooper, N.M. & Turner, A.J. (2008) A new take on prions: preventing Alzheimer's disease. *Trends Biochem. Sci.* **33**, 151-155.

Griffiths, H.H., Morten, I.J. & Hooper, N.M. (2008) Emerging and potential therapies for Alzheimer's disease. *Expert Opin. Ther. Targets* **12**, 693-704.

Funding

This work was funded by the MRC, Wellcome Trust and BBSRC.

Biomolecular modeling and structural bioinformatics

James Dalton, John Davies, Christopher Fallaize, Jonathan Fuller, Sarah Kinnings, Mahesh Kulharia and Richard Jackson

Predicting druggable binding sites at the protein-protein interface

Protein-protein interactions (PPIs) are critical for all aspects of cellular function, a role that is further underlined by their involvement in a large number of disease pathways, and thus they represent attractive targets for therapeutic intervention. A number of small molecules have been successful in targeting and disrupting protein-protein interactions. It is observed that these small molecules bind deeper within the contact surface of the target protein, with higher ligand efficiencies. We address the differences between proteins that bind marketed drugs and proteins that are currently targeted by small molecule protein-protein interaction inhibitors.

We use an energy based pocket detection algorithm (Q-SiteFinder) as a tool to define and characterise the extent of binding pockets on the protein surface. The aim is to compare and contrast different classes of protein interactions, specifically focusing on the properties of occupied pockets i.e. known protein binding sites. We find that in general protein-protein interactions occur in a number of small pockets (54 Å3) whereas current marketed drugs occur predominantly in a single large pocket (260 Å3). PPI inhibitors are shown to occur in relatively small pockets (77 Å3) when compared to current marketed drugs, thus they appear to have properties resembling those of protein-protein interactions. Q-SiteFinder implicitly assumes that the total energy of the pocket defines the ability to bind a small-molecule, thus giving a simple measure of the druggability of the pocket.

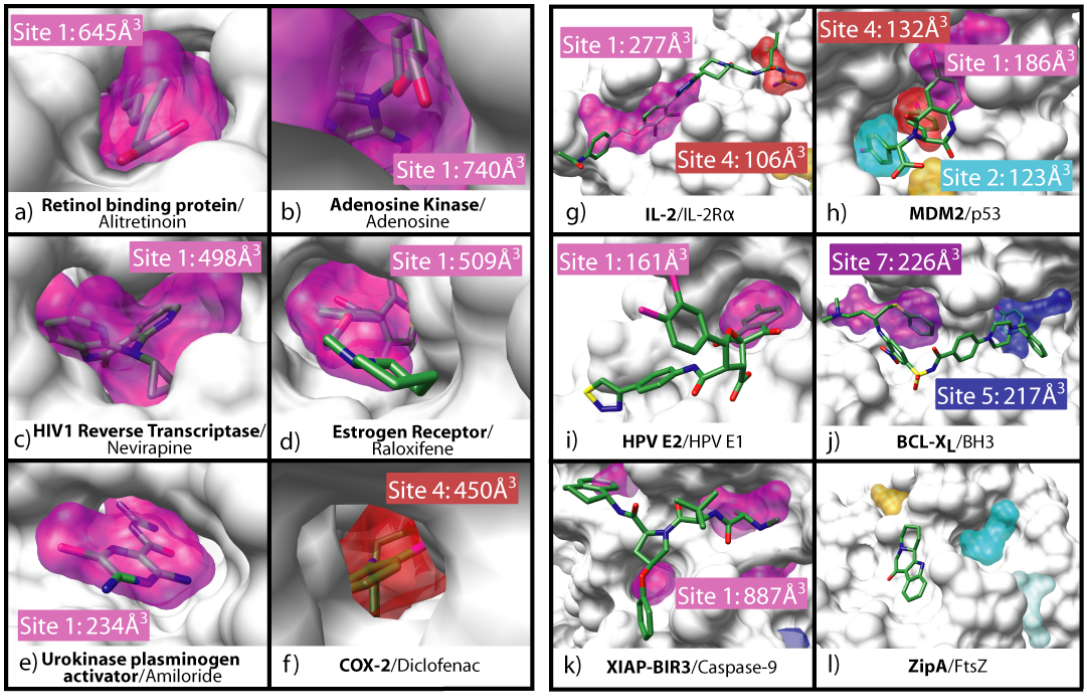

We have further analysed the characteristics of binding pockets involved in protein-drug interactions and protein-protein interactions in both the bound and unbound state. Our analysis suggests that a mechanism of 'conformational selection' may play an important role in the binding of small-molecules to protein interfaces. These results highlight the importance of the dynamical view of proteins with respect to the rational design of small-molecule competitive inhibitors of protein-protein interfaces.

Site similarity analysis for the functional classification of the protein kinases

Methods for analyzing complete gene families are becoming of increasing importance to the drug discovery process, because similarities and differences within a family are often the key to understanding functional differences that can be exploited in drug design. We undertook a large-scale structural comparison of protein kinase ATP-binding sites using a geometric hashing method. Subsequently, we proposed a relevant classification of the protein kinase family based on the structural similarity of its binding sites. Our classification was not only able to reveal the great diversity of different protein kinases and therefore their different potential for inhibitor selectivity but it was also able to distinguish subtle differences within binding site conformation reflecting the protein activation state. Furthermore, using experimental inhibition profiling, we demonstrated that our classification could be used to identify protein kinase binding sites that are known experimentally to bind the same drug, demonstrating that it has potential as an inverse (protein) virtual screening tool, by identifying which other sites have the potential to bind a given drug. In this way the cross-reactivities of the anticancer drugs Tarceva and Gleevec were rationalized.

Homology modeling of protein-ligand interactions

We have developed an automated homology modeling method for the structural prediction of protein-ligand binding-sites, which brings together new and existing ideas. The method is based on the 'induced' fit concept where there is flexibility in both side-chains and ligand. This is implemented by generating a broad range of possible conformations (or rotamers) for side-chains and ligand, which are then refined with a mean-field optimisation calculation, resulting in the lowest available energetic state of the binding-site. SitesModel is accessible for use at "http://www.modelling.leeds.ac.uk/sitesmodel". A tool for selecting the most appropriate template structure based on sequence and ligand similarity is included, together with visualization aids for selecting relevant protein chain(s) and binding-site co-factors. The methods and results are currently being written up for publication.

Modelling protein interactions and docking

In collaboration with the group of Prof. Goody (Max Plank Institute, Dortmund) we have developed a novel knowledge-based scoring function (SIScoreJE) that uses information theory to predict the binding affinity of ligands to proteins for use in structure-based inhibitor design. SIScoreJE efficiently predicts the binding energy between a small molecule and its protein receptor. Protein-ligand atomic contact information was derived from a Non-Redundant Data set (NRD) of over 3000 X-ray crystal structures of protein-ligand complexes. The preferences were calculated using an information theoretic relationship of joint entropy. To test the sensitivity of the method to the inclusion of solvent, Single-body Solvation Potentials (SSP) were also derived from the atomic contacts between the protein atom types and water molecules modeled using AQUARIUS2. Validation was carried out using an evaluation data set of 100 protein-ligand complexes with known binding energies to test the ability of the scoring functions to reproduce known binding affinities. In summary, it was found that a combined SSP/ScoreJE (SIScoreJE) performed significantly better than ScoreJE alone, and SIScoreJE and ScoreJE performed better than other commonly used scoring functions such as GOLD::GoldScore, GOLD::ChemScore, and XScore.

In collaboration with the group of Prof. Brito (University of Coimbra, Portugal) we are currently using molecular docking and pharmacophore modelling to develop novel inhibitors to prevent amyloid fibril formation in familial amyloidotic polyneuropathy. In this disease, single point mutations encode for less stable variants of transthyretin (TTR), which undergo tetramer dissociation and monomer unfolding. The initial tetramer dissociation is thought to be the rate limiting step in the process, and some success has been achieved through

inhibition of this process using small molecule thyroxine mimetics. The aim is to design inhibitors that prevent fibril formation.

Collaborators
Prof. Kanti Mardia (School of Maths, University of Leeds)
Prof. Charles Taylor (School of Maths, University of Leeds)
Dr. Stewart Barber (School of Maths, University of Leeds)
Prof. Rui Brito (University of Coimbra, Portugal)
Prof. Roger Goody (Max Plank Institute, Dortmund, Germany)

Visiting Researchers
Mr. Mahesh Kulharia (Max Plank Institute, Dortmund, Germany)
Mr. Carlos Simoes (University of Coimbra, Portugal)

Publications
Kinnings, S.L., Jackson, R.M. (2009) Binding site similarity analysis for the functional classification of the protein kinase family. *J. Chem. Inf. Model.* **49**: 318-329.

Fuller, J.C., Burgoyne, N.J., Jackson, R.M. (2009) Predicting druggable binding sites at the protein-protein interface. *Drug Discov Today*, **14**: 155-161.

Kulharia, M., Goody, R.S., Jackson, R.M. (2008) Information theory-based scoring function for the structure-based prediction of protein-ligand binding affinity. *J Chem Inf Model.* **48**, 1990-1998.

Dalton, J.A.R. & Jackson, R.M. (2007) An evaluation of automated homology modelling methods at low target template sequence similarity. *Bioinformatics* **23**: 1901-1908.

Funding
These projects were funded by the BBSRC, EPSRC, University of Leeds.

Electrodes for redox-active membrane proteins

Sophie Weiss, Nikolaos Daskalakis, Lukasz Krzeminksi, James Kendall, Steve Evans, Richard Bushby, Simon Connell, Peter Henderson and Lars Jeuken

Introduction

Redox proteins, which are estimated to account for a quarter of all proteins, perform a myriad of functions in biology. They shuttle electrons and catalyse redox reactions in many vital processes, including photosynthesis and metabolism. Dynamic electrochemical techniques have proven to be powerful tools to study these proteins. The thermodynamics and kinetics can be studied in detail if they are electrochemically connected or 'wired' to the electrode surface. The main challenge is to adsorb proteins in their native state on the electrode while efficiently exchanging electrons. Because membrane proteins are more difficult to manipulate experimentally than globular proteins, less work has been reported on the electrochemistry of these proteins. Here, we report a novel approach to link membrane proteins to an electrode surface.

Cholesterol tethers to 'wire' membranes

We have prepared electrode surfaces which enables the characterisation of redox-active membrane enzymes in a native-like environment. For this, we have used the methodology of tethered bilayer lipid membranes (tBLM), in which the lipid bilayer is attached to the electrode surface via special chemical anchors that are bound to the surface on one side and insert into a bilayer leaflet at the other (Fig. 1). Cholesterol derivatives have been synthesised, which, via a hydrophilic linker, are connected to a thiol group that form self-assembled monolayers (SAMs) on gold electrodes. These cholesterol-lipids have been mixed with small thiols to provide space for transmembrane proteins. The surfaces of these mixed SAMs have been characterised in detail and shown to exhibit a complex pattern of phase separation, confirming the demixing of the two thiols schematically shown in Fig. 1.

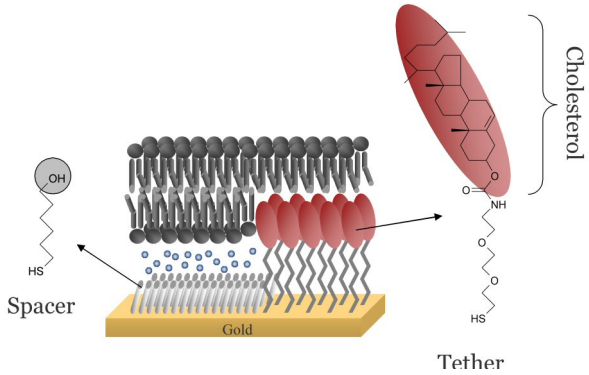

Figure 1: Chemical structures of 6-mercaptohexanol (spacer) and the cholesterol tether molecule used to form tBLMs.

Electric field effects

The tBLMs (without proteins) on gold provide an excellent platform to study the effects that electric fields have on the structure of lipid membranes. Electric-field induced changes in structure and conductivity of the tBLM have been studied at submicroscopic resolution using atomic force microscopy (AFM) and electrochemical impedance spectroscopy (Fig. 2). At electric fields of ≤ 0.45 V across the membrane, it was found that the conductance of the membrane starts to increase and membrane areas of less than 150 nm in size elevate from the surface up to 15 nm in height. The latter observation suggests that pockets of solvent appear or are formed beneath the membrane.

tBLM from bacterial membrane extracts

New protocols have been developed to prepare tBLMs from inner membranes extract from *E. coli*. In contrast to the systems prepared previously with purified membrane proteins, these systems are easier to prepare and more robust in nature.

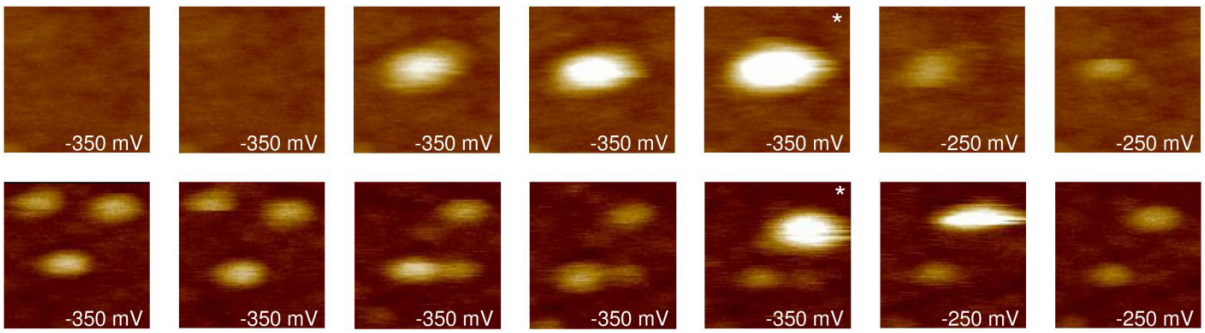

Figure 2: Two selected areas of consecutive AFM images of a tBLM at varying DC potentials (the electric field experienced by the lipid membrane is about 200 mV larger than the applied potential). The size of the selected areas is 200×200 nm and the height scale 18 nm. The indicated potential is applied versus Ag/AgCl. The potential of zero charge (*pzc*) of the substrate 'underneath' the membrane is 0.19 ± 0.13 V vs Ag/AgCl. Thus, when -350 mV is applied the tBLM an electric field of ~0.54 V is applied to the lipid membrane.

The membrane-bound quinones in these tBLM systems still act as substrates for quinone enzymes that are co-immobilised (Fig. 3, left). Using this novel membrane system, the activity of an ubiquinol oxidase from *Escherichia coli*, cytochrome bo_3 (cbo_3) is studied using voltammetry techniques (Fig. 4, left). The apparent K_M of cbo_3 for oxygen with this system was determined to be 1.1 ± 0.4 µM, in good agreement with literature values for whole cell experiments and for purified cbo_3. Increasing the concentration of lipophilic UQ-10 in the membrane leads to an increase in cbo_3 activity (Fig. 3, right). The activity of cbo_3 with long chain ubiquinones appears to be different to previous literature, which uses short chain substrate analogues such as UQ-1, in that typical Michaelis Menten kinetics are not observed using UQ-10. This native-like membrane model thus provides new insights into the interaction of transmembrane enzymes with hydrophobic substrates which contrasts with studies using hydrophilic UQ analogues.

The same tBLM was used to study the diffusion properties of ubiquinol in the membrane. Electrochemical impedance spectra (EIS) were obtained at varying DC potentials covering the potential window in which the voltammetric catalytic wave of cbo_3 is visible (Fig. 4 for one example). These spectra were compared to those obtained after addition of a potent

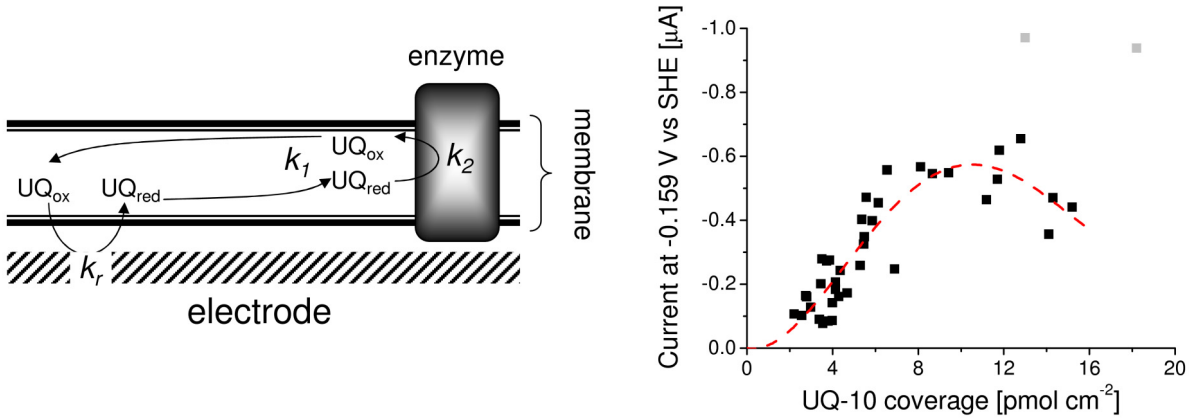

Figure 3: (Left) Schemetic representation of the tBLM systems in the electrochemical, diffusion and enzymatic reaction taking place. (Right) Enzymatic activity of cytochrome bo_3 obtained using the tBLM system prepared from inner membrane extracts from cbo_3. The maximum reduction activity (at high oxygen concentration) of inner membranes (1:9 mixed with *E. coli* lipid extract) is plotted as a function of ubiquinol-10 present in the membrane. The line is included as a guide to the eye.

inhibitor of cbo_3, cyanide, and the difference in impedance was analysed using a derived equivalent circuit, which is similar to that of Open Finite-Length Diffusion (OFLD) or the finite Warburg circuit, but with the boundary conditions modified to account for the fact that

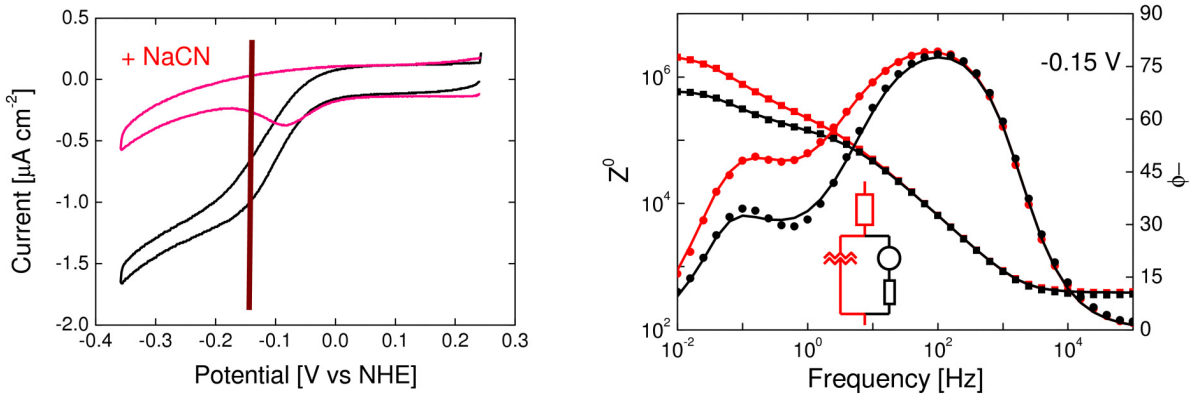

Figure 4: (Left) Typical cylic voltammogram (CV, 10 mV/s) of the tBLM system prepared from *E. coli* inner membranes overexpressing c*bo*$_3$ without (black line) and with (red line) the inhibitor cyanide. (Right) Typical electrochemical impedance spectra (EIS) measured at -0.15 V vs normal hydrogen electrode (NHE) as indicated by the brown bar in the left plot) without (black line) and with (red line) the inhibitor cyanide. The EIS data was analysed by the equivalent circuit shown with the circle representing the derived circuit that models the ubiquinol diffusion in the membrane.

ubiquinol reoxidation is limited by enzyme activity. Analysis of the impedance spectra of the tethered membrane system gave kinetic parameters that are consistent with values obtained using cyclic voltammetry. Importantly, the diffusion rate of ubiquinone (10^{-13} – 10^{-12} cm^2/s) was found to be orders of magnitude lower than accepted values for lateral diffusion (10^{-8} – 10^{-7} cm^2/s). We argue that the obtained diffusion constant represent perpendicular diffusion of quinone across the membrane, corresponding to a 'flip' time between 0.05 and 1 s. This is the first time that the flip time of ubiquinol has been measured.

Future directions

We aim to continue to study the enzyme mechanics of c*bo*$_3$ and other quinone enzymes with particular focus on properties that made UQ a special substrate when compared to aqueous solutes. This data will be substituted with detailed inhibitor studies. In a second project, intact vesicles with fluorescent pH indicators are adsorbed on the surface in order to monitor simultaneously the electron and proton transfer properties of the redox enzymes of interest.

Collaborators and Funding

We thank Prof. Robert B. Gennis (University of Illinois, Urbana, USA) for his help with c*bo*$_3$ and providing several *E. coli* strains. This work is funded by the MCN (FP6), EU (FP7), BBSRC, EPSRC, Royal Society and Philips.

Publications

Dodd, C.E., Johnson, B.R.G., Jeuken, L.J.C., Bugg, T.D.H., Bushby, R.J., Evans, S.D. (2008) Native *E. coli* inner membrane incorporation in solid supported lipid bilayer membranes, *Biointerphases*, **3**, FA59-FA67**.**

Jeuken, L. J. C. (2008) AFM study on the electric-field effects on supported bilayer lipid membranes, *Biophys. J.*, **94,** 4711-4717**.**

Barfoot, R., Sheikh, K., Johnson, B.R.G., Colyer, J., Jeuken, L.J.C., Bushby, R.J., Evans, S.D. (2008) F-actin interaction with ponticulin containing planar phospholipid bilayers, *Langmuir*, **24,** 6827-6836.

Weiss, S. A., Bushby, R. J., Evans, S. D., Henderson, P. J. F., Jeuken, L. J. C. (2009) Characterisation of cytochrome bo3 activity in a native-like surface-tethered membrane, *Biochem. J.*, **417**, 555-560.

Jeuken, L. J. C., Weiss, S. A., Henderson, P. J. F., Evans, S. D., Bushby, R. J. (2008) Impedance spectroscopy of bacterial membranes: Coenzyme-Q diffusion in a finite diffusion layer, *Anal. Chem.*, **80**, 9084–9090.

Structural studies of innate immune signalling proteins

Adam Dale, John Short, Sayaka Sato, Thomas Edwards,
Arwen Pearson and Andrew Macdonald

Introduction

The innate immune response is a highly conserved early defence mechanism against microbial pathogens including viruses. The success of this defence against virus invasion depends on the capacity of the host cell to detect the invader and rapidly induce a programme of gene expression that leads to the production and dissemination of interferons (IFNs), which convert the host environment into one that is hostile to viruses. The innate immune response relies on an array of pattern recognition receptors that detect microbial metabolic products including the nucleic acids of viruses. These receptors, which include the RNA helicases RIG-I and Mda-5, act as an early warning system in the defence against invasion. They function by transmitting signals to critical protein kinases, including TBK1, which phosphorylate transcription factors such as IRF3/7 and NFκB that bind to specific promoter elements and up-regulate the transcription of anti-viral genes including IFNβ.

Studies on the RNA helicases RIG-I and Mda-5

Despite great recent interest, the molecular mechanism of nucleotide recognition and signalling of RIG-I and Mda-5 is unknown. Hence, we have initiated studies with the aim of producing high-resolution structures primarily using X-ray diffraction methods. Homology mapping predicts RIG-I and Mda5 to be composed of a C-terminal helicase domain. Nucleic acid binding assays demonstrate that the helicase of RIG-I binds with high affinity to single stranded RNA with a five prime tri-phosphate (ssRNA), whilst the helicase of Mda-5 has a greater preference for double-stranded RNA (dsRNA). The helicases of these proteins are coupled to two amino-terminal caspase recruitment (CARD) domains, which are necessary for transmitting the appropriate anti-viral signal via protein-protein interactions with other CARD containing proteins. Several constructs comprising different combinations of the domains (Fig 1, top) have been successfully cloned into pGEX GST-fusion vectors and recombinant protein over-expression has been achieved in *E.coli* (Fig 1, bottom). This has enabled the efficient production of high-levels of pure protein for either full-length protein or specific domains (e.g. ~50 mg from 4L culture for RIGI CARD1/2) using glutathione affinity chromatography. In addition, the use of luciferase reporter technology has demonstrated that the CARD fusion proteins are able to efficiently transduce an anti-viral signal to the IFNβ promoter (data not shown). High-throughput crystallization trials are in progress using the in-house robotic facilities present in the Astbury Centre. It is expected that the first 3D structures of these important proteins will solved in Leeds within the next 12 months.

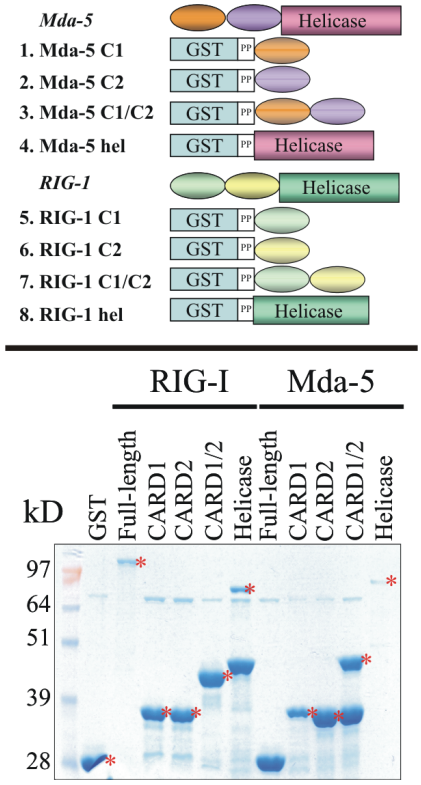

Fig 1. *Top*. Domain organisation of RIG-I and Mda-5 constructs. *Bottom,* Denaturing SDS-PAGE image showing levels of recombinant protein expression in *E.coli*. Expected position of GST-fusion construct is denoted by (*).

Studies on regulators of the innate immune response

Studies from our laboratory have identified the protein optineurin as a critical regulator of the anti-viral response. The mechanism by which optineurin regulates the anti-viral response is currently unknown, although it may require an interaction with the protein kinase TBK1 and upstream signalling proteins that are ubiquitylated. Optineurin is a member of the AHD-family of ubiquitin binding proteins. This family includes the well characterised regulator of NFκB, NEMO. NEMO forms a trimer in response to various stimuli and this higher molecular weight form of the protein is critical for correct functioning. Preliminary experiments have determined that optineurin also forms a higher molecular weight oligomeric structure in response to viral nucleic acids (Fig. 2). Our Royal Society funded studies are analysing the structural and molecular biology of optineurin in greater detail, with the eventual aim of solving the three dimensional structure of this critical mediator of signalling.

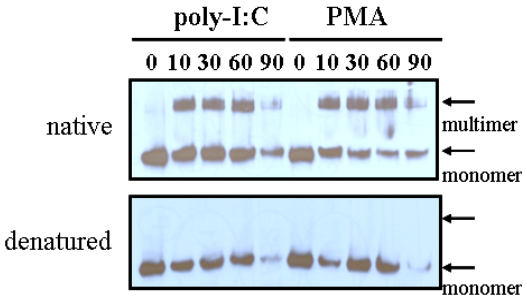

Fig 2. Formation of higher order structures by optineurin. Cells expressing Optineurin were stimulated with the viral dsRNA mimic poly-I:C or treated with the mitogen PMA and lysed at the indicated time-point. Lysates were analysed either by non-denaturing native electrophoresis (top) or by denaturing electrophoresis (bottom).

Publications

Poole, E., Groves, I., Macdonald, A., Pang, Y., Alcami, A. & Sinclair, J. (2009) Identification of TRIM23 as a co-factor involved in the regulation of NFκB by the Human cytomegalovirus gene product UL144. *J. Virol*. *In press.*

Ananieva, O., Macdonald, A**.,** Wang, X., McCoy, C., McIlrath, J., Tournier, C. & Arthur, J.S.C. (2008). ERK5 regulation in naïve T cell activation and survival. *Eur. J. Immunol.* **38**, 2534-47.

Kaiser M., Wiggin, G., Lightfoot, K., Arthur J.S.C., & Macdonald, A. (2007). MSK regulate TCR-induced CREB phosphorylation but not immediate early gene transcription. *Eur. J. Immunol.* **37**, 2583-2595.

McCoy, C.E., Macdonald, A., Morris, N.A., Campbell, D.G., Deak, M., Toth, R., Mcilrath, J. & Arthur, J.S.C. (2007). Identification of novel phosphorylation sites in MSK1 by precursor ion scanning Mass Spectrometry. *Biochem. J.* **402***,* 491-501.

Funding

This work is funded by Research Council UK, Yorkshire Cancer Research, The Royal Society and the University of Leeds.

Aptamers selections and bioinformatics combined extend the AtrA regulon to cell morphogenesis and nutrient uptake

Bart Boomsma, David Cobley, David H. Bunka and Kenneth J. McDowall

In a previous report, we described the identification and characterisation of AtrA, which activates the transcription of *actII*-ORF4, the cluster-situated regulator of the actinorhodin biosynthetic gene cluster in *S. coelicolor*. Subsequent to the publication of this work, we found that overproduction of AtrA promotes morphological development by a mechanism independent of *actII*-ORF4 and the production of actinorhodin. This was the first evidence that AtrA regulates the expression of multiple genes.

Bioinformatic approaches have proven to be powerful tools for the identification of additional binding sites for transcription factors in genomes when the sequences of known sites are available. To obtain multiple sequences recognised by AtrA, we used systematic evolution of ligands by exponential enrichment (SELEX) to produce DNA aptamers. The sequencing of eighteen clones revealed five unique sequences that when aligned produced a consensus resembling the known binding sites in the *actII*-ORF4 promoter.

A WebLogo representation of the consensus sequence derived from AtrA aptamers.

These sequences were then used as part of the PREDetector package to screen the *S. coelicolor* genome. The promoter of *actII*-ORF4 was one of the top hits, thus validating the approach. Another binding site was found upstream of *murC*, which encodes a ligase involved in peptidoglycan biosynthesis. This provides a plausible link to the phenotypic change resulting from AtrA overproduction (see above). Potential sites were also found upstream *murC* orthologues in two other *Streptomyces* species.

Another site was found upstream of *nagE2* and binding confirmed *in vitro* using a gel-shift assay. The product of the *nagE2* gene is a transporter of N-acetylglucosamine, a nutrient inextricably linked to morphological development and antibiotic production. Transcription of the *nagE2* gene is also controlled by DasR, a globally acting repressor that has also been reported to regulate transcription of *actII*-ORF4. The overlapping regulons of AtrA and DasR are being studied in collaboration with the group of Gilles van Wezel, Leiden Institute of Chemistry. A joint research article and invited review are in the process of being submitted.

Collaborators:
Prof. Gilles P. van Wezel (Leiden Institute of Chemistry, The Netherlands)
Prof. Fritz Titgemeyer (Münster University of Applied Sciences, Germany).

Funding
This work was funded by the European Union through the Marie Curie Actions and a BBSRC grant to K. J. M.

A new perspective on the initiation of bacterial mRNA degradation

Louise Kime, Stefanie S. Jourdan, Jonathan A. Stead and Kenneth J. McDowall

In current models of mRNA degradation, the process is initiated by "decapping" to generate a 5'-monophosphate group that stimulates cleavage by RNase E, an endonuclease required for the rapid degradation of many, if not most transcripts in *E. coli*. A key assumption is the commonly held view that RNase E is only able to cleave efficiently those RNAs that have a 5'-monophosphate group. The results presented here show that this is not in fact the case.

In previous reports, we have described the structure and function of the pocket in RNase E and related enzymes that can bind a 5' monophosphate. Last year, we suggested that *E. coli* RNase E was capable of the rapid cleavage of a quadruplexed oligonucleotide lacking a 5'-monophosphate group. We can now report that 5'-biotinylated RNA can also be cleaved rapidly when conjugated to streptavidin prior to incubation with the NTH of RNase E.

RNase E is a tetramer, more precisely a dimer of dimers, and modelling studies have indicated that two RNA-binding channels in a principal dimer could simultaneously contact single-stranded regions in the context of either the quadruplexes or streptavidin conjugates. This raised the possibility that the requirement for the rapid cleavage of substrates that lack a 5'-monophosphate could be as simple as multiple single-stranded regions accessible to RNase E. Michaelis-Menten analysis is consistent with the duplication of contacts increasing the affinity of RNase E for substrates.

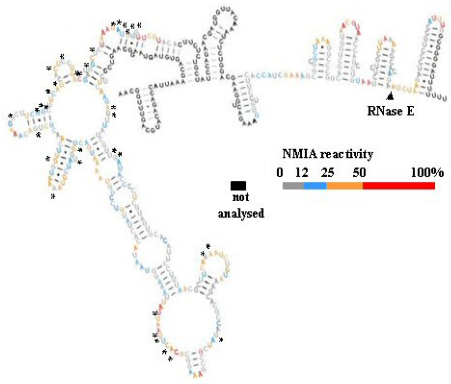

Secondary structure model of *cspA* shown with RNase E recognition sites(*).

Having found that model substrates can be cleaved rapidly by RNase E independent of interaction with a 5'-monophosphate, we extended our analysis to transcripts of *E. coli* and found that *cspA* mRNA can be cleaved rapidly when it has a 5' triphosphate group. We have found similar results for other transcripts including *epd-pgk* mRNA. Moreover, we have probed the structure of *cspA* mRNA using selective acylation of 2'-hydroxyl groups and have confirmed that multiple single-stranded regions are indeed recognised by RNase E.

We propose that the initiation of the decay of many transcripts in *E. coli* is not dependent on "decapping", but rather RNase E cleavages that are facilitated by interaction with multiple single-stranded regions. This model provides a simple explanation for how a change in the rate of translation, as mediated by non-coding RNAs for example, often has an inverse effect on the rate of mRNA turnover. It also explains the recent finding that the decapping enzyme is not essential and only influences the decay of a relatively small proportion of the mRNA pool.

Publications

Jourdan, S.S. & McDowall, K.J. (2008) Sensing of 5'-monophosphate by *Escherichia coli* RNase G can significantly enhance association with RNA and stimulate the decay of functional mRNA transcripts *in vivo*. *Mol. Microbiol*. **67**, 102-115.

Kime, L., Jourdan, S.S. & McDowall, K.J. (2008) Identifying and characterizing substrates of the RNase E/G family of enzymes. *Methods Enzymol.* **447**, 215-41.

McDowall, K.J. (2008) The chemistry, measurement, and modulation of RNA stability. In *Wiley Encyclopedia of Chemical Biology*, Vol 1. Ed. Begley T.P.

Resch, A., Afonyushkin, T., Lombo, T.B., McDowall, K.J., Bläsi, U., Kaberdin, V.R. (2008) Translational activation by the noncoding RNA DsrA involves alternative RNase III processing in the *rpoS* 5'-leader. *RNA*. **14**, 454-9.

Carpousis, A.J., Luisi, B.F., McDowall, K.J. (2009) Endonucleolytic initiation of mRNA decay in *Escherichia coli*. *Prog Nucleic Acid Res Mol Biol*. **85**, 91-135.

Funding
This work was funded by the European Union through the Marie Curie Actions and a BBSRC grant to K. J. M.

Structural and functional studies of oxidases

Mark Smith, Yonca Yuzugullu[¶], Thembi Gaule, Pascale Pirrat, Arwen Pearson,
Didem Sutay[¶], Peter Knowles, Simon Phillips and Mike McPherson

We use structure-based protein engineering and structural tools to dissect the mechanisms of unusual cofactor formation and tuning, oxygen entry routes and catalytic mechanisms of a range of oxidases.

Galactose oxidase: The mechanism of formation of the thioether bond (Tyr272- Cys228) cofactor was studied by kinetic and gel analysis and X-ray crystallography, showing the bond forms autocatalytically even in the absence of oxygen but does not oxidise to a radical state. This may reflect the *in vivo* situation within the Golgi allowing secretion of a processed but inactive enzyme which becomes activated by oxygen once safely in the extracellular environment.

Copper amine oxidase: High pressure xenon has been used to explore the oxygen entry routes to the active site of the *E. coli* enzyme (ECAO). The results of crystallography support studies on other amine oxidases showing defined oxygen pathways. We have studied two peripheral calcium ions by structural, and biochemical studies to explore their role in controlling the proposed oxygen entry routes. In another bacterial amine oxidase we are exploring the ability to produce heterodimers in order to explore the proposal that these enzymes display half-of-site reactivity.

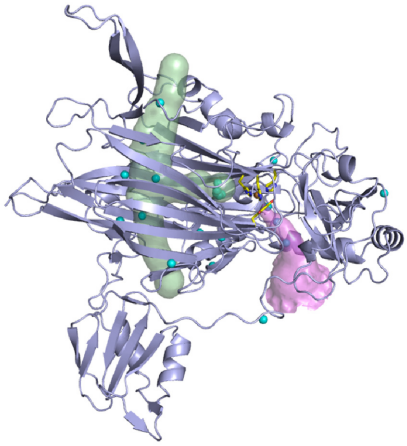

Fig. 2. ECAO monomer with amine entry channel (magenta surface) and putative oxygen entry pathway (green) surface with xenon sites in various AO structures (cyan spheres) and copper (bronze sphere).

Catalase-phenol oxidase: Work involving visiting scientists from METU, Turkey, has focussed on structural, recombinant protein expression and mutagenesis studies on a novel catalase which also displays phenol oxidase activity. This enzyme, from the fungus *Scytalidium thermophilus* has given crystals of the native enzyme which now diffract to ~2.4Å allowing structure determination. Recombinant enzyme and two active site mutants are also being crystallised and characterised.

Collaborators: Galactose oxidase: Prof D.M. Dooley and Dr M. Rogers (Montana) State University. Catalase: visiting scientists to Leeds and Prof. Z. B. Ogel and U. Bakar, Middle East Technical University, Ankara, Turkey.

Funding: This work was supported by funding from BBSRC and the Wellcome Trust.

Publications

Rogers, M., Hurtado-Guerrero, R, Firbank, S J., Halcrow, M.A., Dooley, D.M., Phillips, S.E.V., Knowles, P.F. and McPherson, M.J. (2008) Crosslink formation of the cysteine228-tyrosine272 catalytic cofactor of galactose oxidase does not require dioxygen. *Biochemistry*, **47**, 10428-10439.

Pirrat, P. Smith, M.A., Pearson, A.R., McPherson, M.J. and Phillips, S.E.V. (2008) Structure of the xenon derivative of *E. coli* copper amine oxidase: confirmation of the proposed copper amine oxidase oxygen entry pathway, *Acta Crystallographica F* **64**, 1105-1109.

Kocabas, D.S., Bakir, U., Phillips, S.E.V., McPherson, M.J. and Ogel, Z.B. (2008) Purification, characterization and identification of a novel bifunctional catalase-phenol oxidase from *Scytalidium thermophilum*. *Applied Microbiol. and Biotechnol.*, **79**, 407-415.

Recombinant production of nanostructured self-assembling and therapeutic peptides for tissue engineering

Stuart Kyle, Stephen Parsons, Kier James, Jessica Riley, Eileen Ingham and Mike McPherson

One area of nanomedicine is the development of 3D scaffolds for cell culture. There is current interest in nanostructured self-assembling peptides capable of forming various macroscopic structures such as hydrogels of fibrils and fibres (Fig. 1). Advantages of such materials are biocompatibility, biodegradability and the ability to tailor such 'smart' materials with specific responsive properties by altering the amino acid sequence.

We are developing high yield recombinant production systems for short self-assembling peptides. One family of peptides were rationally designed by the Centre for Self Organising Molecular systems (SOMS). These form β-sheets that hierarchically self-assemble into helical tapes, twisted ribbons (double tapes) fibrils (twisted stacks of ribbons) and fibres (entwined fibrils) with increasing concentration, and/or in response to environmental cues such as pH or temperature.

Our initial studies have focussed on *Escherichia coli* in which yields of 0.6 g/L of peptide have been achieved. We are also exploring yeast and plant expression hosts. A toolkit of fusion proteins, purification tags and cleavage approaches is being developed. A major benefit of biological systems is the ability to generate biofunctionalised peptides of a size that would not be feasible by solid phase synthesis. We characterise the self-assembling properties of the peptides by TEM, AFM, CD and FT-IR. Mammalian cell tissue culture experiments of self-assembling peptide hydrogels as tissue engineering matrices are underway.

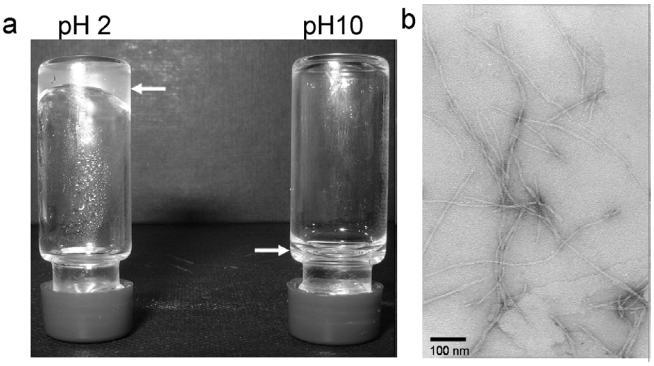

Figure 1. Images of rP11-4(hsl) hydrogel formation. (**a**) A self-supporting hydrogel formed at pH 2 and containing >99% water, adhering to the base of an inverted glass vial while at pH 10 the solution sits at the neck of the vial. The white arrows indicate the locations of the peptide samples. (**b**) TEM analysis of uranyl acetate negative stained samples of pure rP11-4(hsl) showing self assembly of the peptide into semi-rigid fibrils.

Collaborators: Amalia Aggeli, Centre of Self Organising Molecular Systems (SOMS); Rudi Koopmans, Dow Chemicals.

Publications

Riley, J.M., Aggeli, A., Koopmans, R.J. and McPherson, M.J. (2009) Bioproduction and characterisation of a pH responsive self-assembling peptide. Biotechnology and Bioengineering, Published online 22 January 2009 DOI 10.1002/bit.22274

McPherson, M.J., James, K., Kyle, S., Parsons, S., Riley, J. (2009) Recombinant production of self-assembling peptides. Koopmans, R.J. (ed.) In *Engineering aspects of self-organising materials*, *Advances in Chemical Engineering*, **35**, 80-117, Elsevier.

Funding: We acknowledge studentship funding from BBSRC, The Wellcome Trust, Dow Chemical Company and the University of Leeds Institute of Bionanosciences.

Synthesis and chemical biology of natural product-like small molecules

Stephen Bartlett, Jamie Caryl, Christopher Cordier, Teresa Damiano, Adam Nelson, Catherine O'Leary Steele, Alexis Perry, Peter Stockley and Stuart Warriner

Introduction

Synthetic organic chemistry is an immensely powerful tool for chemical biology, which we exploit in a wide range of biological problems. Our publications which were published in 2008 are provided in this report. You may like to browse our website at www.asn.leeds.ac.uk to find out more about what we do!

The synthesis of libraries of diverse natural product-like molecules

Historically, chemists have explored chemical space in an uneven and unsystematic manner: the organic chemistry "universe" is extremely top heavy, with half of molecules in the CAS database being based on just 0.25% of the known molecular scaffolds! A major challenge in chemical biology and medicinal chemistry is to prepare libraries of ligands that populate broad tracts of biologically-relevant chemical space. The development of methods that allow the systematic exploration of such chemical space is a major theme within our research group.

The synthesis of a small molecule library of unprecedented scaffold diversity was described in the 2007 annual report, and this research has recently been published as a VIP article in *Angewandte Chemie*. Our approach has received widespread attention: it was the subject of News & Views articles in *Nature* (Schreiber) and *Nature Chemical Biology* (Waldmann), highlights in *Angewandte Chemie* (Spring) and (on-line) in *Nature Chemistry*, and articles in *Science* and *C&E News*. It was also noted as "Exceptional" by the Biology Faculty of 1000.

More recently, we have described a fluorous-tagged "safety catch" linker which we have applied in the synthesis of skeletally-diverse small molecule libraries. The principles that underpin the design of the linker are outlined in Scheme 1. Crucially, cleavage of both of the bonds that are marked with an arrow (in structure **1**) is necessary for release of products from the linker.

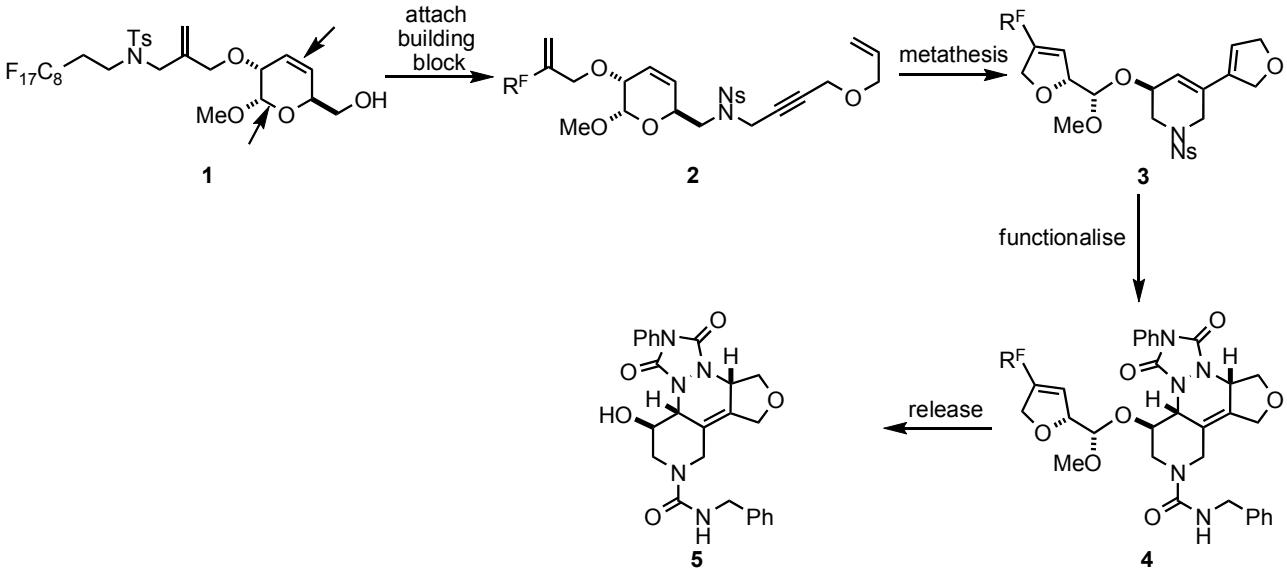

Scheme 1: A fluorous-tagged 'safety catch' linker for preparing skeletally-diverse small molecule libraries. Cleavage of both bonds marked with an arrow is necessary for release from the linker 1.

To start, a building block is attached to the linker **1** (e.g. to give **2**). A metathesis cascade process then leads to cleavage of the cyclic alkene in the linker (e.g. **2** → **3**). Further

functionalisation is possible at this stage (e.g. **3** → **4**). Finally, acid-catalysed acetal hydrolysis leads to release from the linker (→ **5**). Crucially, the design of the linker means that (a) fluorous–solid phase extraction alone is needed to purify the intermediates in the synthesis, and (b) only metathesis products are ever released from the fluorous tag.

Applications of chemical probes of biological systems

We have also reported some novel chemical tools that may be used to interrogate biological systems. We have used the SAM analogue **6** to modulate the function of the *E. coli* methionine repressor, MetJ. The strained cyclooctyne ring of **6** is a "bioorthogonal" tag which may allow the compound to be used as a tool in the purification and analysis of other SAM-binding proteins.

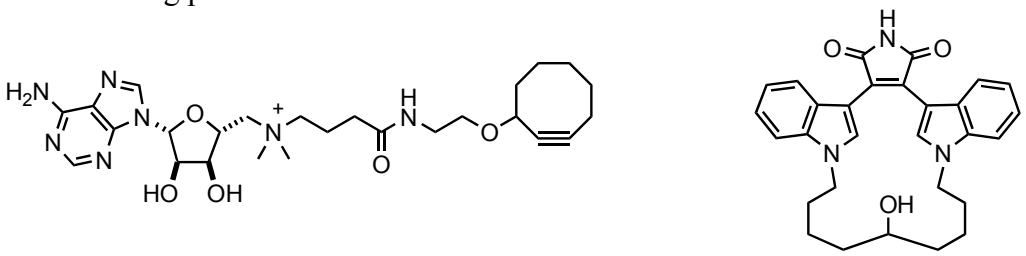

6 **7**

Scheme 2: Some novel probe molecules reported by the Nelson group in 2008.

In addition, the bisindolylmaleimide **7** is an example of a potent inhibitor of glycogen synthase kinase (GSK) 3. In collaboration with Prof. Melanie Welham, University of Bath, we have used such molecules to understand the role of GSK-3 in promoting the self-renewal of murine embryonic stem cells.

Acknowledgements

ASN holds an EPSRC Advanced Research Fellowship to support his research at the biology/chemistry interface. We thank EPSRC, BBSRC, the Wellcome Trust and GSK for funding.

Collaborators

We also thank our collaborators from outside the Astbury Centre. The research into GSK-3 function was undertaken in collaboration with Heather Bone, Julie Letchford and Melanie Welham from the Department of Pharmacy and Phamacology, University of Bath.

Publications

Bolt, A., Berry, A. and Nelson, A. (2008) Directed evolution of aldolases for exploitation in synthetic organic chemistry, *Arch. Biochem. Biophys*. **474**, 318-330.

Leach, S.G., Cordier, C.J., Morton, D., McKiernan, G.J., Warriner, S.L. and Nelson, A. (2008) A fluorous-tagged linker from which small molecules are released by ring-closing metathesis, *J. Org. Chem.* **73**, 2752-2759.

Cordier, C., Morton, D., Murrison, S., Nelson, A. and O'Leary-Steele, C. (2008) Natural products as an inspiration in the diversity-oriented synthesis of bioactive compound libraries, *Nat. Prod. Rep.* 2008, 719-737.

Cordier, C., Morton, D., Leach, S., Woodhall, T., O'Leary-Steele, C., Warriner, S.L. and Nelson, A. (2008) An efficient method for synthesising unsymmetrical silaketals: substrates for ring-closing, including macrocycle-closing, metathesis, *Org. Biomol. Chem.* **6**, 1734-1737.

Horn, J., Marsden, S., Nelson, A., House, D. and Weingarten, G. (2008) Convergent, regiospecific synthesis of quinolines from *o*-aminophenylboronates *Org. Lett.* 2008, 4117-4120.

Joce, C., Caryl, J., Stockley, P.G., Warriner, S.L. and Nelson, A. (2009) Identification of stable *S*-adenosylmethionine (SAM) analogues derivatised with bioorthogonal tags: Effect of ligands on the affinity of the *E. coli* methionine repressor, MetJ, for its operator DNA, *Org. Biomol. Chem.* **7**, 635-638.

Bone, H.K., Damiano, T., Bartlett, S., Perry, A., Letchford, J., Nelson, A. and Welham, M.J. (2009) Involvement of glycogen synthase kinase-3 in regulation of murine embryonic stem cell self-renewal revealed by a series of bisindolylmaleimides", *Chem. Biol.* **16**, 15-27. *The research has been featured by the London Evening Standard and (on-line) by the Daily Telegraph. This paper was highlighted in a preview in Cell Stem Cell (Cell Stem Cell 2009, 4, 98-100).*

Morton, D., Leach, S., Cordier, C., Warriner, S.L. and Nelson, A. (2009) Synthesis of natural product-like molecules with over eighty distinct skeletons, *Angew. Chem., Int. Ed.* **47**, 104-109. *This paper has been featured in News and Views articles in Nature (S. Schreiber, Nature 2009, 457, 153-154) and Nature Chemical Biology (H. Waldmann, Nature Chem. Biol. 2009, 5, 76-77) and in a Highlight in Angewandte Chemie (D. Spring et al, Angew. Chemie. Int. Ed. 2009, 47, 1194-1196). In addition, the paper was selected by the editors of Science as a highlight of the recent literature (Science 2009, 323, 16) and was a research highlight in Chemical and Engineering News and Nature Chemistry. The paper highlighted for its "Exceptional" interest by the Biology Faculty of 1000.*

Murrison, S., Glowacki, D., Einzinger, C., Titchmarsh, J., Bartlett, S., McKeever-Abbas, B., Warriner, S.L. and Nelson, A. (2009) Remarkably slow rotation about a single bond between an sp^3-hybridised carbon and an aromatic ring without *ortho* substituents, *Chem. Eur. J.* **15**, 2185-2189.

O'Leary-Steele, C., Cordier, C., Hayes, J., Warriner, S.L. and Nelson, A. (2009) A fluorous-tagged 'safety catch' linker for preparing heterocycles by ring-closing metathesis, *Org. Lett.* **11**, 915-918.

Free-energy surfaces of proteins from reversible folding simulations

Lucy Allen, Sergei Krivov and Emanuele Paci

λ -repressor is a five helix bundle protein which has been extensively studied experimentally, and found to be a very fast, two state folder. We have used a recently developed method for analysing equilibrium trajectories, developed by Krivov *et al*., to study in detail the folding behaviour of a coarse-grained, structure-based model of the protein. The analysis, which provides an unprojected representation of the energy landscape, reveals complexity in the folding process which is hidden by traditional geometric analyses. The accuracy of structure-based models for describing the behaviour of real proteins has been widely debated. Nevertheless, they do predict features which are believed to be characteristic of the folding landscapes of real proteins, such as the presence of intermediates and downhill folding. Thus, whilst the results of our simulations do not necessarily reflect the true folding behaviour of λ -repressor, they are undoubtedly useful for understanding the general features of landscapes.

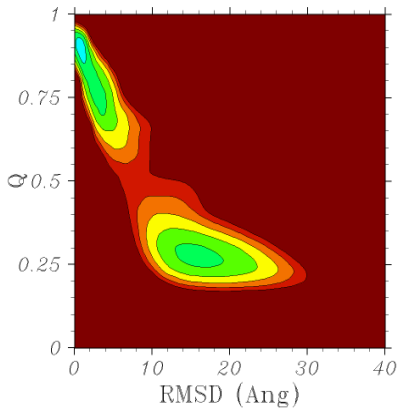

Figure 1: Equilibrium trajectory of λ-repressor model, projected onto geometric coordinates

Fig. 1 shows a projection of a 30μs trajectory of the λ-repressor model at its melting temperature, in which over 600 folding events are observed, onto a plane defined by two geometric reaction coordinates, the fraction of native contacts (Q) and the root mean square distance from the experimental native structure (RMSD). Folding appears to be two-state, with a barrier of around 4 k_BT.

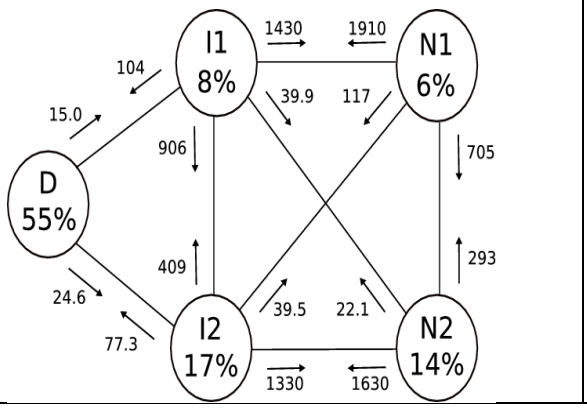

Figure 2: Simplified equilibrium kinetic network for λ-repressor model. States are represented as circles: five are present, two native (N1 and N2), two intermediate (I1 and I2) and denatured (D). The relative populations of the states are shown within the circles. Transitions between states are shown as arrows, with the rates of exchange in μs^{-1} also displayed.

The more detailed, unprojected analysis, however, reveals greater complexity. Fig. 2 shows the simplified equilibrium kinetic network for the trajectory. An obligatory intermediate, which was hidden in the geometric projection, is present, and both the native and intermediate states are divided into two substates, leading to two parallel major folding pathways, D→I1→N1 and D→I2→N2.

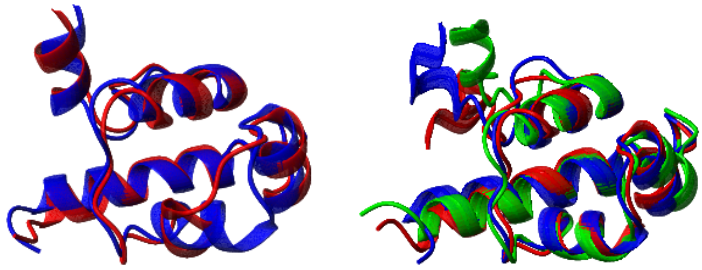

Figure 3: Representative structures of the native substates (left), and intermediate states (right).

A structural analysis of the different states reveals small differences between the intermediate and native states. In the intermediate states (shown in Fig. 2), helices 1-4 are formed and natively docked, but helix 5 is only partially formed and is detached from the rest of the protein. The differences between the intermediate and native sub-states are even more subtle, and are localised to the loop region between helices 2 and 3, which is more flexible in state N2 (Fig. 2, right-hand panel).

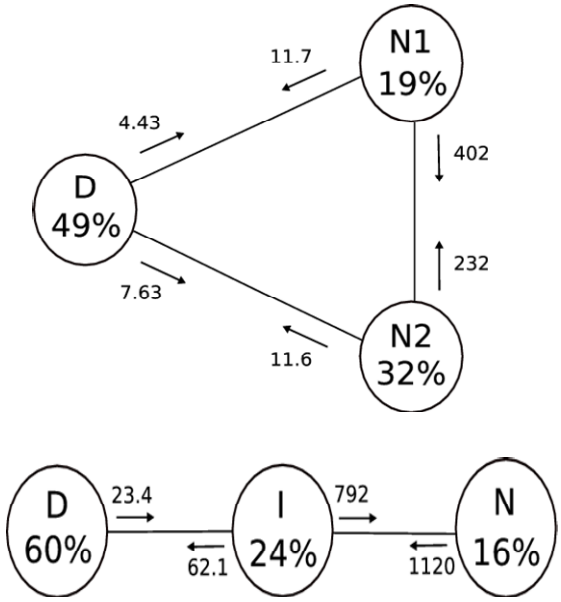

Figure 4: simplified equilibrium kinetic networks for the two modified proteins. One mutant no longer populates an intermediate state (top), the other folds via a single pathway (bottom).

Using this information about the individual states, we have been able to modify individual interactions to perturb the energy landscape. By strengthening three interactions between helix 4 and 5, we destabilized the intermediate states so they were not populated during folding. As a result, the modified protein folded 3 times slower than the wild type, indicating that, in this case, the intermediate plays an important, accelerating role in folding. We also designed another mutant in which two interactions were introduced in the helix 2-3 loop region: this had the effect of depopulating the N1 and I1 states so that folding occurs via a single pathway. Again, this modification slowed folding, this time by a factor of 2, suggesting that parallel pathways may also play an important role in fast-folding.

It is well known that experimental probes of protein folding are often localised and therefore may not be sensitive to structural changes in distant parts of the protein. This work shows that an analogous problem exists in simulation: the projection of reversible trajectories onto geometric reaction coordinates can hide important features of the folding pathway. Such features can, however, be uncovered by a more detailed analysis such as the unprojected representation used here. This detailed analysis reveals important characteristics of the folding landscape of a structure-based model of a fast-folding protein which help to explain how it folds so quickly.

Funding
This work was funded by the EPSRC.

Exploring the energy landscape of proteins using mechanical forces: simulations and theory

Zu Thur Yew, Sergei Krivov and Emanuele Paci

Introduction

The mechanical properties of proteins can be probed by pulling two residues (e.g., the *N* and *C*-termini) and measuring the unfolding force or equivalently, the unfolding time. These experiments have not only been instrumental in furthering our understanding of the determinants of mechanical resistance, but also given us insights into the energy landscapes of proteins.

The interpretation of mechanical unfolding experiments however, relies on two main assumptions:

(i) The free-energy difference between any two states is a linear function of the applied force.

(ii) The distance between the two residues being pulled apart is a good reaction coordinate; i.e., this distance can uniquely "identify" *all* the states along the unfolding pathway.

Using molecular dynamics simulations of a coarse-grain model of a protein (one bead per residue), we investigated the validity of the above assumptions.

The Hammond effect in forced unfolding

Even when unfolding pathways are qualitatively similar at *all* forces, the specifics of the energy landscape such as the "locations" (along some reaction coordinate) of the minima or transition states are expected to change if the applied force is significantly larger than zero. Yet, mechanical unfolding experiments are usually analysed with a model due to Bell: $\Delta G(F) = \Delta G(0) - Fx_u$ where x_u is the difference in the extensions of the transition and native states, and is assumed to be *independent* of the applied force.

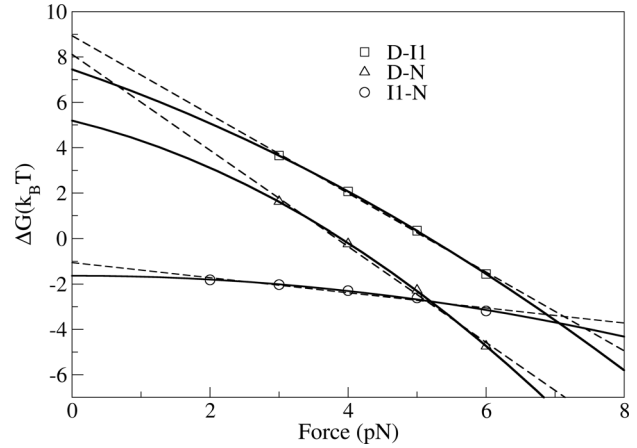

Figure 1: Free-energy differences between pairs of states as a function of the applied force. The dashed lines represent fits of the data to the Bell model while the solid lines are fits to the Hammond corrected model.

The simplicity of the protein model allowed us to simulate to convergence and hence, accurately compute the free-energies between various states (i.e., N, I1 and D) as a function of the applied force (Fig. 1). It is clear that $\Delta G(F)$ for any pair of states is not linear in the applied force (Fig. 1, dashed line). If Bell's model is supplemented by a correction term that takes into consideration the movement of the transition state (the Hammond effect), the curvature in $\Delta G(F)$ can be fully accounted for (Fig. 1, solid line). That x_u can change significantly, even in a small range of forces (0-6 pN), suggests that the parameters extracted from Bell's model are likely to be quite different from the true values at zero force. Indeed, the parameters should instead be interpreted as that of the system in a narrow range of forces; that is, the range of forces that was applied in the experiment.

The free-energy landscape under force is "multi-dimensional"

We determined the free-energy landscape of our simplified protein model using a method that clusters conformations into "states" based on the dynamical behaviour of the conformations rather than geometrical properties such as the RMSD. The output of the analysis is a description of the free-energy landscape as a network of states (EKN) as shown in Fig. 2.

It is immediately apparent from the EKN that the free-energy landscape evolves in a complex fashion as the applied force is increased. The force not only induces the appearance of a "new state", I2, but also parallel pathways between pairs of states that are otherwise inaccessible in the absence of a force.

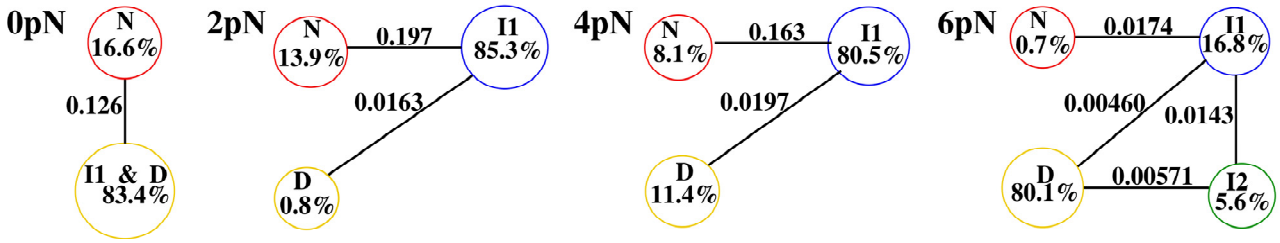

Figure 2. Equilibrium network of states (EKN) in the presence of applied force. The numbers in the circles represent the populations of the states while those on the lines are the rates of transition between states (ns^{-1}).

Such changes (e.g., the appearance of parallel pathways) cannot be predicted or captured by 1D free-energy profiles defined along variables like the extension.

Intriguingly, the EKN suggests that rate of unfolding is not solely determined by the height of the unfolding barrier - an intrinsically 1D notion - but also by the loss or gain in unfolding pathways at different forces. In this regard, preliminary results on the same system have indicated that the number and nature of the unfolding pathways change depending on the magnitude of the applied force (data not shown). These results also suggest that if the unfolding kinetics of a protein is measured in a broad range of forces (e.g., 5-200 pN), it is then possible to at least identify the "architecture" of the EKN and its associated parameters.

Acknowledgements

This work was funded by the EPSRC, INTAS, and the Wellcome Trust. Discussions with Edward Causton, Peter Olmsted and David Brockwell are gratefully acknowledged.

Publications

Yew, Z.T., Krivov, S. & Paci, E. (2008) Free-Energy landscapes of proteins in the presence and absence of force. *J. Phys. Chem. B* **112**, 16902–16907

Expression, purification and activities of the entire family of membrane sensor kinases of *Enterococcus faecalis* and studies of quorum sensor FsrC and essential sensor VicK

Pikyee Ma, Hayley M. Yuille, Victor Blessie, Nadine Göhring, Zsófia Iglói,
Peter J. F. Henderson and Mary K. Phillips-Jones

Introduction

Two-component signal transduction systems are the main mechanism by which bacteria sense and respond to their environment, and their membrane-located histidine protein kinases generally constitute the sensory components of these systems. Relatively little is known about their fundamental mechanisms, three-dimensional structures and even the precise nature of the molecular signals sensed, because of the technical challenges of producing sufficient quantities of these hydrophobic membrane proteins. However, previous work by our group established that these challenges can be overcome. To determine how widely applicable our approach with such proteins might be, and to learn more about the roles of such kinases in processes such as virulence and quorum sensing, we evaluated the successes of expressing in *E. coli* and purifying the entire genome complement of membrane sensor kinases of *Enterococcus faecalis*, an important agent of hospital-acquired infection in the UK, and undertook detailed studies of two of these proteins, VicK and FsrC, that have known functions.

Results.

All but one of the 16 intact membrane sensor kinases was expressed successfully in *E. coli* inner membranes and purification of the hexa-histidine 'tagged' recombinant proteins was achieved for thirteen of the intact kinases. Thirteen intact kinases possessed autophosphorylation activity in the absence of added signal when assayed in membrane vesicles or as purified proteins (examples shown in Fig. 1). Signal testing using two of the functionally-characterised kinases of this bacterium, VicK and FsrC, was successful in confirming known or putative signals for these sensors. Glutathione and possibly redox potential were direct modulators of VicK activity *in vitro*, and the activity of quorum sensor FsrC was strongly activated in response to its pheromone signal GBAP (Fig. 2), confirming the use of such an *in vitro* approach to identify signals for these proteins. Further work is now in progress to identify signals and inhibitors for all the sensor kinases of this bacterium.

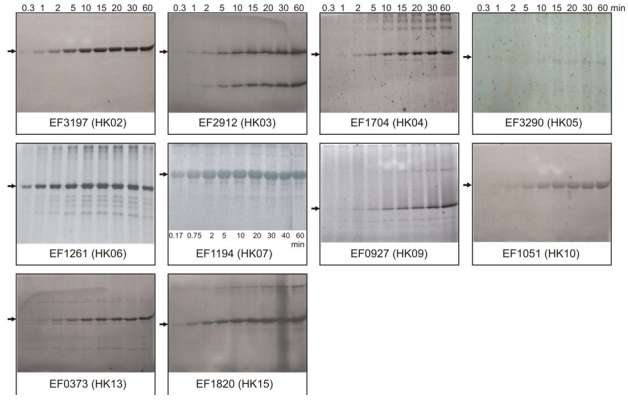

Fig. 1. Autophosphorylation activities of purified *E. faecalis* sensor kinases in the absence of known signal

Collaborators

Professors Peter Henderson and Simon Phillips at Leeds, Professor Jiro Nakayama in Japan, Professor Anna-Brit Kolsto in Oslo, Professor Mike Williamson in Sheffield, Professor Richard Neutze in Goteborg and Professor Mike Peck at the Food Research Institute in Norwich.

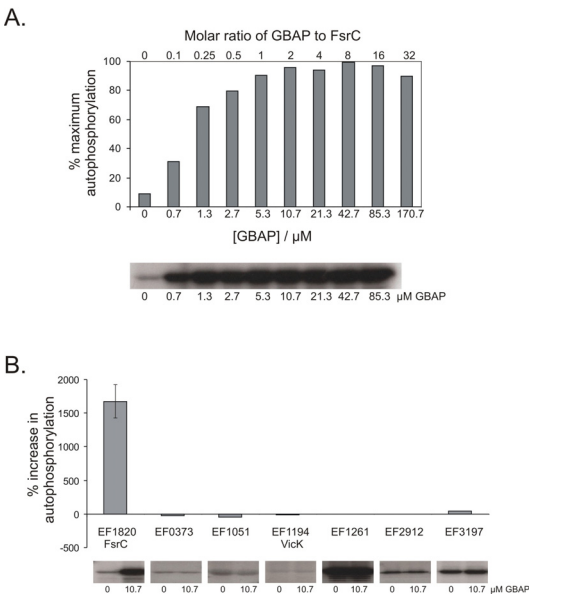

Fig. 2. Specific increases in FsrC autophosphorylation activity in response to its pheromone signals GBAP

Publications

Trinh, C.H., Liu, Y., Phillips, S.E.V. & Phillips-Jones, M.K. (2007) Structure of the response regulator VicR DNA-binding domain. *Acta Crystallog. Sect. D*. **63,** 266-269.

Moody, R.G., Phillips-Jones, M.K. and Williamson, M.P. (2007) NMR assignment of the *Rhodobacter sphaeroides* fasciclin-1 domain protein (Fdp). *Biomol NMR Assign.* **1,** 11-12.

Henderson, P., Szakonyi, G., Leng, D., Ma, P., Blessie, V., Yuille, H.M. & Phillips-Jones, M.K. (2007) Bacterial membrane drug efflux and receptor proteins. *Drugs of the future* **32A**, 6-6.

Ma, P., Yuille, H.M., Blessie, V., Göhring, N., Iglói, Z, Nishiguchi, K., Nakayama, J., Henderson, P.J.F. & Phillips-Jones, M.K. (2008) Expression, purification and activities of the entire family of intact membrane sensor kinases from *Enterococcus faecalis. Mol. Membr. Biol.* **25,** 449-473.

Funding

This work was funded by the BBSRC and the European Membrane Protein consortium, EMeP

Systematic analysis of the self-assembly mechanism of β_2-microglobulin into amyloid fibrils

Wei-Feng Xue, Timo Eichner, Andrew L. Hellewell, John P. Hodkinson, Carol L. Ladner, Eva Petrik, Geoffrey W. Platt, Katy E. Routledge, David P. Smith, Ricardo J. L. Tomé, Nathalie Valette, Lucy Woods and Sheena E. Radford

Introduction

Many neuro-degenerative and age-related diseases are associated with the formation of protein aggregates known as amyloid. Despite an increasing number of proteins and peptides being recognised as amyloidogenic, the molecular mechanisms of amyloid formation remain elusive. In particular, the distribution of species formed during different stages of assembly, the structural properties of populated oligomeric species and the nature of the fibril product itself remain unclear. Because the understanding of how amyloid self-assembly occurs is of paramount importance for a molecular interpretation of amyloidosis and for the rational development of therapies against amyloid disease, we have recently characterised the assembly mechanism of β_2-microglobulin (β_2m) into long-straight (LS) amyloid-like fibrils *in vitro* in detail. Using a novel systematic modelling approach, we demonstrated that an assembly mechanism *via* monomer addition through a hexameric structural nucleus is most consistent with all available experimental data. Equally interestingly, fragmentation was revealed as the dominating secondary process accelerating fibril assembly. We are now working to shed light on the effects of agitation-promoted fragmentation on the physical and biological properties of β_2m LS fibrils using tapping mode atomic force microscopy (TM-AFM) and statistical single particle image analysis.

Systematic analysis of nucleation-dependent polymerisation

To dissect the assembly mechanism of β_2m-LS fibrillogenesis in the context of the kinetic, thermodynamic and structural aspects of its nucleated assembly mechanism, we have developed a new experimental and theoretical approach for the analysis of the mechanism of amyloid fibril formation. Using this novel systematic approach, a large number of possible models for assembly was tested (Fig. 1), allowing us to conclude that an assembly model involving monomer addition through a hexameric structural nucleus (hexameric thermodynamic nucleus under concentrations employed) with fragmentation as a secondary process is most consistent with all of the available experimental data.

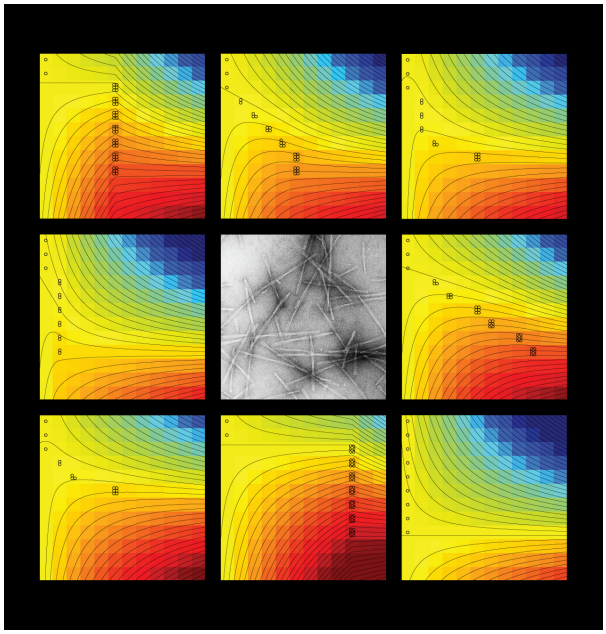

Figure 1: Systematic analysis of the nucleated assembly mechanism of β_2m fibrils. Using a flexible modular modelling approach, many different possible assembly mechanisms were tested against experimental data of the concentration-dependence of the rates of β_2m fibril assembly. Depicted are illustrations of several of the different assembly free energy profiles tested (coloured from red representing positive unfavourable, to blue representing favourable free energy changes) as function of protein concentration (y-axis) and oligomer size (x-axis from monomer to the left to 12-mer to the right). An EM image of the final fibril product is shown in the centre (1x1 μm). The highest free energy species as function of concentration are illustrated using circles.

From this study, we were able to provide new information about the nature of nucleated amyloid assembly mechanisms and the secondary processes that accelerate fibril formation. The method also enables the prediction of the presence of oligomeric species populated during the lag phase of assembly that is consistent with independently performed experiments using mass spectrometry and analytical ultracentrifugation. Efforts are now focused on the impact of fibril fragmentation on the observed rates of fibril growth, the nature of oligomeric species populated and their roles in fibril assembly under physiological conditions.

Effects of fragmentation on the rates of fibril formation

Following up on the observation that fibril fragmentation is a key secondary process that accelerates fibril growth, the ability to fragment fibrils may present a significant process in hastening the onset of amyloid diseases *in vivo*. To understand this important process, we have created fibril samples under carefully controlled mechanical conditions provided by a precision stirrer custom built by the workshop of School of Physics and Astronomy. We are currently developing TM-AFM single-particle image analysis methods, including automated fibril recognition software programme (Fig. 2) that enables analysis of a large number of individual fibrils, to quantitatively characterise the changes in the length distribution and other properties of fibrils upon fragmentation.

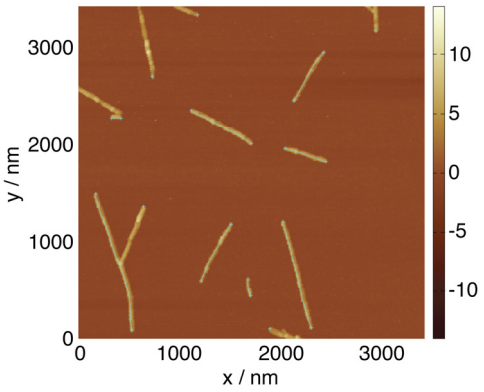

Figure 2: Typical TM-AFM image data of LS fibrils of β_2m processed by automated single particle analysis software developed in house. The colour bar represents height (in nm). Fibril ends and fibril contours are automatically determined by the software programme are represented by cyan + symbols and lines, respectively.

Collaborators

This project was performed in collaboration with Alison Ashcroft, Eric Hewitt, Steve Homans and Stuart Warriner of the Astbury Centre for Structural Molecular Biology.

Publications

Jahn, T.R. & Radford, S.E. (2008) Folding *versus* aggregation: Polypeptide conformations on competing pathways. *Archives in Biophys and Biochem.* **469**, 100-117.

Jahn, T.R., Tennent, G.A &. Radford, S.E. (2008) A common β-sheet architecture underlies *in vitro* and *in vivo* β_2-microglobulin amyloid fibrils. *J. Biol. Chem.* 283, 17279-17286

Platt, G.W., Routledge, K.E., Homans, S.W. & Radford, S.E. (2008) Fibril growth kinetics reveal a region of β_2-microglobulin important for nucleation and elongation of aggregation. *J. Mol. Biol.* **378**, 251-263.

Xue, W.-F., Homans, S.W., Radford, S.E. (2008) Systematic analysis of nucleation-dependent polymerisation reveals new insights into the mechanism of amyloid self-assembly. *Proc. Natl. Acad. Sciences. USA.* **105**, 8926– 8931.

Funding

We are grateful to the University of Leeds, BBSRC and The Wellcome Trust for financial support. We thank Keith Ainley for technical assistance.

Elucidating a generic mechanism of β_2-microglobulin amyloid assembly at neutral pH

Timo Eichner, Andrew Hellewell, John P. Hodkinson, Carol L. Ladner, Eva Petrik, Geoffrey W. Platt, Katy E. Routledge, David P. Smith, Ricardo, J. L. Tomé, Nathalie Valette, Lucy Woods, Wei-Feng Xue and Sheena E. Radford

Introduction

Although numerous measurements of amyloid assembly of different proteins under distinct conditions *in vitro* have been performed, the molecular mechanisms underlying the specific self-association of proteins into amyloid fibrils remain obscure. Elucidating the nature of the events that initiate amyloid formation remains a particularly difficult challenge because of the heterogeneity and transient nature of the species involved. Here we have used site-directed mutagenesis to create five proline to glycine variants in the naturally amyloidogenic protein β_2-microglobulin (β_2m). One of these variants, P5G, populates the native state and a non-native species containing a *trans* P32 backbone conformation in equal proportion at pH 7.5 at equilibrium. By exploiting the slow interconversion of these species and varying the protein concentration and temperature we show that the non-native species is able to assemble into amyloid fibrils spontaneously at neutral pH in the absence of seeds. Comparison of these results with amyloid formation of the wild-type protein in the presence of Cu^{2+} ions and of the species ΔN6, a variant of β_2m found in *ex vivo* amyloid deposits and known to have enhanced amyloid potential, using similar approaches leads us to propose a generic mechanism for β_2m amyloid assembly consistent with the wide range of studies of this protein published to date. Crucially, all of these studies are linked by the switch of the native *cis* P32 to a *trans* isomer, forming a non-native and aggregation-prone monomeric intermediate, the population of which is controlled by the amino acid sequence proximal to P32 and the solution conditions.

The non-native state I_T is a common precursor of amyloid assembly

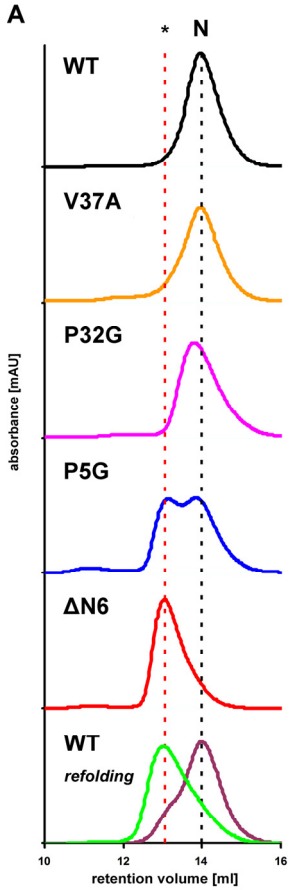

Figure 1: Analytical SEC traces (obtained at 5°C in 100 mM Tris HCl pH 8.0) of 80 μM wild-type β_2m (black), V37A (orange), P32G (pink), P5G (blue) and ΔN6 (red) after incubation overnight at pH 7.5, 25 mM sodium phosphate, 37°C. 'WT *refolding*' denotes the elution profile of wild-type β_2m refolded on ice and analysed by SEC (at 5°C) either 2 min (4°C) after dilution (green) or after incubation for 10 min at 37°C (plum). The vertical dotted lines indicate the retention volume of native wild-type β_2m (~14 ml) (black, N) or of ΔN6 (~13 ml) (red, *).

Fig. 1 shows the size-exclusion chromatograms of wild-type β_2m and the variants V37A, P32G, P5G and ΔN6 at a concentration of 100 μM following their incubation overnight at pH 7.5, 37°C. The elution profiles show that the wild-type protein and V37A elute as a single, sharp peak while the variant P5G elutes as two major components indicating that a non-native species (labelled *) is co-populated with the native state under the conditions employed. By contrast with the behaviour of P5G and wild-type β_2m, ΔN6 elutes as a single peak with a retention volume similar to that of the non-native P5G species. This suggests that the species eluting with native P5G is a non-native conformer in slow equilibrium with the native state. Consistent with this, wild-type β_2m denatured in 8 M urea and refolded by 8-fold dilution of the denaturant at pH 7.5, 4°C traps the folding intermediate I_T for sufficient time to allow its fractionation

by SEC and reveals a single peak that elutes at the same volume as ΔN6. Incubation for longer times, results in the formation of the native state *via trans-cis* proline isomerisation and a peak on SEC that elutes subsequent to the early folding intermediate (Fig. 1). The species giving rise to the two peaks in P5G, therefore, are consistent with native and non-native conformers of the protein that are in slow equilibrium, presumably rate-limited by the isomerisation of P32.

NMR techniques give rise to the structure of the amyloidogenic intermediate

To confirm the analytical SEC data on a structural level ^{1}H-^{15}N correlation (HSQC) spectra at pH 7.5, 25°C from wild-type β_2m (black), ΔN6 (red), P32G (magenta) and P5G (blue) were recorded (Fig. 2A). The spectra reveal small, but significant, chemical shift differences between the different species resolved by SEC (Fig. 2A), with the spectrum of P5G displaying doubling of several resonances, consistent with the view that P5G populates the native and I_T state to similar proportions at equilibrium under the conditions applied. Observed differences in chemical shift between wild-type β_2m and ΔN6 indicate that the non-native intermediate I_T exhibits a native-like structure, but with some reorganisation compared with the wild-type protein. Intriguingly, judging the peak intensities of the amide bond vectors of 69E indicates that P5G does not only resemble the structure of wild-type β_2m and ΔN6 but also very precisely their intermediate backbone dynamics. Further work is focussed on elucidation of the structure of ΔN6, so that its enhanced amyloid propensity relative to the wild-type proteins may be understood in molecular detail.

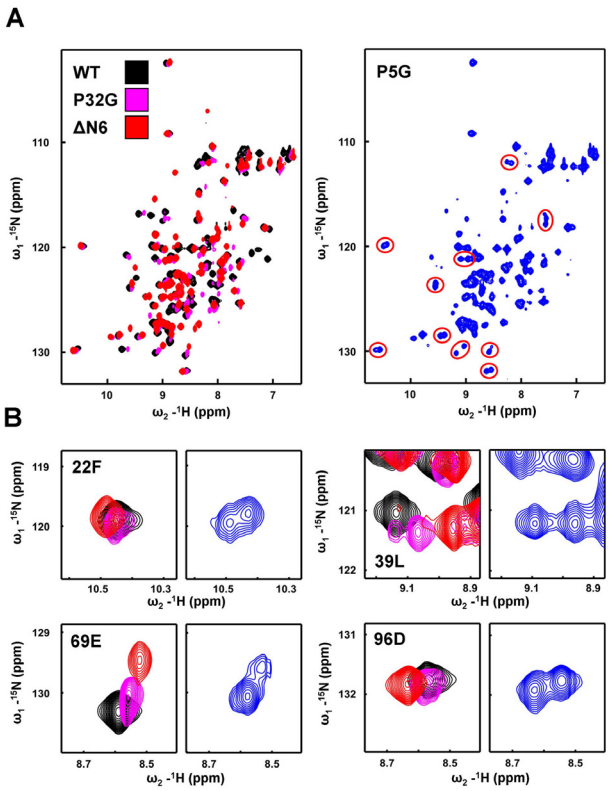

Figure 2: NMR ^{15}N-HSQC experiments of wild-type β_2m, P5G, P32G and ΔN6 at pH 7.5, 25°C. (A) 500 µM wild-type β_2m (black), 500uM P32G (pink) 500 µM ΔN6 (red) and 1 mM P5G (blue). (B) Zoom in: peaks represent the amid bond vectors of 22F, 39L, 69E and 96D.

Collaborators

This project was performed in collaboration with Steve Homans, Arnout Kalverda and Gary Thompson of the Astbury Centre for Structural Molecular Biology.

Publications

Eichner, T. & Radford, S.E. (2009) A generic mechanism of β_2-microglobulin amyloid assembly at neutral pH involving a specific proline switch. *J. Mol. Biol.* **105**, 8926-31.

Funding

We are grateful to the University of Leeds and The Wellcome Trust for financial support. We thank Keith Ainley for technical support.

Exploring the folding energy landscape for immunity proteins Im7 and Im9

Alice I. Bartlett, Claire T. Friel, Gareth J. Morgan, Clare L. Pashley and Sheena E. Radford

Introduction

Elucidating the role of a protein's primary amino acid sequence in controlling the search for the native conformation is of fundamental importance. Progress towards this goal requires the structural and energetic characterisation of all species encountered on the folding energy landscape. The transient and heterogeneous nature of the species populated early in folding makes them difficult to characterise. By using a range of biophysical approaches it is possible to obtain detailed information about the properties of these species. In particular, kinetic methods are crucial for obtaining information on transition state ensembles. In combination with computational simulations data from biophysical experiments can be used to create atomistic models of transition state and intermediate state ensembles.

We are investigating the folding landscapes of the colicin immunity proteins, Im7 and Im9. We have previously shown that these four-helical proteins fold to their native states *via* distinct kinetic mechanisms at neutral pH: Im7 transiently populates a compact, on-pathway intermediate (Fig. 1), while Im9 does not. The folding intermediate of Im7 is composed of three of its four native helices, docked in a non-native manner and stabilised by both native and non-native interactions.

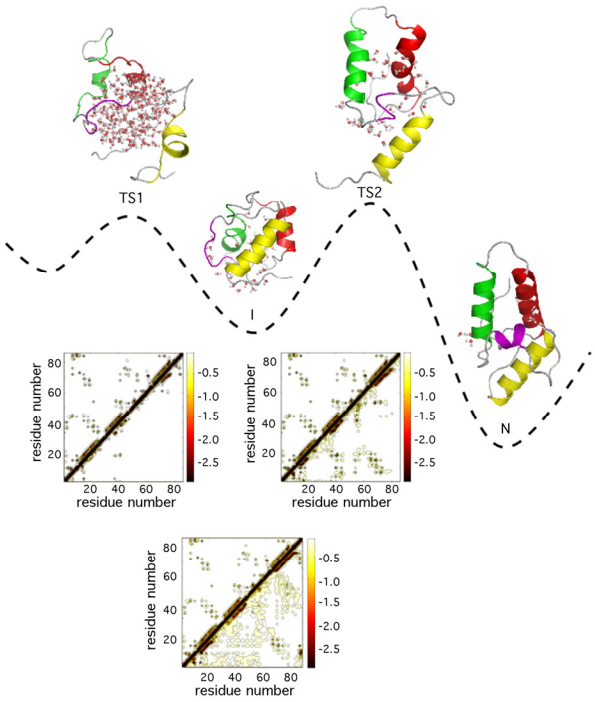

Figure 1: Schematic of the folding landscape of Im7. Ribbon diagram representations of selected cluster centres of TS1, I, TS2 and N are shown. The native helices are coloured red (helix I), green (helix II), purple (helix III) and yellow (helix IV). Water molecules within a 12Å sphere around the centre of masses of TS1, I, TS2 and N are shown. The average interaction energy maps of TS1, I and TS2 (below the diagonal) are compared with that of N (above the diagonal). The scale on the right is in kcal/mol.

Characterisation of the first transition state ensemble

When refolding of Im7 is initiated, the protein populates its intermediate state within the first millisecond of the reaction. By combining ultra-rapid mixing with stopped-flow fluorescence measurements of wild-type Im7 and 16 variants we were able to determine Φ-values for first transition state (TS1 in Fig. 1), as well as the intermediate (I) and rate-limiting transition state (TS2). These Φ-values were then used in restrained MD simulations to provide an all-atom description of the entire Im7 folding landscape (see Fig. 1). The transition state for formation of the intermediate is an expanded species (β_T = 0.2) predominantly stabilised by long-range contacts between residues that form helices I and II in the native structure. These interactions are not sufficient to establish the native topology of Im7. Further collapse and mispacking of hydrophobic residues occurs as the intermediate forms, establishing a native-like topology in

which helices I, II and IV pack together. Non-native interactions in the intermediate species occlude the site which allows helix III to dock onto the developing structure. Reorganisation of these non-native interactions forms the rate-limiting step in Im7 folding. Analysis of the contributions of native and non-native interactions at different stages of folding demonstrates that the Im7 sequence is not optimized for efficient folding. Rather it appears that the folding landscape of this small protein is the result of comprise between evolutionary pressures for function (colicin binding) and folding efficiency.

Current work

Urea-denatured Im7 has been shown to contain transient residual structure, with clusters of interacting hydrophobic side-chains being observed in the regions corresponding to native helices. In more recent work, a number of Im7 variants that significantly populate the denatured state under non-denaturing conditions have been created, with a view to gaining further insights into the dynamics of the unfolded chain, and how this may impact on subsequent events in folding. Biophysical characterisation of the properties of these variants is on-going. Current kinetic studies of Im7 folding have focused on examining hydrophobic core packing in this small helical protein. Over-packing substitutions, in which side chain size is increased, were created to probe the specificity and malleability of core-packing in the folding intermediate and rate-limiting transition state. In parallel, polar groups have been introduced into the Im7 core to determine the solvation status of core residues at different stages of folding. The majority of Im7 core positions become buried from solvent early in folding prior to population of the intermediate species. However, key regions involved in docking of the short helix III remaining solvent exposed until after the rate-limiting transition state has been traversed. When these regions are over-packed Im7 fails to fold correctly and the intermediate species becomes highly populated at equilibrium.

We have also used Im7 to develop a system that allows protein stability to be measured *in vivo*, and allows for the directed evolution of protein stability independently of function. By fusing Im7 into the antibiotic resistance protein β-lactamase, we can infer the stability of the inserted protein by measuring the antibiotic resistance of cells expressing the fusion construct. We compared the thermodynamic and kinetic stability of isolated Im7 variants measured *in vitro* to the antibiotic resistance that those mutants confer in the context of the fusion protein, and found a striking correlation over a wide range of stability. The mutations that stabilized the protein mapped predominantly to residues in the binding site of Im7 for its cognate nuclease, colicin E7. This showed that the evolution of Im7 has involved a tradeoff between stability and function. This method allows a new approach to understanding the forces that have shaped the evolution of today's protein sequences.

Publications

Friel, C.T., Smith, D.A., Vendruscolo, M., Gsponer, J. & Radford, S.E. (2009) The mechanism of formation of a folding intermediate reveals the competition between functional and kinetic evolutionary constraints. *Nat. Struct. Mol. Biol.* **16**, 318-324.

Funding and acknowledgments

This work is funded by the BBSRC. We thank Keith Ainley for technical support.

Collaborators

Joerg Gsponer & Michele Vendruscolo (University of Cambridge), Jim Bardwell (University of Michigan, USA), Barbara Imperiali (MIT, USA).

Single molecule protein folding and kinetics

Jennifer Clark, Maarten F. M. Engel, Karine Deville, Opas Tojira and Sheena E. Radford

Introduction

Single molecule fluorescence resonance energy transfer (smFRET) permits the study of biological macromolecules, in this case proteins, beyond the bulk ensemble. Ensemble averaged observations can result in the occlusion of rarely populated yet scientifically relevant species. A single molecule approach, with sufficient temporal and special resolution can allow us a window into motions beyond the scope of ensemble techniques.

SmFRET has been described as a spectroscopic ruler. Proteins are labelled with suitable fluorophores at selected points within the protein of interest and the energy transfer between fluorophores provides information as to their spatial separation.

Diffusion-based FRET studies

The B domain of protein A (BdpA) is one of the fastest folding proteins studied to date. Its simple three helix topology in combination with its rapid rate of folding has made this protein an excellent model to study protein folding both *in vitro* and *in silico*. Whilst BdpA is a simple model for these studies its speed of folding provides experimental challenges and the postulated mechanism of folding remains under debate. Here, we address the information provided by single molecule proximity ratio histograms for studies of protein folding. Proximity ratios provide information as to the spatial separation between fluorophore sites within the protein. In addition, the width of the proximity ratio histograms contains information about the dynamics of the dyes attached to the protein, the intra-ensemble dynamics and inter-ensemble exchange dynamics. Variants of BdpA, designed to possess cysteine residues which allow site-specific labelling were produced and used as a probe for single molecule folding studies. Using smFRET and ensemble FRET, the thermodynamic properties of these molecules have been probed, and the kinetic parameters determined using laser induced temperature jump and smFRET experiments.

Using a Monte Carlo simulation method we have developed, information previously hidden within single molecule frequency histograms can be delineated, establishing the rate constants for folding and unfolding of BdpA with a greater accuracy than using laser induced temperature jump measurements. This model can be expanded to other protein systems, increasing the amount of information available to the single molecule experimentalist.

Immobilised protein studies

In addition to protein folding, two very different areas of research are under investigation in our laboratory using smFRET. Using a liposome-based immobilisation strategy (Fig. 1) the oligomeric state and conformational dynamics of the evolutionarily conserved Sec complex (SecYEG) are being studied using total internal reflection (TIRF) FRET. SecYEG is part of a complex larger secretory pathway, whose multiple components are each postulated to undergo conformational rearrangements during the course of protein translocation. In addition, protein-protein interactions can be studied using this approach, another key process in the translocation mechanism. Importantly, the single molecule approach obviates the need of ensemble approaches to synchronise these motions in order to study them.

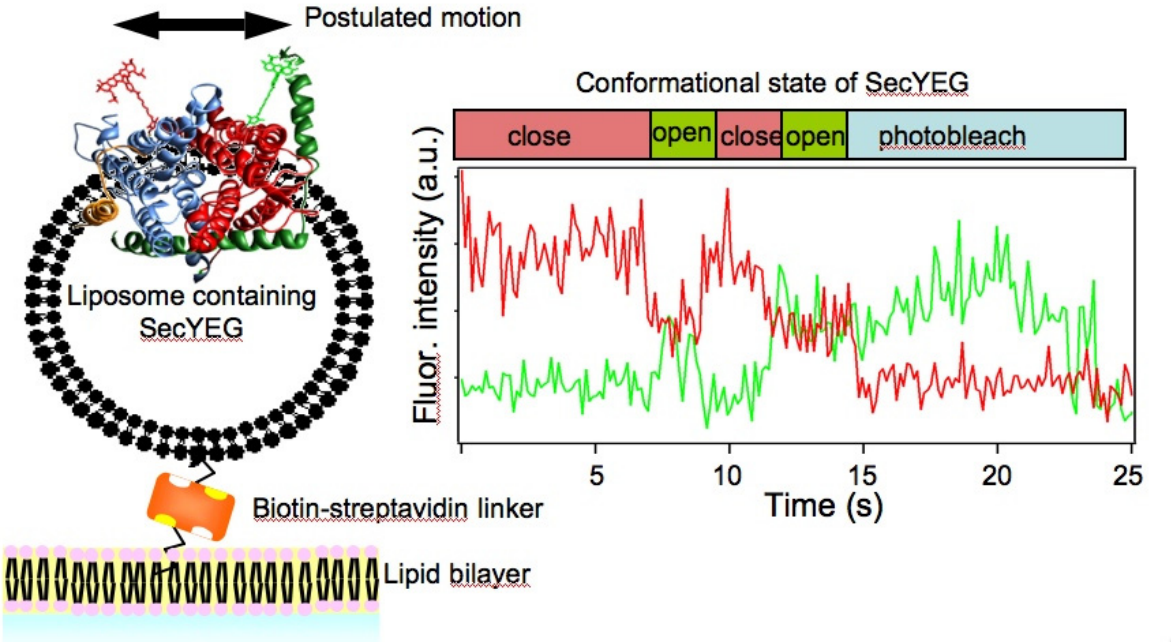

Figure 1: Schematic of TIRF-FRET immobilisation system (left) and the response, observed by TIRF-FRET, on the opening and closing of the SecYEG channel (right).

Single molecule amyloid studies

Finally, the aggregation and amyloid formation of the proteins, islet amyloid polypeptide (IAPP) and ß-2-microglobulin ($ß_2$m) are being probed using fluorescence correlation spectroscopy (FCS). FCS provides a measure of size and, when used in conjunction with a maximum entropy deconvolution algorithm, provides an unique opportunity to observe the population of multiple oligomeric species in real time ranging from monomeric protein to large, potentially fibrillar species. Used in combination with more traditional biophysical techniques, FCS is an exciting method to examine the species populated during an amyloid assembly reaction and in the future examine which species are affected by through the addition of small molecule additives.

Publications

Clark J., Gell C., Smith D. A. & Radford S. E. (2009) Folding dynamics of BdpA determined using a single molecule diffusion FRET method. *Submitted*

Collaborations

Ian Collinson (University of Bristol), Steven A. Baldwin, Roman Tuma and Thomas Wilkop (Astbury Centre for Structural Molecular Biology, Leeds), D. Alastair Smith (Avacta Group Plc).

Funding and Acknowledgements

We acknowledge the Wellcome Trust, Diabetes UK, European Molecular Biology Organization, BBSRC and the University of Leeds for funding. We thank Keith Ainley for technical support.

Targeting the functions of the Human Papilloma Virus 16 oncoproteins with RNA aptamers.

Clare Nicol, G. Eric Blair and Nicola J. Stonehouse

Introduction

Human papillomaviruses are DNA tumour viruses that are responsible for the development of cervical cancer. Approximately 50% of cervical cancers have been shown to contain HPV16 DNA. The major factors responsible for the initiation of carcinogenesis are the viral oncoproteins E6 and E7. This project focuses on HPV16 E7, a small hydrophobic protein which has been shown to form multiple interactions with a variety of cellular proteins, many of which are involved in cell cycle control. We have developed RNA aptamers as molecular tools to investigate some of these protein-protein interactions. Previous work has identified aptamers which alter the cell cycle distribution and induce apoptosis in an E7-expressing cell line that originates from a human cervical carcinoma (SiHa cells).

An aptamer that inhibits the interaction between E7 and the cell cycle control protein pRb.

Using a panel of GST-E7 mutant proteins, we performed binding assays to identify regions of the E7 protein involved in the interaction with our aptamers. Of particular interest is aptamer A2 which confers the greatest level of apoptosis in E7-expressing cells. Aptamer A2 binds GST-E7 mutant proteins in which there are deletions in the C-terminal zinc binding domain, however fails to bind when there are mutations in the N-terminus (Fig. 1).

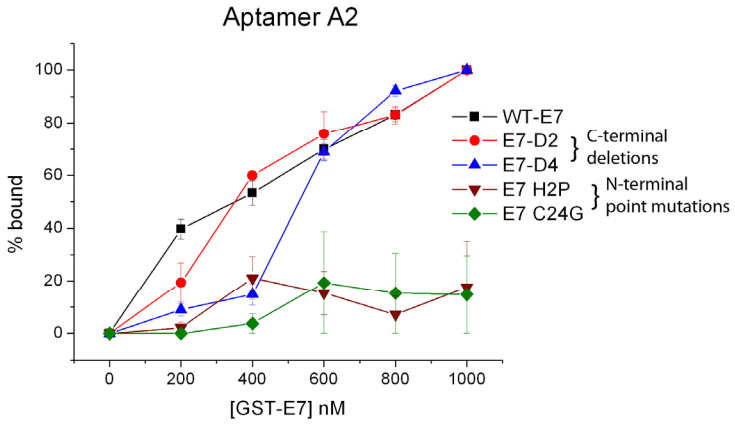

Figure 1. Aptamer A2 fails to bind to GST-E7 mutant proteins in which modifications are made at the N-terminus. Aptamer was 5' labelled with [γ ^{32}P]-ATP and incubated with increasing concentrations of bead-bound protein, GST only beads were included to maintain a constant volume of beads throughout. The percentage of bound RNA was quantitated by scintillation counting. A2 was probed for binding to wild-type GST-E7, or C-terminal deletion mutants GST-E7-Δ2 and GST-E7-Δ4 or N-terminal point mutants GST-E7 H2P and GST-E7 C24G.

This indicates that A2 requires residues in the N-terminus of E7 for binding, which is also the region known to be involved in the interaction with cell cycle control protein pRb. To test whether A2 could disrupt the interaction between E7 and pRb, GST pull-down assays were performed. Fig. 2 shows that with increasing concentration of aptamer A2 there is reduced interaction between GST-E7 and pRb. Interestingly, aptamers with a high sequence similarity do not share this activity which suggests that a specific conformation of A2 is responsible.

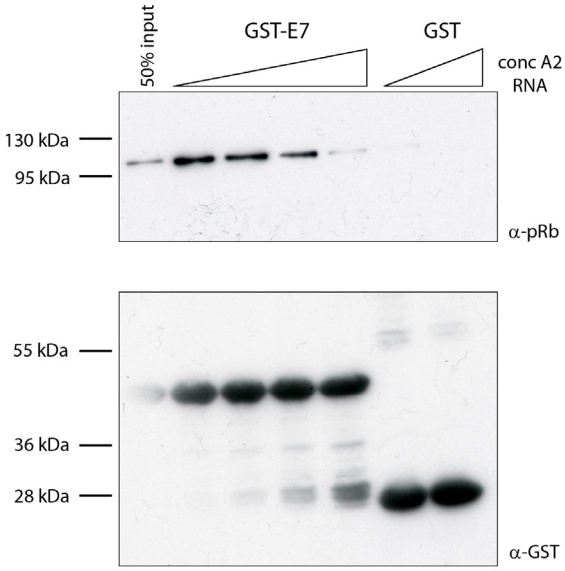

Figure 2. Aptamer A2 disrupts the interaction between GST-E7 and pRb. 5 μg of GST-E7 bound to glutathione magnetic beads was incubated with a HaCaT cell lysate for 1 hour at 4°C in the absence of aptamer A2 or in the presence of increasing concentrations of A2 (0, 1, 2.5 and 5 μg of RNA). Bead bound GST alone was incubated with the highest concentration of aptamer used. GST proteins and interacting partners were isolated from the reaction using a magnet, eluted in Laemmli buffer and analysed by SDS-PAGE and Western blot using antibodies to pRb and to GST.

Collaborators
Lawrence Banks, International Centre for Genetic Engineering and Biotechnology, Trieste, Italy
Sybille Mittnacht, ICR, UK
Andrew Macdonald, University of Leeds

Funding
Funding from BBSRC and Yorkshire Cancer Research is gratefully acknowledged.

The FMDV replication complex

Matthew Bentham, Sophie Forrest, Kris Holmes, David J. Rowlands and
Nicola J. Stonehouse

Foot and mouth disease (FMD) is highly contagious and sometimes fatal disease of cloven hoofed animals, which has a global impact on animal husbandry – both in terms of reducing productivity and preventing trade. The cost of the U.K. outbreak in 2001 has been estimated at over £9 billion.

Foot-and-mouth disease virus (FMDV), the etiological agent of FMD, has a relatively small (~ 9 Kb), single-stranded, RNA genome. Due to the presence of an internal entry ribosome site and a polyA tail, the viral genome is directly translated into a single poly-protein. Subsequent cleavage gives rise to 13 fully mature proteins, although a number of the partial cleavage products are functional proteins in themselves. Replication of the genome is primarily performed by 3Dpol – a virally encoded RNA-dependent-RNA polymerase. This provides templates for subsequent rounds of translation as well as genomes for packaging into viral particles. Remarkably, for a virus infecting a eukaryotic cell, the entire replication cycle can be completed in under 3 hours.

We have been working towards a greater understanding of the replication complex of FMDV and the generation of inhibitors. We have developed a 'minimal' functional polymerase assay, consisting of; template RNA, a primer, 3Dpol and UTP. Using this assay we have screened a large number of RNA aptamers, some of which are inhibitory.

In common with all other picornaviruses, of which FMDV is a family member, infection results in a major rearrangement of cellular membranes. Replication complexes are usually found within small vacuoles suggesting a significant role for membranes in genome replication. We can emulate this *in vitro*, by the addition of liposomes to our polymerase assay, which resulted in an enhancement of polymerase activity (see Fig. 1).

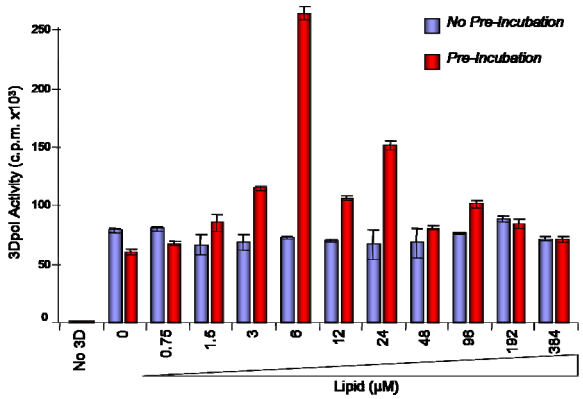

Figure 1. Liposome enhancement of polymerase assays. Polymerase assays were performed by either pre-incubating 2.5 µM 3Dpol with liposomes (red bars) or by simply mixing the complete assay with liposomes (blue bars). Only by pre-incubation of 3Dpol with liposomes is the enhancement of polymerase activity seen. Interestingly, the presence of a high concentration liposomes reduces the enhancement, suggesting that 3Dpol is required to associate with liposomes at a critical ratio.

The related poliovirus (PV) 3Dpol has been shown to self-assemble into planar and tubular 'arrays'- thought to be necessary for efficient replication. In contrast to the structural information available for PV, the crystal structure of FMDV 3Dpol does not support the formation of higher order structures. However, we have shown by TEM that FMDV 3Dpol is able to form higher order structures, but only in the presence of all other components of the polymerase assay (see Fig. 2). We have demonstrated that none of the components (i.e. template, primer, 3Dpol or UTP) alone has the ability to form higher order structures and that the formation of these structures is time dependent i.e. more structures are seen as the assay

proceeds. Further characterization of these structures is ongoing, together with investigations into a possible role for membranes in the promotion of their formation.

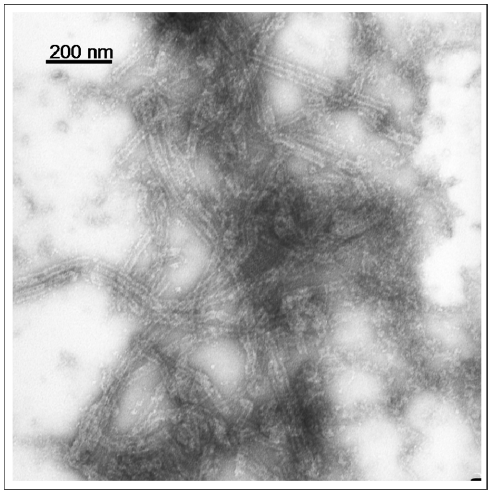

Figure 2. Electron micrograph of a replication assay consisting of polyA template, oligoT primer, UTP and 3Dpol after 30 minutes. Samples were negatively stained with 4% (w/v) uranyl acetate and viewed at 80 KeV using a Jeol microscope.

Collaborators
Esteban Domingo, Universidad Autonoma de Madrid
Nuria Verdaguer, IBMB-CSIC, Barcelona
Graham Belsham, Danish Institute for Food and Veterinary Research, Denmark

Funding
Funding from BBSRC is gratefully acknowledged.

The staphylococcal PcrA helicase requires the action of both the replication initiator RepD and SSB proteins to unwind the small plasmid pCER*oriD*

Gerard P. Lynch, Neil H. Thomson and Christopher D. Thomas

Background

The *pcrA* gene is almost ubiquitous in Gram-positive bacteria and encodes an essential but poorly processive helicase. Although the role of PcrA in Gram-positive bacteria such as the human pathogen *Staphylococcus aureus* remains unclear, it has been shown to be important for the rolling circle replication of the pT181 family of staphylococcal plasmids.

Using our 3 kb model plasmid pCER*oriD* as substrate, we have studied the mechanism by which PcrA unwinds duplex DNA into its component single-stranded form. Work has previously focused on how PcrA is recruited by the plasmid replication initiator protein RepD to partially unwind negatively supercoiled plasmid DNA, but recent advances with linearised plasmid DNA substrates have highlighted additional roles of RepD and single-stranded DNA binding protein (SSB) in stimulating the unwinding activity of PcrA.

Recent findings

Atomic force microscopy (AFM) was used to visualise the recruitment and unwinding of linear pCER*oriD* by PcrA. RepD can nick and religate at its cognate origin of replication, *oriD,* forming a transient covalent attachment with the plasmid pCER*oriD* via the active site residue Y191. Digestion of pCER*oriD* with HindIII results in a linear DNA fragment with *oriD* located at one end. The RepD mutant R189K retains the ability to nick at *oriD* but cannot religate. This mutant was used to form a stable DNA:protein replication initiation complex (Fig. 1A). The complex is recognised by the PcrA helicase, which alters the terminal appearance of the DNA fibre once bound (Fig. 1B). On the addition of ATP, the helicase appears to translocate along the DNA (Fig. 1C). Interestingly the terminal end of the DNA fibre is still in contact with the position of the helicase, suggesting that not only is R189K important for recruitment of PcrA, but it is also essential in "clamping" the helicase onto the DNA. Under such conditions the DNA appears to remain in double-stranded form after passage of the helicase. Full unwinding of pCER*oriD* is only seen in the presence of SSB, which sequesters single-stranded DNA (Fig. 1D). The combination of RepD-R189K for formation of the initiation complex plus visualisation by AFM thus represents a powerful tool for the study of PcrA helicase activity.

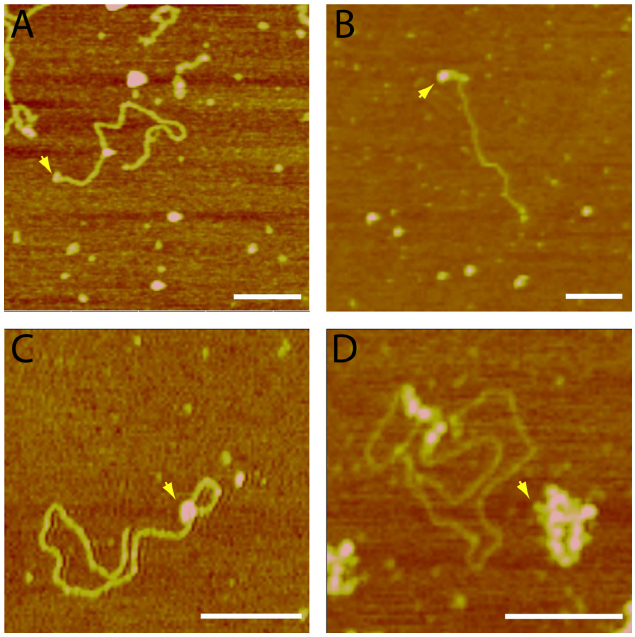

Fig. 1 AFM image in air of linearised pCER*oriD* in the presence of various components of the rolling circle replicative apparatus. **A**, R189K; **B**, R189K and PcrA; **C,** R189K, PcrA and ATP; **D**, R189K, PcrA, ATP and SSB. Yellow arrows indicate components described in the text. The white scale bar represents 200 nm.

Acknowledgements

We thank Neil Crampton and Sergio Santos Hernandez for assistance with the AFM work.

Funding

This work was funded by the BBSRC.

Cross-specificity in the dimerisation of pT181 family Rep proteins

Christopher D. Thomas

Background

Our model plasmid is pC221, a member of the staphylococcal pT181 family. Rolling circle replication of pC221 is initiated by the RepD protein, which is specific for the cognate origin of replication, *oriD*. Within the pT181 family the Rep proteins are highly conserved; *ori* binding specificity is mediated via a 6 aa region in the C-terminus of the protein and the cognate inverted complementary repeat ICRIII at the origin of replication. At normal copy number, the Rep proteins of pC221 and pT181 do not complement one another.

The Rep proteins are dimeric, each subunit contributing one nucleophilic tyrosine residue to the initiation and termination processes. Previous dimerisation studies between a hexahistidine-tagged 39 kDa Rep protein and a series of truncated 34 kDa variants identified a 25 aa dimerisation determining region within the C-terminus of the protein, immediately prior to the 6 aa binding specificity region. Thus RepC will form a heterodimer against RepD if 15 key residues in the dimerisation determining region of the latter are swapped to match the RepC sequence.

Recent findings

We have now extended dimerisation studies to the other prototype Rep proteins of the pT181 family. In each case, fusion proteins between the conserved 21 kDa region of RepD and the divergent C-terminal 14 kDa domains of RepE (pS194), RepI (pUB112), RepJ (pC223) and RepN (pCW7) have been constructed. Each has been challenged in a dimerisation assay against RepD or RepC.

Despite the clear discrimination between RepC and RepD, not all Rep dimers were found to be mutually exclusive. Instead, the RepDN fusion was found to rapidly form heterodimers with RepC but not RepD; conversely, RepDE, RepDI and RepDJ formed heterodimers somewhat more slowly with RepD but not RepC. This matches the sequence alignments of the 25 aa dimerisation determinant, and suggests key amino acids involved at the dimer interface. Site directed mutagenesis of residues in this region has been conducted, and critical interactions identified through the solubility of the resultant proteins.

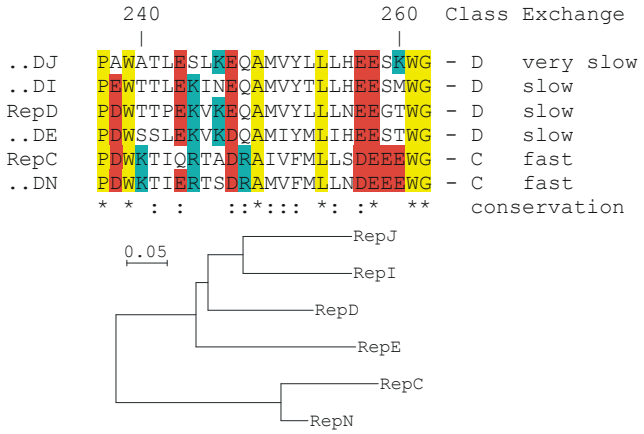

Sequence relationships of the dimerisation region.

The relationships within dimerisation "classes" contrast with the sequence relationships within the adjacent 6 aa specificity region (and the corresponding ICRIII sequences). For example, RepE and RepN complement each other for replication yet are of different dimerisation groups. Similar sequence-based pairings are apparent for RepC and RepJ. This suggests that relatively few classes of dimerisation and DNA sequence specificity have been combined to produce the range of Rep proteins currently known, yet raises the likelihood that significant populations of Rep heterodimers will form when certain compatible plasmids co-exist within the same cell. To explore this effect we are currently examining the specificity of such heterodimeric Rep proteins against "heteromeric" ICRIII combinations.

Applications of atomic force microscopy to DNA

Daniel J. Billingsley, Sergio Santos, William A. Bonass, Jennifer Kirkham, Neil H. Thomson

Introduction

The atomic force microscope is a versatile technique that is particularly suitable for studying biological material since it can image in native-like environments on unstained tissues and molecules. There are many imaging modes, but the most prevalent is amplitude modulation (AM AFM) where a micro-sized cantilever with a sharp probe at the end is made to vibrate near a surface and its dynamics are monitored to obtain information about the sample. Since the instruments' invention perhaps the most widely studied biomolecular sample has been DNA, where the conformation of the backbone can be resolved on sufficiently dilute samples. Sample preparation is relatively simple and imaging can be performed in both ambient and liquid conditions, with the latter allowing studies to be performed in physiological-like conditions. To date, numerous studies into DNA using AFM have been performed, including investigations into DNA structure, condensation behaviour, and DNA-protein interactions.

Humidity-controlled AFM of DNA

Dynamic studies of DNA-protein interactions have historically been performed by operating the AFM under bulk liquid. Imaging under liquid can prove difficult as molecular adhesion to the surface is reduced, and molecular motion leads to detrimental effects on imaging. We have performed investigations into how the humidity of the environment when imaging in air affects image contrast. Interesting effects were observed when imaging was performed at high humidity. Local changes in molecular conformation were observed over the entire scan area (see Fig. 1), in addition to DNA condensation effects. This can be attributed to increased molecular mobility, a result of a bulk water layer condensing onto the surface at high humidity. The finding that DNA gains a certain degree of mobility at high humidity could have applications in studying DNA-protein interactions, in which a certain amount of rotation or movement of the complex is often a prerequisite. Imaging at high humidity could provide a possibility to image biological interactions, without the inherent difficulties associated with imaging under liquid.

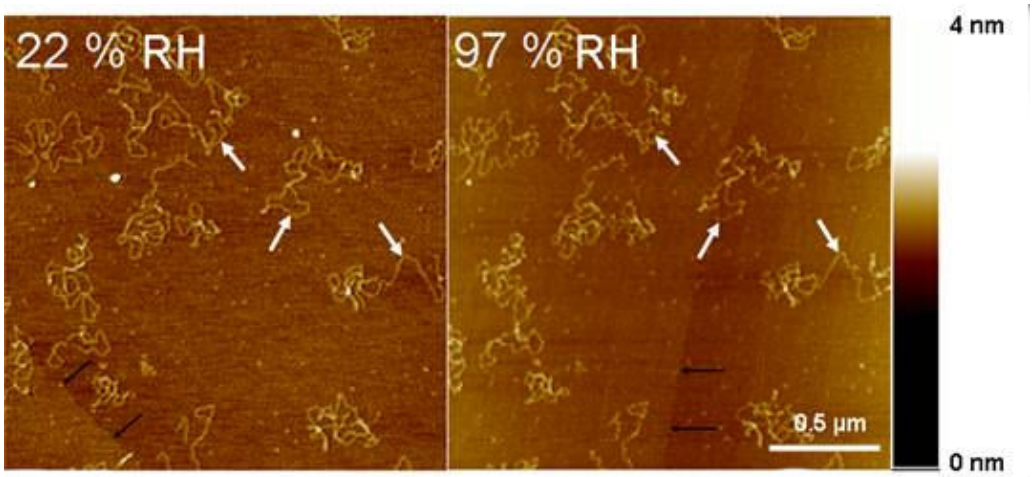

Figure 1. Comparison of imaging at low humidity (left) and high humidity (right) for supercoiled plasmid prepared on Ni(II)-mica. At high humidity the DNA begins to regain mobility and local conformational changes can be observed. A number of these changes are indicated with white arrows. Also apparent in these images is a moving water monolayer caused by non-equilibrium effects (indicated with black arrows).

Cantilever dynamics affect image contrast generation

The dynamics of the cantilever in AM AFM have also been investigated, since these provide topography, phase, and amplitude contrast in AM-AFM. In short, lateral and topographic resolution can vary dramatically with even slight changes in operational parameters or the geometry of the probe. Due to the complexity of the tip-sample interactions numerical simulations are typically used to interpret AM AFM data. Topography and lateral contrast might also vary widely from scan to scan depending on cantilever-sample properties, environmental conditions and operational parameters. Nevertheless our studies have shown that it is possible to distinguish between artifacts induced by the non-linear dynamics of the cantilever and true surface features. Over the past year we have also been developing new methods based on models and experiments to increase resolution and contrast. Examples of the improvements relative to standard methods are shown in Fig. 2.

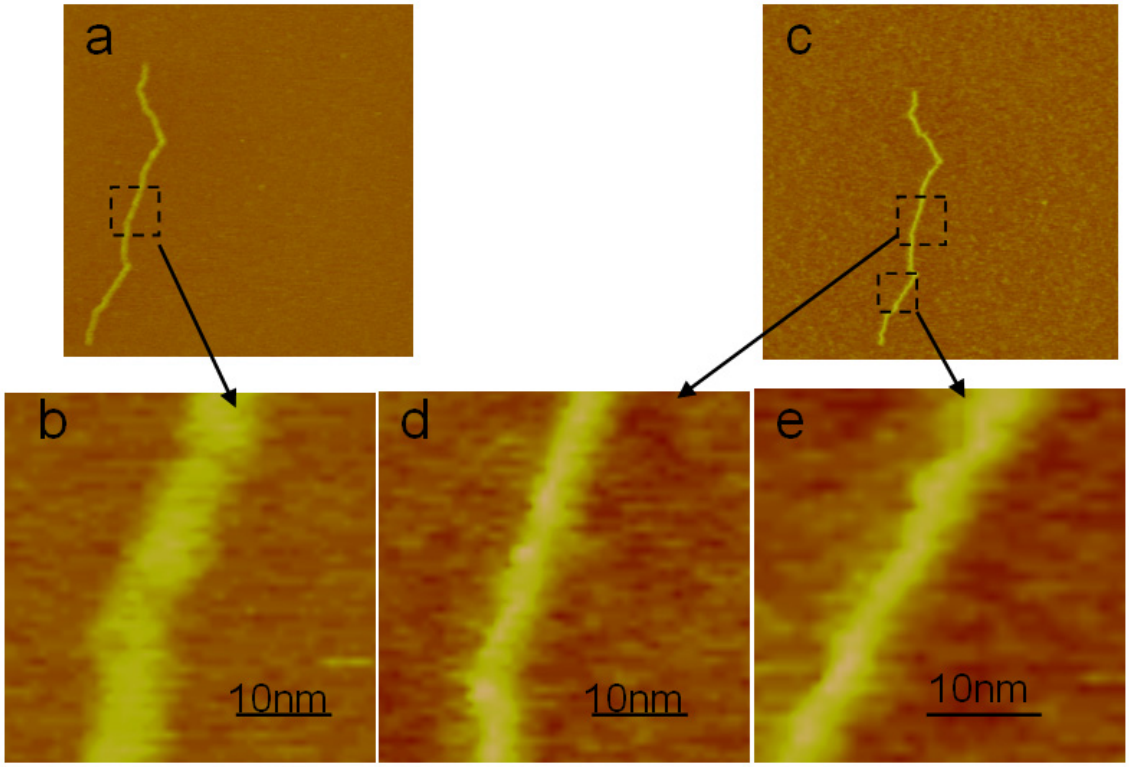

Figure 2. Topographic images of an 800bp dsDNA fragment obtained by: (a) and (b) standard AM AFM methods ; (c), (d) and (e) new procedures based on finer control of the cantilever amplitude and applied force.

Funding

This work was funded by the EPSRC White Rose Doctoral Training Centre, the BBSRC and Asylum Research Corporation.

Cryo-electron microscopy of the vacuolar ATPase motor reveals mechanical and regulatory complexity

Stephen P. Muench, Chun Feng Song, Clair Phillips,
Michael A. Harrison & John Trinick

Introduction

The vacuolar ATPase (V-ATPase) is a large and highly complex ATP-driven molecular motor, which acts as a transmembrane proton pump in almost all eukaryotic cells. Its central roles in cell physiology include energising secondary active transport, maintaining the acidity of intracellular compartments and pumping acid out of the cell. Unregulated function or loss of the V-ATPase is associated with kidney disease, inherited deafness, osteoporosis and in metastasis and multidrug resistance of some tumors. The V-ATPase has evolved from the same ancestral pump as F_1F_0-ATP synthase, the primary source of ATP synthesis, with both sharing a common rotary catalytic mechanism linked to proton pumping. Despite the importance of both motors, understanding of their subunit arrangements is poor, with the ~900kDa V-ATPase containing over 30 subunits of as many as 14 different types.

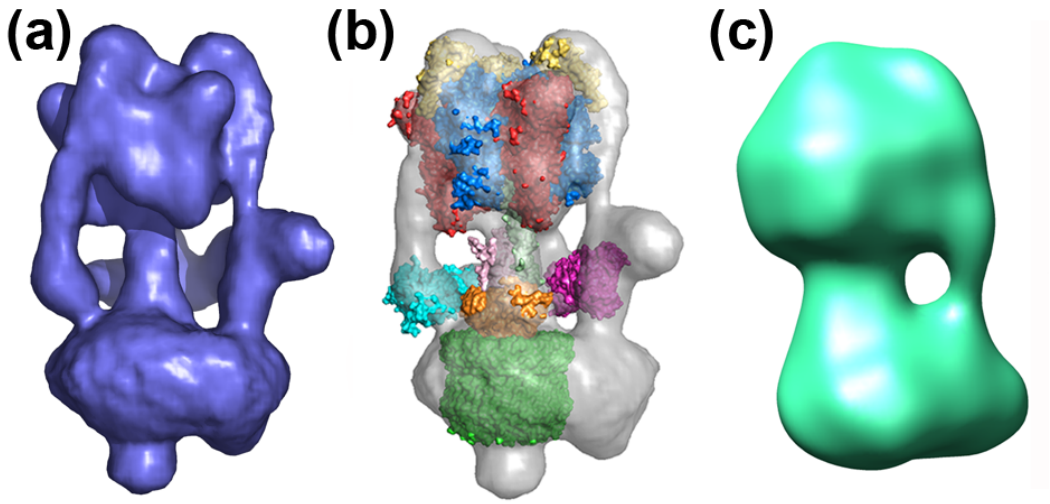

Figure 1. Side views of the V-ATPase cryo-EM reconstruction, with a solid surface (a), a transparent surface showing the fitting of the known X-ray structures (b) and the 32Å resolution cryo-EM reconstruction of the related F_1F_0-ATP synthase by John Rubinstein and co-workers (c).

Results

Using single particle cryo-EM, the structure of the tobacco hornworm (*Manducca sexta*) V-ATPase has been solved to 16.5Å, which is ~2 fold higher than previous cryo-EM models of either the V-ATPase or the related mitochondrial F_1F_0 ATP synthase (Fig. 1). As a result of producing a highly detailed structural model of the V-ATPase we have been able to fit all of the known subunit structures in order to gain a much better understanding of their positions and inter-connectivity. We have been able to show that 3, rather than 1 peripheral stalks link the catalytic V_1 and proton translocating V_0 domain, demonstrating greater complexity than that found in the F_1F_0 ATP synthase. The V-ATPase operates via a rotary mechanism, and one or more of these stalks are likely to have 'stator' functions. Furthermore, the role of the C and H subunits in V-ATPase regulation can now be understood at a structural level, with both subunits playing key parts in maintaining the structural integrity of the network of 3 peripheral stalks. Thus the model provides new insights into the organisation of key components involved in mechanical coupling between the domains and regulation of activity.

Publications

Muench, S.P., Huss, M., Feng Song, C., Phillips, C., Wieczorek, H., Trinick, J. & Harrison, M.A. (2009) Cryo-electron microscopy of the vacuolar ATPase motor reveals its mechanical and regulatory complexity. *J. Mol. Biol*. **386**, 989-999

Funding

This work was funded by the BBSRC and Deutsche Forschungsgemeinschaft.

Collaborators

Markus Huss and Helmut Wieczorek are from Fachbereich Biologie, Universität Osnabrück, Germany.

Structure of a bacterial Type-I DNA methyltransferase with a bound antirestriction protein from phage T7 using electron microscopy

Christopher K. Kennaway and John Trinick

Introduction

Bacteria protect themselves from invading foreign genetic material (from phage, plasmids, cosmids, etc.) by several means, one of which is the type I Restriction Modification (R-M) system. R-M systems act to limit the spread of pathogenic traits such as antibiotic resistance by horizontal gene transfer. The bacterium's own DNA is modified by addition of methyl groups at specific sites, and when DNA lacking any modification is encountered the 'foreign' DNA is destroyed by an endonuclease. The double stranded breaks are distant from the initial recognition site due to the action of a DNA translocase. The DNA methylation, translocation and restriction functions are all carried out by a type I complex made of three types of subunits: S (specificity), M (methyltransferase) and R (restriction endonuclease and translocase), assembling as $R_2M_2S_1$. DNA methylation alone requires a M_2S_1 complex. Type I R-Ms are specifically inhibited by DNA mimic proteins produced by phage. In this work a complex of $M_2S_1$with Ocr, an antirestriction protein from phage T7, was studied by electron microscopy (EM).

Results

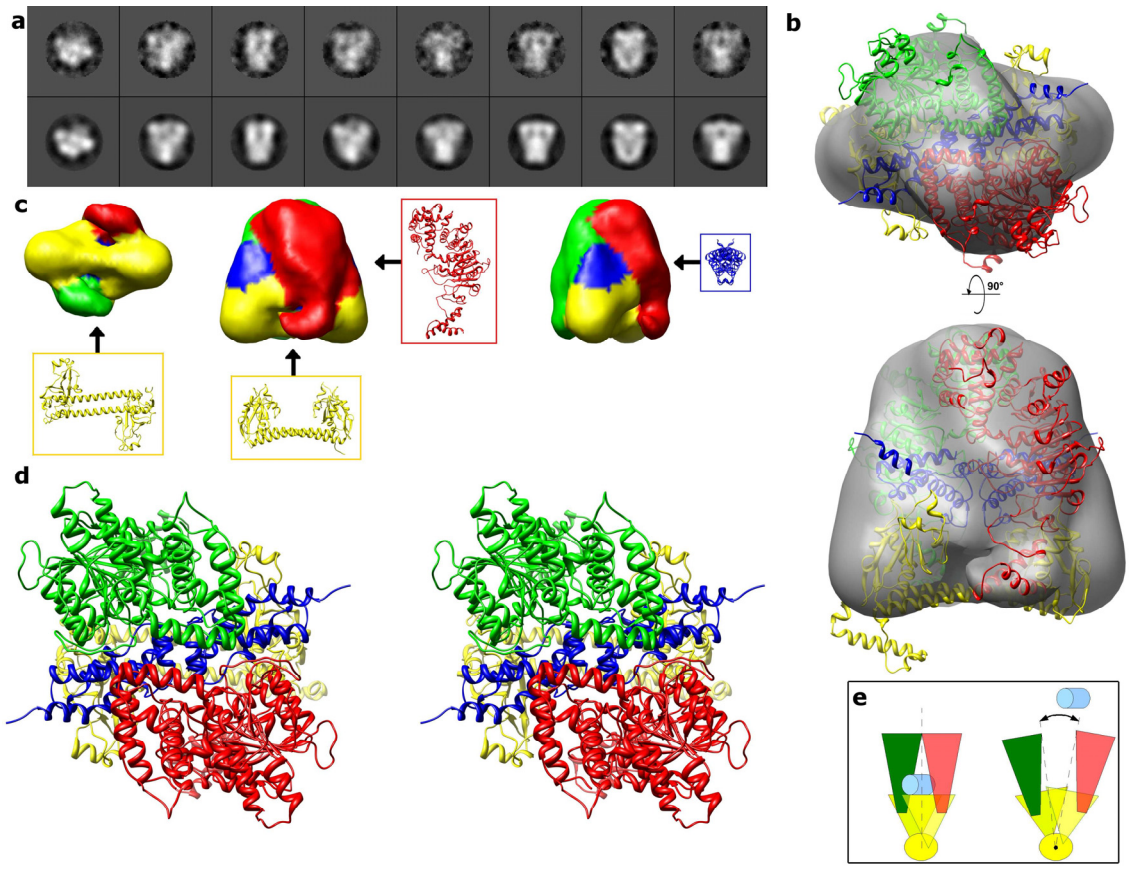

Figure 1. EM data, 3D reconstructions and model for the M_2S_1-ocr complex. **a**: Eight selected EM class average images (top row) with their corresponding reprojections of the EM map (second row), showing a range of views. **b**: Two orthogonal semi-transparent surface representations of the EM 3D reconstruction each with a view of the modelled coordinates fitted as a rigid body (green and red – M; blue – ocr dimer; yellow – S). **c**: 3 surface views of the M_2S_1-ocr EM 3D reconstruction coloured according to proximity to the fitted coordinates, with the positions of individual protein chains indicated with arrows. **d**: A stereo view of the M_2S_1-ocr atomic model. **e**: Schematic diagram of proposed mechanism of clamping and release of DNA substrate (light blue) facilitated by twisting of the coiled-coil (yellow, viewed end-on).

Negative stain electron microscopy of M_2S_1-Ocr assemblies (~200 kDa) showed a homogeneous array of particles with a variety of orientations visible on the carbon substrate. Single particle analysis and three dimensional reconstruction image processing techniques resulted in a 3D density map, which was judged by Fourier shell correlation to be about 18 Å resolution. X-ray crystallographic structures of individual subunit proteins were modified using homology modelling methods and automated docking programs. The resulting atomic assembly matched the EM density when fitted either manually or computationally. Similar atomic models were also constructed for the M_2S_1-DNA complex, giving a complete explanation of how the proteins come together and bind their target sequence. This model also encompassed bending of the DNA backbone, flipping out the adenine bases, sequence recognition, and catalytic site formation.

Conclusions

The new EM structure and computational model of M_2S_1-Ocr rationalise, for the first time, a large body of experimental data obtained using many different methods over many years. A mechanistic explanation of the Type I methyltransferase enzymes is suggested by the model, which clearly indicates locations for further analyses such as the M-S and M-M interfaces. When combined with data on M.EcoR124I**,** the model also suggests that a dynamic opening and closing of the protein, driven by a flexing and twisting of the conserved coiled-coil region within S, is required to open up the M-M interface to allow either DNA binding or attack of the Ocr antirestriction protein, a protein that "disguises itself" as DNA.

Publications

Kennaway CK, Obarska-Kosinska A, White JH, Tuszynska I, Cooper LP, Bujnicki JM, Trinick J, & Dryden DT. (2009) The structure of M.EcoKI Type I DNA methyltransferase with a DNA mimic antirestriction protein. *Nucleic Acids Res.* **37**, 762-70.

Collaborators

A Obarska-Kosinska, I Tuszynska and J Bujnicki (Poznan) and J White, L Cooper and D Dryden (Edinburgh)

Funding

Grant funding from the BBSRC gratefully received.

Dynamics of viral RNA dependent RNA polymerase studied by hydrogen-deuterium exchange and mass spectrometry

Roman Tuma

Introduction

Several copies of RNA-dependent RNA polymerase (protein P2) reside within the icosahedral polymerase complex (PC, Fig. 1A) of dsRNA bacteriophages from the *Cystoviridae* family. P2 is involved in PC assembly and replicates ssRNA precursors into dsRNA segments within the complex. During replication RNA is translocated through a template tunnel to the active site. Initiation is primer-independent and requires stacking of the first two nucleotide bases against a priming platform within the C-terminal domain. However, during elongation the platform and the C-terminal domain (red in Fig. 1B) have to swing out of the way and allow the nascent dsRNA to exit. The C-terminal domain is clamped to the rest of the enzyme by a C-terminal α-helix (Fig. 1B). Dissociation and perhaps local unfolding of this helix may be necessary in order to allow the domain motion and RNA exit. We have investigated local dynamics and stability of different regions of the P2 polymerase by hydrogen-deuterium exchange and mass spectrometry (HX-MS).

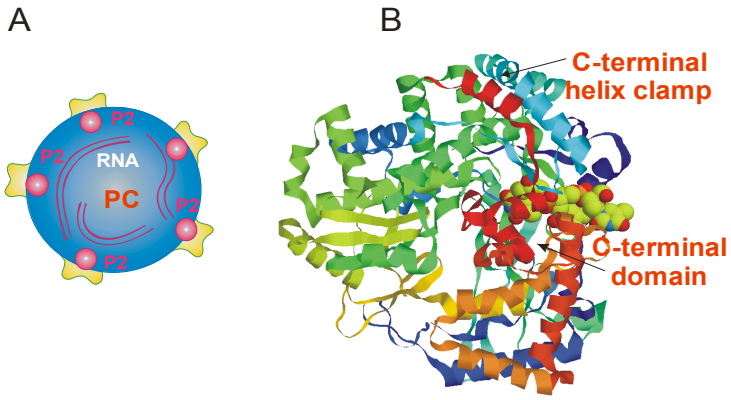

Figure 1 (A) P2 polymerase (pink) replicates the viral RNA genome inside the virion (blue) (B) Location of domains within the P2 structure. The C-terminal domain is red while the palm domain is cyan.

Results

HX-MS monitors incorporation of deuterium at amide sites along the polypeptide chain with 10-20 amino acid resolution. This enables to identify regions that exhibit slow or no exchange, such as the middle palm domain (Fig. 2). This domain holds the active site together and consequently is considerably rigid. On the other hand the N-terminus exchanges fast (Fig. 2 left). The C-terminal clamp docks against the rigid core and exhibits intermediate exchange on the timescale of minutes. This suggests that the helix dissociates from the rigid catalytic core and allows the whole C-terminal domain

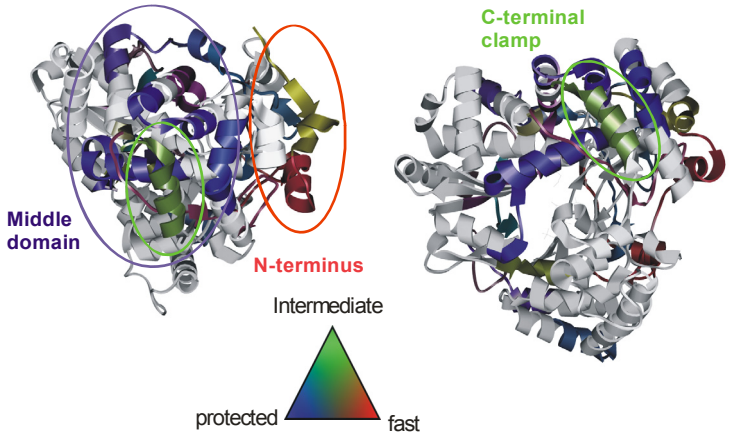

Figure 2 Kinetics of deuterium incorporation mapped onto the three-dimensional structure. Deuterium incorporation into peptic fragments was monitored by high-resolution Fourier-Transform Ion Cyclotron Resonance (FT-ICR) mass spectrometry. The colour of each region is a blend of red, green and blue, weighted by the number of fast exchanging ($t_{1/2}$ < 60 sec), medium to slow exchanging ($t_{1/2}$ min to hours) and protected ($t_{1/2}$>8h) sites. The scale triangle is shown below. (Left) A side view showing the three regions of interest. (Right) A 90 degree rotated view down the central channel showing the C-terminal clamp (green) latched against the protected palm domain (blue).

to undock from the active site, effectively releasing the nascent dsRNA during elongation.

Present research

In the current model the C-terminal domain and the clamp helix are expected to become significantly exposed during RNA elongation. We are testing this hypothesis by performing HX labelling during RNA polymerisation. In addition, we are taking advantage of the high-resolution FT-ICR and map the dynamics of the polymerase within the virion. This will shed light on the molecular mechanism of polymerase regulation during virus maturation.

Publications

Suchanova, B. & Tuma, R. (2008) Folding and assembly of large macromolecular complexes monitored by hydrogen-deuterium exchange and mass spectrometry. *Microbial Cell Factories* **7**, doi:10.1186/1475-2859-7-12.

Collaborators

This work was carried out by Violeta Manole and Dr. Ari Ora, University of Helsinki, in collaboration with Profs Sarah Butcher (University of Helsinki) and Peter Prevelige (University of Alabama at Birmingham, USA).

Funding

Funding from Euroscope programme of the European Science Foundation and participating countries is gratefully acknowledged. Support for the high-resolution FT-ICR mass spectrometry facility at University of Alabama at Birmingham, USA, is provided by a grant from the US National Institutes of Health.

Mechanistic characterisation of an ADP-dependent kinase

Zhenlian Ling, Jeff Hollins, Tom McAllister, Laura Erdmanis, Stuart Warriner,
Arwen Pearson and Michael Webb

Introduction

We are currently the investigating the mechanism of an unusual ADP-dependent kinase which is required for the light-dark regulation of carbon fixation in C_4 plants. In this class of plants, CO_2 is shuttled from the mesophyll to the bundle sheath via temporary fixation as C_4 organic acids before decarboxylation to regenerate CO_2 (which is then a substrate for Rubisco) and pyruvate. The chloroplast enzyme pyruvate, orthophosphate dikinase (PPDK) in the mesophyll then regenerates the substrate for temporary fixation phosphoenolpyruvate. We are interested in the mechanism of PPDK regulatory protein (PDRP) which binds to PPDK and reversibly phosphorylates a threonyl residue in the phospho-carrier domain of PPDK using ADP as a phosphate source as shown below. This reaction inactivates the protein in response to the transition to darkness; upon illumination PDRP reactivates PPDK via a phosphate-dependent phosphotransferase activity to generate pyrophosphate and active protein.

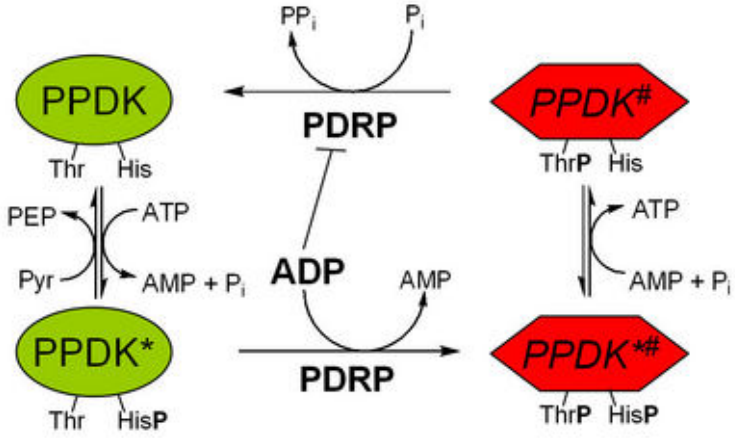

Purification of PDRP isoforms from maize, *Arabidopsis thaliana* and *Escherichia coli*

We wish to investigate the mechanism and structure of this unusual ADP-dependent kinase and are currently attempting to recombinantly overexpress and purify multiple isoforms of the protein from plants together with a putative homologue from *E. coli*, the biochemical function of which is not known. We have purified this bacterial homologue and have demonstrated, using isothermal titration calorimetry that it does bind ADP with micromolar affinity. We are now characterising the binding of this protein to other nucleotides and peptide substrates while continuing attempts to purify the plant proteins in addition to developing new biochemical assays in order to assay the unusual reactions catalysed by PDRP.

Collaborators

Dr Chris Chastain, Minnesota State Moorhead, USA
Dr Julian Hibberd, University of Cambridge
Professor Jim Burnell, James Cook University Australia

Funding

Funding from BBSRC and EPSRC is gratefully acknowledged

The reconstruction and evolution of metabolic networks

John W. Whitaker, Thomas E. Forth, Phillip M.R. Tedder,
Glenn A. McConkey and David R. Westhead

Introduction

Metabolic reconstruction is an essential aspect of the genomic analysis. The reconstruction of an organism's metabolic network can be used to identify drug targets in pathogens or can be used to increase the productivity of organisms used in industry. We consider three aspects of metabolic reconstruction: high-throughput reconstruction of metabolic networks, the evolution of metabolic networks and a detailed reconstruction of the metabolic network of *Plasmodium falciparum*.

High-throughput reconstruction of metabolic networks

Owing to advances in DNA sequencing technologies the rate at which new genome sequences are released is increasing. To allow the reconstruction of metabolic networks from these sequences there is an increasing need for accurate automated methods. To this end a high-throughput metabolic reconstruction tool called SHARKhunt has been developed and has been used to reconstruct the metabolic networks of a 121 eukaryotes. The reconstructed metabolic networks are made publicly accessible through the website metaTIGER (www.bioinformatics.leeds.ac.uk/metatiger). In an extension of this work, we are developing methods that are able to predict function using data integration methods that will be applicable to genes that cannot be annotated using more standard homology based procedures such as SHARKhunt, and these will lead to more complete reconstructed networks.

The evolution of parasite metabolic networks

To investigate the evolution of the metabolic networks of the 121 eukaryotes that are in the metaTIGER website the enzyme sequences were used to create a comprehensive database of 2,257 maximum-likelihood phylogenetic trees, some containing over 500 organisms. The trees can be viewed using an advanced interactive tree viewer or high-throughput tree searching is available which can identify trees containing horizontal gene transfer (HGT) events. HGT is now realised to have played an important role in evolution of eukaryotes. The metaTIGER phylogenetic trees were used to make high-confidence HGT predictions in ten groups of unicellular eukaryotes (see Fig 1).

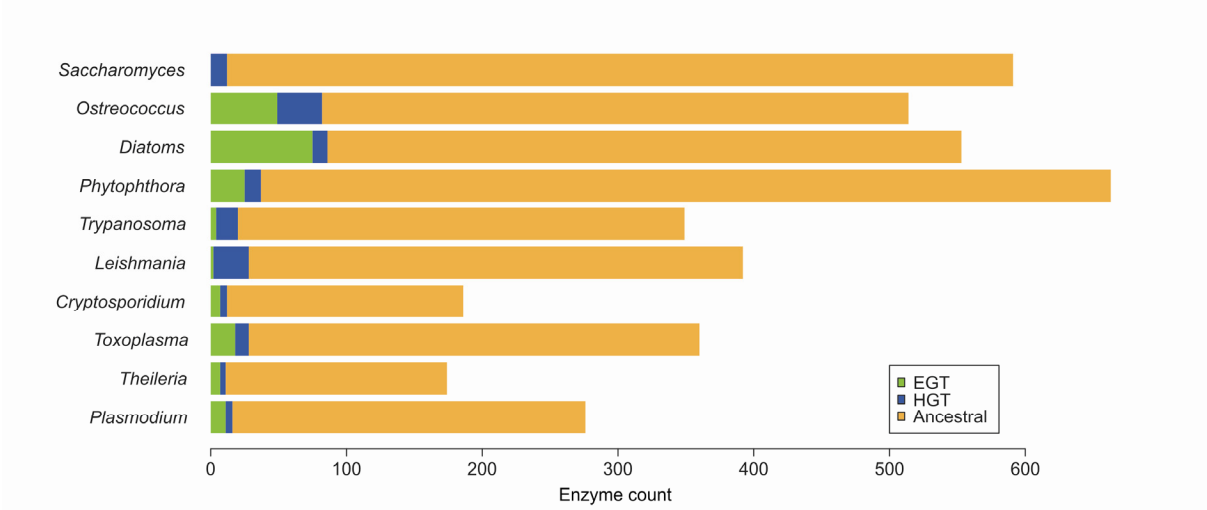

Figure 1. Predicted levels of gene transfer of metabolic enzymes. The bar chart shows the total number of enzymes that were identified as being present in each organism group. The number of enzymes that were predicted as being EGTs and HGTs are indicated with green and blue respectively.

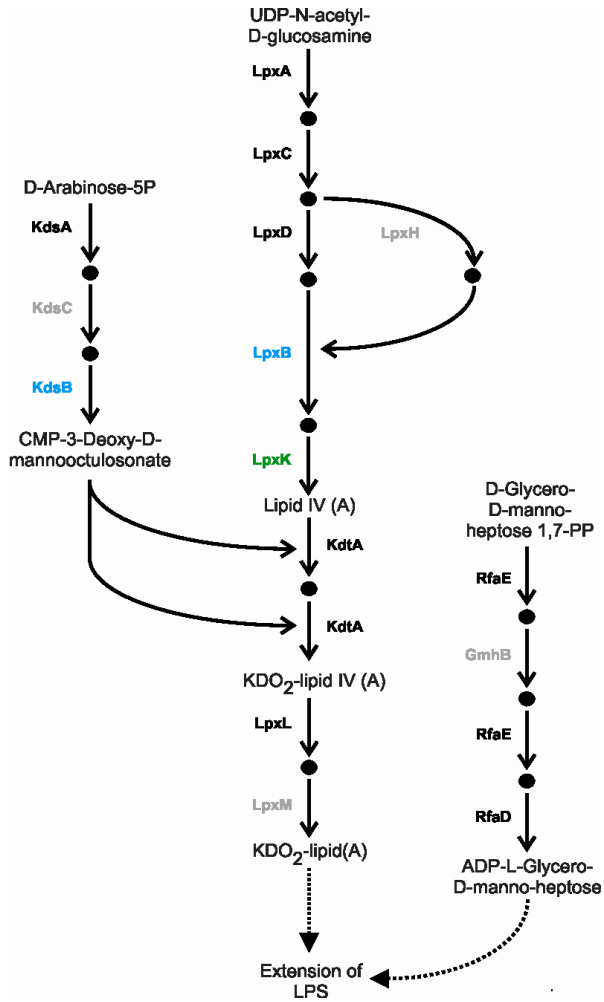

Figure 2. Lipopolysaccharide biosynthesis in *Phytophthora*. Enzymes that carry out reactions are labelled by *E. coli* gene name. The genes of the enzymes coloured blue were predicted as being HGTs and the genes of the enzymes coloured green were predicted as being an EGT. Enzymes coloured black were predicted as being present in both *Phytophthora* genomes with profile match E-values ≤ 10-10. Enzymes in grey were predicted as being present in at least one *Phytophthora* genome with E-values 10-1≥E>10-10.

Comparison of the levels of HGT identified many enzymes whose genes had been transferred during endosymbiosis event in which organisms had acquired a plastid. Some of the HGTs relating to plastid acquisition support the involvement of Chlamydia in the establishment of the plastid. In the parasites *Trypanosoma* and *Leishmania* 5-7% of enzymes were predicted as being of bacterial origin; some of these enzymes may be make good targets for drug development. The sets of HGT predictions relating to endosymbiosis were found to have greater connectivity than random suggesting that whole pathways, or at least pairs of enzymes, had been transferred during endosymbiosis. Enrichment analysis was carried out and found enrichment of enzymes in lipid and carbohydrate metabolism. The lipopolysaccharide biosynthesis pathway was identified as being transferred in the genome of the plant pathogen *Phytophthora* (see Fig 2). This pathway has never before been identified in *Phytophthora* and may prove essential to its pathogenicity thus providing new strategies for controlling its infection.

A detailed reconstruction *Plasmodium falciparum*

The group is also constructing and analysing the metabolic network of *P. falciparum*. Since no single resource on malaria metabolism is complete, the first stage of this project is to create a consensus based network reconstruction by collating information from varied and incompatible sources. As well as using publicly available information, our SHARKhunt tool mentioned above is making major contribution to this endeavour. We are also increasing the number of metabolic and transport functions that can be attached to malaria gene predictions using our homology independent malaria gene function prediction program PAGODA ((http://www.bioinformatics.leeds.ac.uk/~bio5pmrt/PAGODA_basic.html).

In addition to adapting existing tools, new software has been developed to allow easy definition and editing of metabolic networks. The use of Flux Balance Analysis (FBA) on the complete metabolic network will let us predict critical enzymes to the growth and survival of *P. falciparum*. This computational technique is able to identify critical reactions within the reaction network and predict the effects of disrupting them.

In the lab we culture *P. falciparum* in human erythrocytes with two aims. Firstly, to take measurements that let us define the goal of the metabolic network: the weighted list of chemical compounds that metabolism must create in order to allow growth and reproduction. Secondly, to test the numerical predictions of FBA by measuring parasite growth rates in the presence of compounds designed to disrupt critical reactions. With the aim of directly testing computational predictions we are conducting trials using fluorescence cytometry to more accurately and reproducibly measure growth.

Publications

Whitaker, J.W., Letunic, I., McConkey, G.A. & Westhead, D.R. (2009) metaTIGER: a metabolic evolution resource. *Nucleic Acids Res.* **37**: D531-8.

Pinney, J.W., Papp, B., Hyland, C., Wambua, L., Westhead, D.R. & McConkey, G.A. (2007) Metabolic reconstruction and analysis for parasite genomes. *Trends in Parasitology* **23**: 548-554.

Funding

This work was funded by the BBSRC and the EPSRC.

Bioinformatics: predicting disease causing mutations and genes

Matthew Care, Lucy Stead and David Westhead

Genetic disorders range from simple monogenic (Mendelian) traits governed mainly by mutations in a single gene, to oligogenic disorders involving the interaction of a few genes, through to complex disorders affected by many genes. As the number of genes involved increases, the effect of interactions between genes and environment tends to increase, whilst disease penetrance decreases giving weak disorder-gene correlations. Linkage analysis is often low resolution resulting in linkage-intervals of a few hundred genes. There is an increasing effort to use computational methods to prioritise candidate genes within these linkage-intervals.

We have combined a deleterious SNP prediction system with an existing method for human disease gene prediction. For this method, each linkage interval (or benchmark window) is related to a particular genetic disorder with a corresponding phenotypic description. A protein interaction network is used to produce a set of all potential complexes for all proteins encoded by the genes in the linkage interval. A text mining approach is then used to create a distance matrix relating all of the phenotypic descriptions within the OMIM database of human genetic diseases, giving a phenotype similarity score (PSS) of each pair of records. For each complex in the linkage interval the phenotype similarity scores are used to determine interacting proteins that are involved in genetic disorders with similar phenotypes to that of the target disorder. This guilt-by-association approach is based on the assumption that diseases with overlapping phenotypes are sometimes caused by mutations in genes that are part of a single functional module, a hypothesis that is backed up by several examples. In addition, a deleterious SNP prediction method is employed to provide a complementary set of attributes. Predictions are made for all of the single nucleotide polymorphisms that cause amino acid substitutions (non-synonymous SNPs), present in both the proteins in the interval and their interaction partners, classifying them as potentially deleterious or neutral. Finally the SNP and PSS measures (along with attributes describing the protein interactions) are submitted to a machine learning tool to give a confidence rating of each protein's involvement in the target disorder. These confidences are then used to rank the proteins within a linkage-interval.

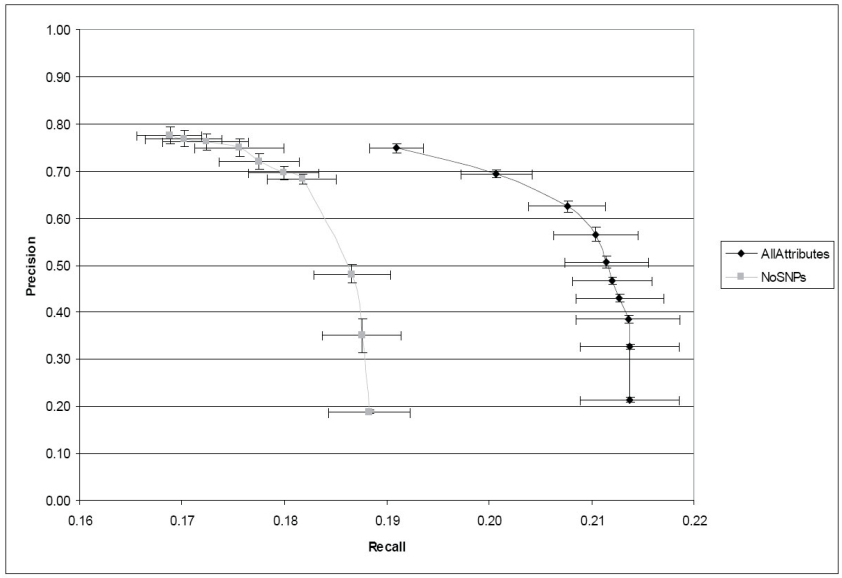

Figure 1: Plot of recall against precision for 10 Mb benchmark-windows. Recall = number of targets ranked 1st/total number of windows. Precision = number of targets ranked 1st/subset of windows that are > threshold. Using 'All-Attributes' gives a recall of 21%, far removed from the 1.5% expected by chance alone. The plot shows that for every precision threshold the addition of SNPs increases recall, with the highest 'All-Attributes' precision (75%) still having a recall (19.1%) that is greater than the lowest precision predictions made without SNPs (recall = 18.8%).

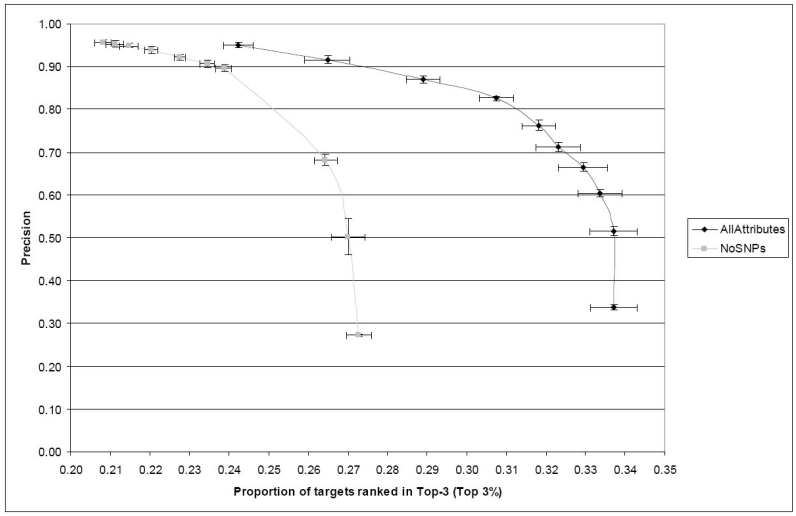

Figure 2: Plot of recall against precision for the 10 Mb benchmark-windows. Here we are looking at ranking the target within the top 3 positions in the window (top 3%; average 100 genes in 10Mb window), giving us an alternative definition of recall/precision: Recall = number of targets ranked within-top-3/total number of windows. Precision = number of targets ranked within-top-3/subset of windows that are > threshold. Using 'All-Attributes' gives a total recall of 34%, far removed from the 3% expected by chance alone. The plot shows that for every precision threshold the addition of SNPs increases recall, with the highest 'All-Attributes' precision (95%) maintaining a recall of 24%. Whilst 'No-SNPs' reaches a marginally higher precision (25%) it does so at the lower recall of 21%.

Our combination of robust machine learning tool (random forest) and attributes with differing biological relevance produced a highly accurate disease gene prediction system. Benchmarking results showed that for a 10Mb window (averaging 100 genes) we could produce an overall precision (ranked 1st) of 75% whilst maintaining a recall of 19%. We were able to obtain a precision of 95% (recall 24%) if we considered ranking the target (known disease gene) in the top 3 positions (top 3%) of the windows.

Identifying disease-causing variation in voltage-gated potassium channel genes

Recent extensions of the disease gene and mutation prediction work relate to a specific family of proteins, the voltage-gated potassium (Kv) channels. These open in response to a change in voltage across the membrane, allowing the selective passage of K^+ ions into, or out of, the cell and are involved in a number of important physiological roles including the generation of the heartbeat and transmission of signals through the central nervous system. This explains their association with diseases such as cardiac arrhythmogenesis and epilepsy. Early diagnosis and treatment of these diseases will be facilitated by revealing the underlying genotype-phenotype relationship of Kv channels, i.e. which polymorphisms (in isolation or in combination) in the genes that encode these channels lead to each disease.

Association studies enlist large numbers of patients to try and reach this goal. These studies have allowed a number of SNPs (Single Nucleotide Polymorphisms) to be labelled as either disease-causing/ mutation or benign/ polymorphism. However, it can take several years to gather results, and they can be confounded by multiple testing errors. The aim of this research is to create a computational method that can predict the effect of SNPs within Kv channel genes and, therefore, highlight those that should be further investigated by association studies. The method employs 'machine learning' whereby the computer receives data on classified SNPs (classed as either disease-causing or neutral) and attempts to find a pattern that successfully distinguishes between the 2 classes. Once the pattern is created, it can be applied to unclassified SNPs to predict the probability that they cause disease.

Creation of this method requires information about the Kv channel family to be collated and stored. This data is made publicly available via a website called KvDB

(www.bioinformatics.leeds.ac.uk/KvDB). The machine learning tool requires that each SNP has many 'features' associated with it, such as location within the gene and, if appropriate, within the protein structure. The latter requires the accurate identification of the transmembrane segments within the protein sequence. A new method for accurately predicting the transmembrane segments within Kv channels has, therefore, been created and is also available via KvDB. The location of classified SNPs and experimentally-induced mutations will be mapped onto known Kv channel structures for further analysis before the final machine-learning method is completed and tested, as this may indicate other features of interest.

Predicting disease-causing genetic variation within voltage-gated potassium channels will help reveal the genotype-phenotype relationships of these channels and aid in the early diagnosis and treatment of diseases such as cardiac arrhythmogenesis.

Collaborators

Dr Ian Wood (Institute of Membrane and Systems Biology, University of Leeds)
Dr Chris Needham and Andy Bulpitt (School of Computing, University of Leeds)
Dr James Bradford (Paterson Institute for Cancer Research)

Publications

Care, M.A., Bradford, J.R., Needham, C.J., Bulpitt, A.J., and Westhead, D.R. (2009). Combining the interactome and deleterious SNP predictions to improve disease gene identification. *Hum. Mutat*. **30***,* 485-492.

Care, M.A., Needham, C.J., Bulpitt, A.J. and Westhead, D.R**.** (2007). Deleterious SNP prediction: Be mindful of your training data! *Bioinformatics* **23**, 664-672.

Funding

BBSRC for all reported work.

Identification of the ribonucleoprotein complex required for efficient export and translation of herpesvirus intronless mRNAs

James Boyne, Brian Jackson, Adam Taylor, Kevin Colgan and Adrian Whitehouse

Introduction

The nuclear export of mRNA composes one part of a larger network of molecular events that begin with transcription of the mRNA in the nucleus and end with its translation and degradation in the cytoplasm. During trafficking to the cytoplasm, a nascent mRNA undergoes numerous co-transcriptional processing steps, including 5' capping, splicing to remove introns and 3' polyadenylation. Of these events it has become clear that splicing is particularly important for mRNA nuclear export, as recruitment of multiprotein complexes required for mRNA export are bound to mRNA in a splicing dependent manner. Two multiple protein complexes, namely, hTREX and the EJC bind at separate locations on spliced mRNA. hTREX, which comprises Aly, UAP56 and the multiprotein ThoI complex, is recruited exclusively to the 5' end of the first exon, providing 5'-polarity and therefore directionality observed in mRNA export.

However, in contrast to the majority of mammalian genes, analysis of herpesvirus genomes has highlighted that most lytically expressed viral genes lack introns. Herpesviruses replicate in the nucleus of the host mammalian cell, and therefore require their intronless mRNAs to be exported out of the nucleus to allow viral mRNA translation in the cytoplasm. This therefore leads to an intriguing question concerning the mechanism by which the viral intronless mRNAs are exported out of the nucleus in the absence of splicing. To circumvent this problem, and to facilitate viral mRNA export, γ-2 herpes viruses encode the ORF 57 protein. ORF 57 interacts with Aly, binds viral RNA, shuttles between the nucleus and the cytoplasm and promotes the nuclear export of viral mRNA.

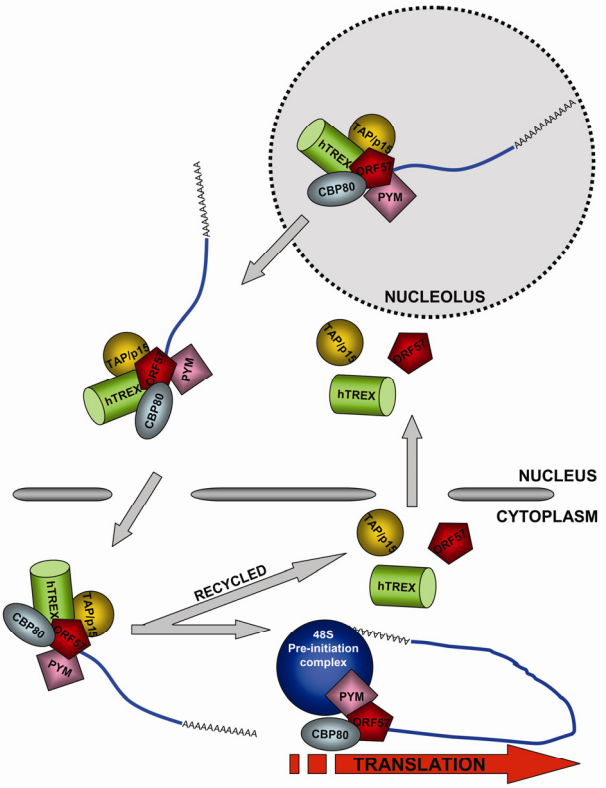

KSHV ORF57 mimics splicing to recruit the necessary nuclear export factors onto viral intronless transcripts and also mimics an EJC to enhance their translation

We are currently investigating how an intronless viral mRNP is assembled in KSHV and what role ORF57 plays in that process. We have shown that ORF57 interacts with hTREX and is essential for the recruitment of hTREX onto intronless viral mRNA transcripts. Importantly, ORF57 does not recruit the EJC to intronless viral transcripts. Moreover, we are currently determining how ORF 57 recognises the viral mRNA and allows recruitment of hTREX. This is the first system that has distinguished between hTREX and EJC *in vivo* and demonstrates that recruitment of hTREX alone to mRNA transcripts is sufficient for their nuclear export. Therefore, we believe this viral system is an exciting model to further study mRNA export mechanisms. We propose a model for herpesvirus mRNA export, whereby ORF57 mimics splicing in order to recruit the mRNA export machinery to intronless viral mRNAs.

Moreover, the inability of ORF57 to recruit the EJC may have implications for the efficiency of translation of the viral intronless mRNAs, as recent data suggests that the EJC promotes

efficient translation of spliced mRNAs by several mechanisms. One such mechanism involves the cellular protein, PYM, which links the EJC to the 48S pre-initiation complex. Therefore, we have investigated whehter KSHV ORF57 has any role in enhancing translation as well as nuclear export. We have shown that ORF57 sediments predominantly with the 40S ribosomal subunit and enhances translation of viral intronless transcripts. Moreover, we have demonstrated that ORF57 interacts with PYM and components of the 48S pre-initiation complex and functions to recruit PYM onto a viral intronless mRNA. Significantly, siRNA-mediated depletion of PYM ablates the interaction between ORF57 and components of the 48S pre-initiation complex and dramatically decreases the translation of KSHV intronless mRNAs. Therefore, we propose a model whereby ORF57 also mimics an EJC enabling efficient translation of intronless KSHV transcripts.

Publications

Boyne, J.R. Colgan, K.J. & Whitehouse, A. (2008). Herpesvirus saimiri ORF57: a post-transcriptional regulatory protein. *Frontiers in Bioscience,* 13, 2928-2938.

Emmott, E., Dove, B.K., Howell, G., Chappell, L., Reed, M.L., Boyne, J.R., You, J.H., Brooks, G., Whitehouse, A. & Hiscox, J.A. (2008). Viral nucleolar localisation signals determine dynamic trafficking within the nucleolus. *Virology*, 380, 191-202.

Boyne, J.R., Colgan, K.J. & Whitehouse, A. (2008). hTREX complex recruitment to Kaposi's sarcoma-associated herpesvirus intronless mRNA is essential for nuclear export. *PLoS Pathogens,* 4(10):e1000194.

Colgan, K.J., Boyne, J.R. & Whitehouse, A. (2009). Identification of a response element in a herpesvirus saimiri mRNA recognised by the ORF57 protein. *Journal of General Virology,* 90, 596 – 601.

Colgan, K.J., Boyne, J.R. & Whitehouse, A. (2009). Uncoupling of hTREX components demonstrates that UAP56 and hTHO-complex recruitment onto herpesvirus saimiri intronless transcripts is required for replication. *Journal of General Virology, In Press.*

Acknowledgements

This project is funded by the BBSRC, Wellcome Trust and Yorkshire Cancer Research.

Development of a herpesvirus-based bionanosubmarine

Stuart McNab, Julian Hiscox and Adrian Whitehouse

Introduction

The continuing advances and understanding in the field of molecular and cellular biology, and the underpinning genetic control mechanisms, has allowed the creation and development of non-traditional means for treating disease to be pursued such as gene therapy and bionanomedicine. We are currently developing a bionanosubmarine which delivers therapeutic genes to the correct cell types. The bionanosubmarine is based on elements of Herpesvirus saimiri (HVS). We have previously shown that HVS can infect a variety of human cell types and upon infection the viral genome can persist as a non-integrated episome in both *in vitro and in vivo* studies. Therefore, HVS has great potential to be developed as a bionanosubmarine. To achieve this, the infectious delivery system of HVS needs to be retained, but the viral genes need to be deleted and replaced with therapeutic genes.

The bionanosubmarine comprises a two tier system created in tissue culture. It utilises the biosafety of an amplicon vector plasmid coupled with the natural infectivity of the wild type virus. The system creates a virus like particle (VLP) containing the transgene of interest expressed from an amplicon vector. The VLP particle is essentially the wild type viral coat preferably lacking, or with minimal immuno-stimulatory antigens exposed. The VLP is generated by a helper-virus genome which contains all the necessary structural genes while remaining replication deficient.

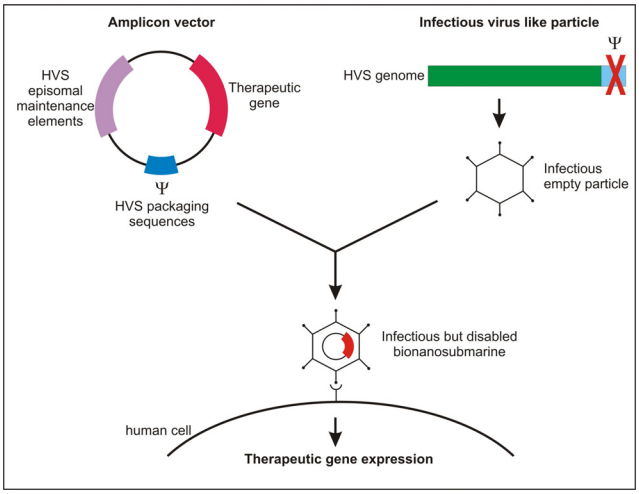

An amplicon is a gutless vector derived from a viral genome. The amplicon contains a transgene, the related expression sequences, and the *cis*-acting sequences required for replication, cleavage, and packaging into the VLP. The amplicon carries no transacting virus genes and consequently does not induce synthesis of virus proteins. Therefore, these vectors are non-toxic for the infected cells and non-pathogenic for the inoculated organisms. Another major advantage of the amplicon system is the removal of most of the virus genome, this consequently creates a transgene capacity equivalent in size to the wild type virus genome.

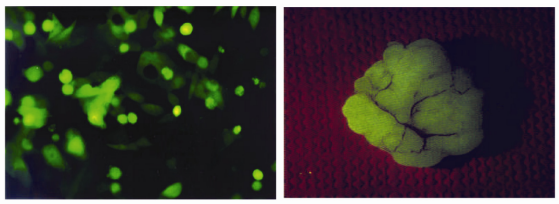

Bowel cancer cells infected the HVS in vitro and in vivo

To date, we have produced a bionanosubmarine, namely the VLP containing the amplicon. We have demonstrated that the bionanosubmarine is exported from the culture cell in the normal manner of the wild type virus and can then be harvested from the culture system and is still infectious. In particular, we have used these VLPs expressing GFP to show that we can

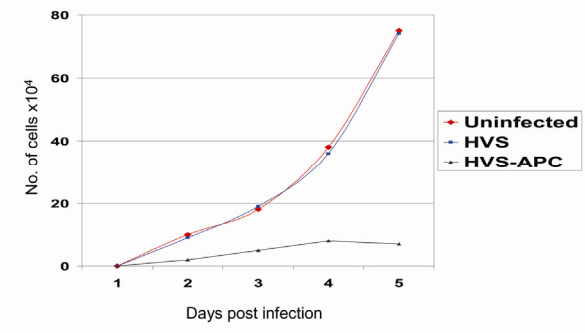

efficiently infect human colorectal cancer cells. Moreover, we have engineered the herpesvirus to express a functional copy of APC colorectal cancer tumour suppressor gene. Upon infect of colorectal cancer cells this APC-expressing VLP inhibits their growth of colorectal cancer cells *in vitro* and is now being tested in animal bowel cancer models.

Publications

Macnab, S., White, R.E., Hiscox, J.A. & Whitehouse, A. (2008). Production of an infectious Herpesvirus saimiri-based episomally maintained amplicon system *Journal of Biotechnology,* 134, 287-296.

Griffiths, R., Harrison, S.M., Macnab, S. & Whitehouse, A. (2008). Mapping the minimal regions within the ORF73 protein required for Herpesvirus saimiri episomal persistence. *Journal of General Virology*, 89, 2843 – 2850.

Gao, J., Coulson, J.M., Whitehouse, A. & Blake, N. (2009). Reduction in RNA levels rather than retardation of translation is responsible for the inhibition of MHC Class I antigen presentation by the glutamic acid rich repeat of Herpesvirus saimiri ORF73. *Journal of Virology,* 83, 273-282.

Acknowledgements

This project is funded by the University of Leeds Interdisciplinary Institute of Bionanoscience.

Repressosome formation and disruption regulates the KSHV latent-lytic switch

Faye Gould and Adrian Whitehouse

Introduction

The etiological agent of Kaposi's Sarcoma, Kaposi's sarcoma associated herpesvirus virus (KSHV), is the most recently identified human tumour virus. KSHV has two distinct forms of infection, latent persistence and lytic replication. The switch between these phases is important as lytic replication plays an essential part in the pathogenesis and spread of KSHV infection. The KSHV Rta protein is the key gene product which regulates viral lytic gene expression as sustained transient expression of Rta in a KSHV-latently infected cell line leads to the stimulation of its own expression and consequently viral lytic replication. This implicates the Rta protein as the molecular switch for reactivation and initiation of the KSHV lytic replication cycle.

We are currently investigating the host cell-Rta interactions to further understand the role of KSHV Rta in the latent-lytic switch. We have demonstrated that KSHV Rta interacts with the cellular protein, Hey-1. Hey-1 functions as a transcriptional repressor, acting as adapter protein that binds to specific DNA binding sites within gene promoters, and subsequently recruits transcriptional repressosome complexes. The interaction between KSHV Rta and the transcriptional repressor protein Hey-1 is a particular intriguing one. Why would Rta interact with a transcriptional repressor protein, given the role of Rta in transcriptional activation and initiating the lytic replication cycle? However, we have shown that the Hey-1- Rta interaction is an essential interaction playing a pivotal role in regulating the KSHV latent-lytic switch.

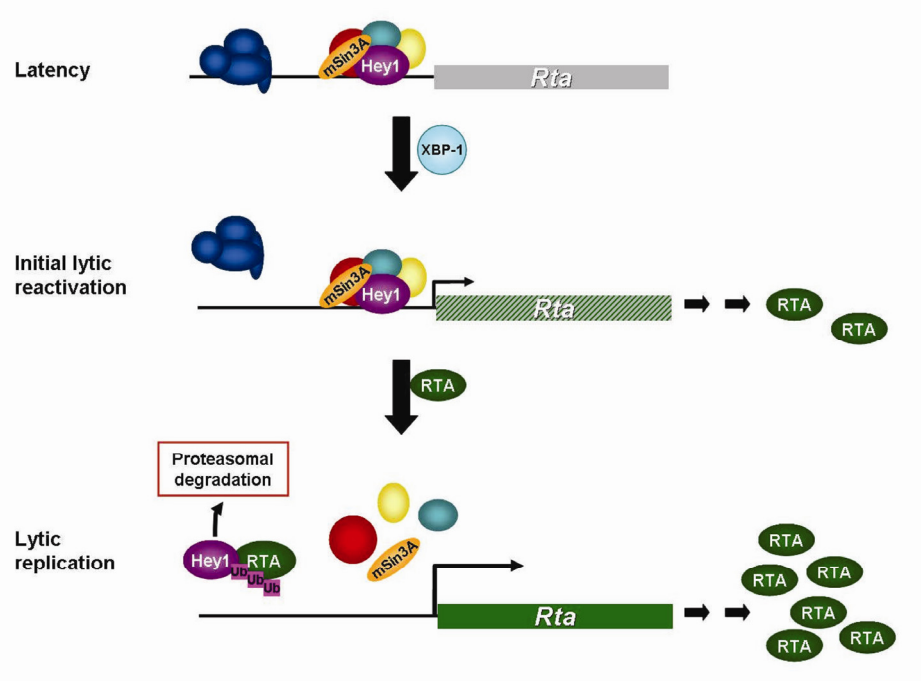

Recently, it has been shown that Rta is a novel E3 ubiquitin ligase that targets a number of transcriptional repressor proteins for degradation by the ubiquitin-proteasome pathway. Therefore, we believe we have identified a novel target for Rta's ubiquitin ligase activity. We have demonstrated that Hey1 is a target for Rta-mediated ubiquitination is degraded by the proteasome. Moreover, a Cys plus His-rich region within RTA is important for Rta-mediated degradation of Hey1. We also showed that Hey1 represses the Rta promoter and binds to the RTA promoter. An interaction was also observed between Hey1 and the co-repressor mSin3A and this interaction was abolished in the presence of Rta. Additionally, mSin3A associated with the Rta promoter in unreactivated, but not reactivated, BCBL1 cells. Moreover, siRNA knockdown of Hey1 in KSHV-latently infected rKSHV.219 HEK 293T cells led to increased levels of Rta expression upon reactivation, but was insufficient to induce complete lytic reactivation. These results suggest that other additional transcriptional

repressors are also important in maintenance of KSHV latency. Taken together our results suggest a contributory role for Hey1 in the maintenance of KSHV latency, and that disruption of the Hey1 repressosome by Rta-targeted degradation may be one step in the mechanism to regulate lytic reactivation. This project will provide valuable information on KSHV reactivation that may ultimately lead to the identification of specific antiviral targets to inhibit ORF 50–host cell interactions which may be developed as a novel treatment for this important human pathogen.

Publications

Wilson, S.J., Tsao, E., Webb, B.L., Ye, H., Dalton-Griffin, L., Tsantoulas, C., Gale, C.V., Du, D., Whitehouse, A. & Kellam, P. (2007). XBP-1 transactivates the KSHV ORF50 promoter, linking plasma cell differentiation to KSHV reactivation from latency. *Journal of Virology,* 81, 13578-13586.

Harrison, S.M. & Whitehouse, A. (2008). Kaposi's sarcoma associated herpesvirus (KSHV) Rta and cellular HMGB1 proteins synergistically transactivate the KSHV *ORF50* promoter. *FEBS Letters,* 50, 3080-3084.

Acknowledgements

This project is funded by the Wellcome Trust and BBSRC.

Design and synthesis of small molecule probes for the study of protein recognition

Fred Campbell, Maria Filby, James Muldoon, Jeffrey P. Plante, George Preston, Alison E. Ashcroft, Thomas A. Edwards, Martin J. Parker, Sheena E. Radford, Stuart Warriner and Andrew J. Wilson

Introduction

Our group is interested in the development of small functional molecules that are used to study protein recognition and self assembly. Specifically, we have designed receptors to recognise protein surfaces and inhibit α-helix mediated protein-protein interactions (PPIs). We are also interested in elucidating mechanisms of amyloid assembly using a photoactive chemical probe. The current report describes our latest synthetic efforts in these areas.

α-Helix mimetics

We have set out to design and synthesise libraries of small molecules that recapitulate the key structural and recogntion features of an α-helix. Such compounds are proposed to inhibit α-helix mediated PPIs and we previously described the solution phase syntheses a series of aromatic oligoamide scaffolds. In the past year we focused on developing the syntheses of Fmoc protected monomers (Fig. 1), which in turn allowed us to carry out shorter, more convergent oligomer syntheses.

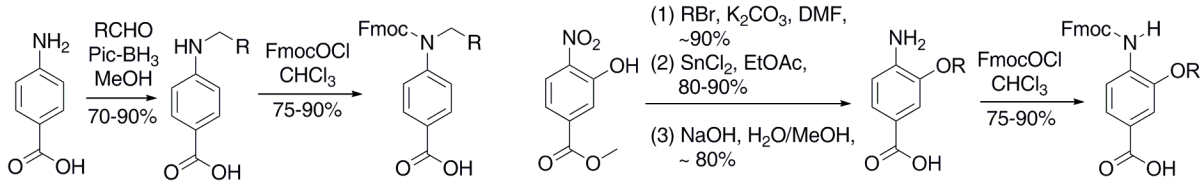

Figure 1 Synthesis of monomers that form the building blocks of aromatic oligoamide helix mimetics

Design and synthesis of ruthenium complexes for recognition of protein surfaces

Alongside our interest in controlling α-helix mediated PPIs, we have synthesised a series of ruthenium complexes as shown in Fig. 2. These are designed to recognise less well defined protein surfaces with high affinity and selectivity by multivalent presentation of recogntion arms from the core Ru(Bipy)$_3$ scaffold onto the protein-surface. Our current and future studies are focusing on recognition of proteins such as cytochrome *c* and will rely on fluorescence titration and isothermal titration calorimetry.

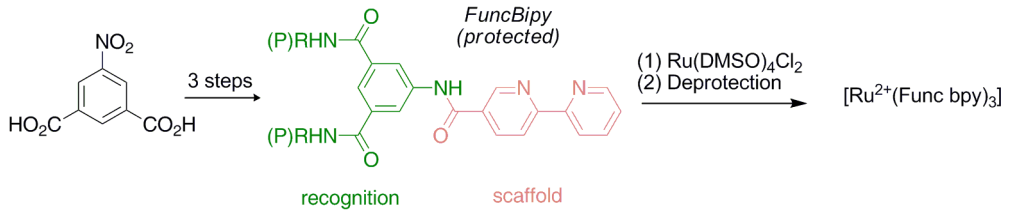

Figure 2 Synthesis of one of the bpy ligands and ruthenium complex

Chemical biology of amyloid formation

Our final area of interest concerns self assembly of amyloid fibrils using photocrosslinking. Proof-of-principle experiments using trifluoromethyldiazirinephenylalanine (tfmd-Phe) incorporated into A$\beta_{16\text{-}22}$ – a peptide that forms amyloid fibrils – established that the probe does not perturb fibril formation. Irradiation of such fibrils at 350 nm initiates trapping *via* a highly reactive carbene and trapped products could be sequenced using IMS-MS to identify

the position of crosslinking. Tfmd-Phe is not commercially available and must be synthesised *via* a multi-step route. We have recently adapted our method to employ an organocatalytic alkylation in a key step of this synthesis (Fig. 3). Ongoing studies concern incorporation of this probe into different and multiple sites within $A\beta_{16\text{-}22}$.

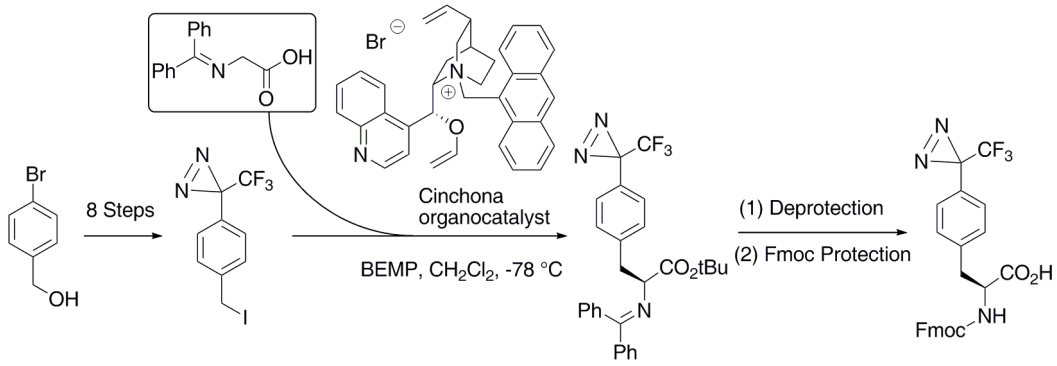

Figure 3 Synthetic route for tfmd-Phe derivative.

Collaborators

We gratefully acknowledge Nicholas Fletcher and Serin Dabb (University of Belfast) for synthesis of bypyridine precursors.

Publications

Smith, D. P., Anderson, J., Plante, J., Ashcroft, A. E., Radford, S. E., Wilson, A. J. & Parker M. J. (2008) Trifluoromethyldiazirine: an effective photo-induced cross-linking probe for exploring amyloid formation. *Chem. Commun.,* 5728-5730.

Plante, J., Campbell, F., Malkova, B., Kilner, C., Warriner, S. L. & Wilson, A.J. (2008) Synthesis of functionalised aromatic oligamide rods. *Org. Biomol. Chem.*, **6**, 138-146.

Campbell, F., Plante, J., Carruthers, C., Hardie, M. J., Prior, T. J. & Wilson, A. J. (2007) Macrocyclic Scaffolds Derived From Para-Aminobenzoic Acid. *Chem. Commun.* 2240-2242.

Funding

We gratefully acknowledge BBSRC, EPSRC, the University of Leeds and The Wellcome Trust for financial support of this research.

pH-driven DNA nanostructures and devices

Dejian Zhou

Introduction

Over the past two decades, DNA has been demonstrated as an extremely powerful and versatile building material for nanotechnology and a range of novel DNA nanostructures, devices and molecular motors have been constructed. However, most such DNA molecular motors are powered by DNA fuels that often leads to slow operation speed and suffers system poisoning due to accumulation of waste DNAs. As a result, their performance gradually degrades after a few cycles, a major factor limiting their potential applications. On the other hand, a pH-driven DNA molecular motor, using a single DNA strand containing 4 stretches of cytosine (C) rich domains, is extremely robust and shows no performance degradation after 30 full operational cycles. It can reversibly switch its conformation between a closed 4-stranded i-motif structure in slightly acidic pHs and a random coil (or duplex on hybridization to a complementary strand) in neutral to basic pHs. Such conformational changes produce well-defined, highly reversible nanoscale contraction/extension motions. The resulting closing and opening of the DNA motor is accompanied significant forces (~ 10 pN). Here we show such forces could be harnessed to construct a reconfigurable DNA nanotriangle.

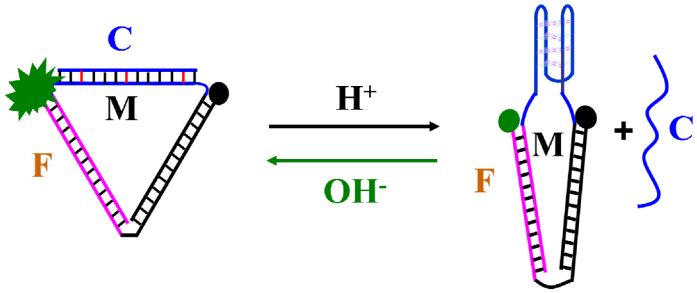

Figure 1. Schematic illustration of the reversible configuration of the DNA nanotriangle.

Fig. 1 shows the construct and principle of the pH-driven DNA nanotriangle. It is made of three single-stranded DNAs, **F**, **M** and **C**. **M** has three unique sequence domains: the first and the last domains, each containing 20 bases, are fully complimentary to the two corresponding domains of **F**, while the middle 25 base domain, with 4 stretches of CCCC, is complementary to **C**. Three mismatches between **C** and **M** middle domain are engineered to tune the melting temperature such that **C** can hybridize/dehybridize to/from the middle domain reversibly in a pH dependent manner. In neutral to basic pHs, all three DNA strands are hybridised together to form a rigid DNA nanotriangle (open state). When the pH is reduced to slightly acidic, the middle domain of **M** folds into an i-motif, leading to dehybridization of the **C** and closing of the nanotriangle. This system can be cycled a number of times by sequentially adding base/acid to change the pH.

Native gel electrophoresis has confirmed that they can assemble into the respective DNA structure with expected gel shift mobility. To readout such structural changes optically, the 5' and 3' ends of **F** are labeled with a rhodamine green and a quencher (dabsyl), and the Förster resonance energy transfer (FRET) between the fluorophore and the quencher is used to confirm the structural reconfiguration. When the structure is in the open state, the fluorophore is separated far away from the quencher, resulting in inefficient energy transfer and hence strong fluorescence. Whereas in the closed state, the fluorophore and quencher are brought to the close proximity to each other, resulting in efficient energy transfer and strong quenching of the fluorescence.

Fluorescence spectra of the DNA nanotriangle at pHs 5.0 and 8.0 are given in Fig. 2A.

Both spectra are characteristic for rhodamine green that peaks at ~ 532 nm, except the fluorescence at pH 8.0 being over twice as strong as that at pH 5.0. The pH dependent fluorescence is consistent with that the DNA nanotriangle is in an extended, open state at pH 8.0, where a big quencher-dye distance leads to little/no quenching, but adopts a contracted, closed state at pH 5.0, where a small quencher-dye distance leads to efficient quenching.

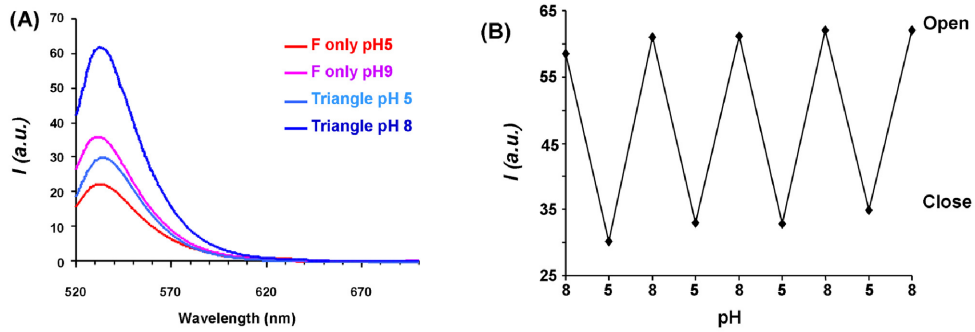

Figure 2 (**A**) Fluorescence spectra of the DNA nanotriangle (0.5 μM) at pH 5 (light blue) and 8 (dark blue) and the control with DNA F only (0.5 μM) at pH 5 (red) and 9 (purple). (**B**) Fluorescence intensity of the DNA nanotriangle at different pH cycles (corrected for dilution following each acid/base addition).

A control with the dual-labelled **F** only reveals a much smaller pH-induced fluorescence change (Fig. 2A), confirming the observed fluorescence change is specific to the DNA nanotriangle. Fig. 2B shows the cyclical changes of the fluorescence at 532 nm as a result of a series pH cycles recorded within 1 min after each pH change. This system shows highly repeatable changes in fluorescence intensity as the pH is sequentially cycled between 5.0 and 8.0. No observable changes in the operational amplitude (changes of the fluorescence intensity) are detected after 4 cycles, suggesting this system is robust and highly reversible. It is noteworthy that the response of this system is fast and completes in 1 min after each pH change, 1-2 orders of magnitude faster than other DNA-fuelled systems.

In summary, we have constructed a simple, robust DNA nanotriangle that can be easily and precisely reconfigured *via* the change of environmental pH. Compared to other DNA fuelled systems, our system has the advantages of clean switching mechanism (no DNA waste is produced), significantly faster response (1 min, 1-2 orders of magnitude faster), robust and highly reversible (no performance degradation). This robust, reconfigurable DNA nanostructure will be an excellent building block for the construction of more complex nanostructures, and may have broad applications as novel nanomechanical and electronic devices as well as novel drug delivery system.

Publications

Wang, W., Yang, Y., Cheng, E., Zhao, M., Meng, H., Liu, D. & Zhou, D. (2009) A pH-driven, reconfigurable DNA nanotriangle. *Chem. Commun.* 824-826.

Wang, W., Liu, H., Liu, D., Xu, Y., Yang, Y. & Zhou, D. (2007) Use of inter-particle i-motif for controlled assembly of gold nanoparticles. *Langmuir* 23, 11956-11959.

Collaborator

Prof. Dongsheng Liu, National Centre for Nanoscience & Technology, Beijing, China

Funding

This work was supported by the Royal Society and the National Science Foundation of China.

Coarse-grained simulations of lipid bilayers: the role of composition and the nature of interactions with detergents and peptides

Brett T. Donovan, Nigel Hooper, Richard Bingham and Peter D. Olmsted

Introduction

Phospholipid bilayers comprise an astonishingly large number of lipid species, as well as myriad proteins. In the last decade, the Singer-Nelson mosaic model of a homogeneously mixed membrane has been challenged by the "raft" hypothesis: that small domains rich in cholesterol and fully saturated lipids can exist and play important roles in processes such as cell signalling. Lipid bilayers have many other degrees of freedom that contribute to their function: in addition to lipid composition, lipid bilayers are typically asymmetric (comparing the outer and inner leaflets), contain proteins that influence shape and function (e.g. caveolin), and can respond easily to applied electric fields.

Phase behaviour and detergent effects

"Raft" domains were first inferred from detergent extraction experiments, and have been correlated with the presence of certain proteins. Hence, there is much yet to learn about the role of composition and the phase of lipid bilayers, as well as the nature of interactions between membranes and proteins. We have been developing simple coarse-grained models with which to study these issues: a four bead lipid is sufficient to describe saturated and unsaturated (kinked) lipids, which can be used to answer qualitative issue about phase separation on length scales much larger than possible in atomistic simulations. A simple model for detergents, which can be mapped to those in widespread use, has allowed us to distinguish different routes by which membranes are dissolved: in addition to addressing detergent dissolution, this is useful for understanding topological changes that occur in complex membranes such as the ER and the Golgi apparatus.

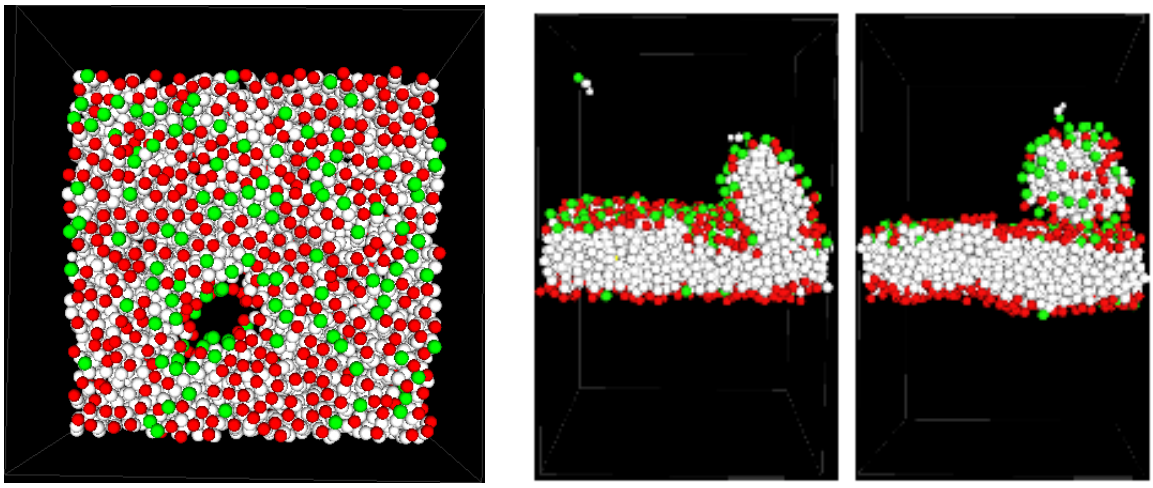

Figure 1 – Cartoons of pore formation and budding driven by excess detergent (green) adsorbed on one leaflet of a lipid bilayer**.**

Peptide-membrane interactions

Alpha-helical peptides can aggregate in membranes, form pores, and lyse membranes. We have developed a coarse-grained model with which to understand these processes: the peptide is assumed to be folded in a rigid alpha helix, with a hydrophobic moment determined by the sequence of amino acids around the helix. We have delineated how the hydrophobic moment and peptide length influences the orientation of peptides. This work will be continued next to study aggregation and folding in more realistic (but still coarse-grained) models.

Electroporation
Electroporation is widely used to deliver drugs and other vectors to cells. Despite general use, its mechanism is still poorly understood. We have considered the interaction between the applied electric field and the dipole moment in typically phospholipid head groups. The action of tilting the dipole moment can destabilize the membrane and induce an instability that could be a precursor to pore formation.

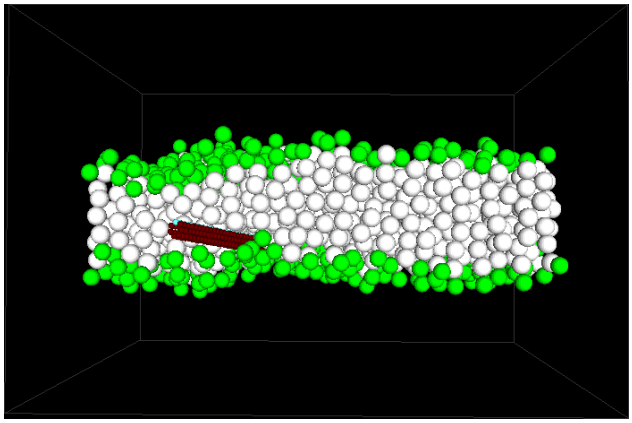

Figure 2 Illustration of a short and mainly hydrophobic (coarse-grained) peptide lying within the plane of a bilayer.

Collaborators
Stephen Smye, Leeds Teaching Hospitals.

Funding
Funding from EPSRC is gratefully acknowledged.

Conserved structure of compact myosin 2 in species separated by at least 600 million years of independent evolution

Hyung-Suk Jung, Stan A. Burgess, Neil Billington and Peter J. Knight

Introduction

The myosin 2 family not only comprises those isoforms found in muscle cells that drive muscle contraction, but also those responsible for intracellular movements such as cytokinesis or neuronal dynamics. Myosin 2 forms filaments from which myosin heads interact cyclically with actin, powered by hydrolysis of ATP. The C-terminal halves of the two heavy chains comprising each myosin molecule associate to form an α-helical coiled-coil tail while the N-terminal halves fold separately to form the two heads. Each head has a motor domain, containing actin and ATP binding sites, connected to the tail by an α-helical lever that is stabilised by an essential light chain (ELC) and a regulatory light chain (RLC). Across the Animal Kingdom, myosin 2 includes isoforms whose activity is regulated in different ways. Vertebrate smooth muscle myosin (SmM) is activated by phosphorylation of the RLC whereas scallop striated adductor muscle myosin (ScM) is activated by calcium binding to its ELC. The paired heads of inhibited molecules from myosins regulated by phosphorylation have an asymmetric arrangement with motor-motor interactions. Both myosins can form compact molecules distinct from the extended molecules found at high salt concentrations. For SmM from turkey gizzard, our recent electron microscopy had shown that the compact conformer has the tail folded back close to the heads, and we obtained a detailed structure of the head region and the path of the folded-up tail. It was unknown whether such interactions were a common motif for inactivation used in other forms of myosin-linked regulation. Therefore we have compared structures of the compact molecules of SmM and ScM, using negative-stain electron microscopy and single particle image processing.

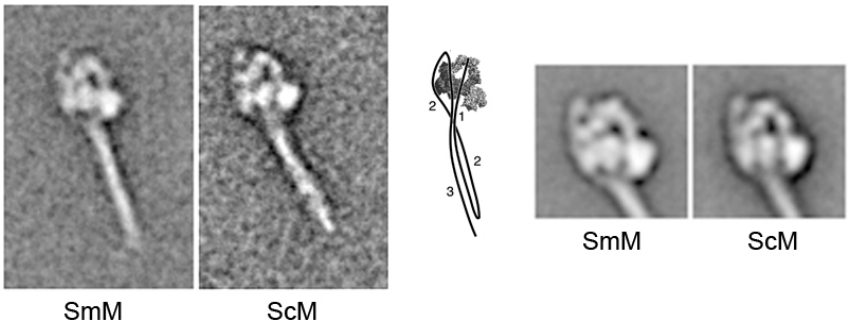

Figure 1 - Close similarity of compact molecules of turkey gizzard smooth muscle myosin (SmM) and scallop striated muscle myosin (ScM). The central diagram explains how the appearances originate from the two heads and the three segments of the folded-up tail.

Myosin 2 forms the same compact structure in scallop and turkey

At the resolution of the electron microscope images (~2 nm), these two remote members of the myosin 2 family are indistinguishable (Fig. 1). Not only are the shapes and asymmetric dispositions of the two heads the same, but the tail folds at apparently identical sites and wraps around the left head in an identical way. A test of whether two datasets are indeed indistinguishable is to combine them and use image processing to align them together and group similar molecules together into classes. If the datasets are indistinguishable, both will contribute roughly equally to the classes. On this basis too, we find no differences in structure. Thus these myosins which have different regulatory mechanisms and which diverged from a common ancestral myosin at least 600 Myr ago have retained the same quaternary structure for this inhibited state. Conservation across such a large evolutionary distance suggests that this conformation is of fundamental functional importance, though we do not yet understand the role that it plays in the life of the muscle cell.

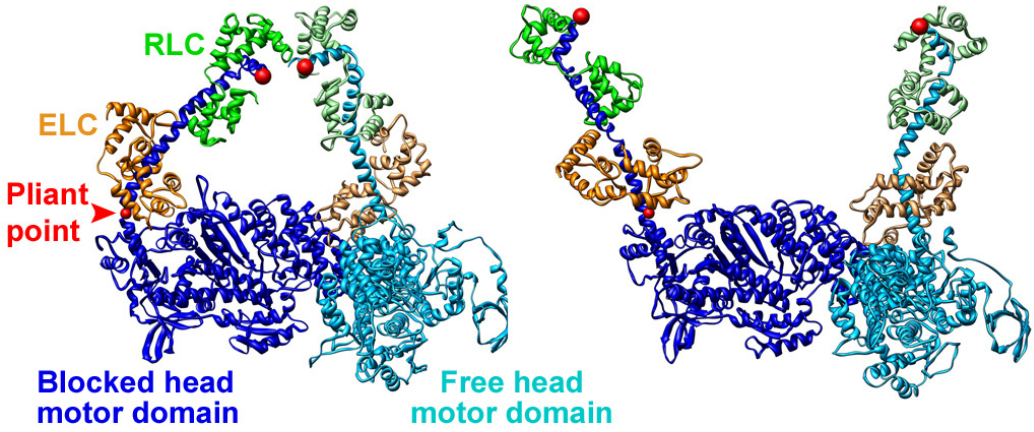

Figure 2 - Structure of scallop myosin heads inferred from our images of the inhibited state (left), contrasted with available scallop head structures (right). The red spheres at the ends of both the two levers have to join onto a single tail: easy for the left-hand model; impossible for the right-hand one.

Scallop head has to bend to form the compact structure

The close similarity of the compact scallop molecules to the smooth muscle ones implies that the heads have the same shape in both species. It is therefore interesting to note that there is a disruption of the heavy chain α-helix at the motor-lever junction in the SmM head (the 'Pliant point'; Fig. 2) that has so far not been seen in any ScM head crystal structure. This bend brings the ELC into new contacts with the motor domain, but the importance of these contacts in the regulatory mechanism remains to be discovered.

Collaborators

Prof. Joseph Chalovich, East Carolina University, Greenville, NC, USA
Prof. Peter D. Chantler, Royal Veterinary School, London, UK

Publications

Jung, H.S., Burgess, S.A., Billington, N., Colegrave, M., Patel, H., Chalovich, J.M., Chantler, P.D. & Knight, P.J. (2008). Conservation of the regulated structure of folded myosin 2 in species separated by at least 600 million years of independent evolution. *Proc. Natl. Acad. Sci. USA*. **105**, 6022-6026.

Funding

Funding from BBSRC and NIH is gratefully acknowledged.

Structural and enzymatic studies on a novel substituent of *Mycobacterium tuberculosis* lipoarabinomannan

Susanne Stalford, Martin Fascione and Bruce Turnbull

Introduction

Tuberculosis (TB) remains a major threat to world health, with approximately eight million cases of TB resulting in two million deaths per annum. The WHO has highlighted the urgent need for more effective anti-TB drugs and for rapid, specific and sensitive diagnostic tests for the causative agent, *Mycobacterium tuberculosis* (Mtb). The lipid-anchored polysaccharide, lipoarabinomannan (LAM, Fig 1), is a major component of the Mtb cell wall, and an important virulence factor for the bacterium. Mannose residues that cap the dendritic arabinan chains of LAM, facilitate entry of Mtb into alveolar macrophages, following interaction with the macrophage mannose receptor. LAM then promotes the intracellular survival of Mtb by down-regulating the immune response and providing anti-oxidative protection for the bacterium.

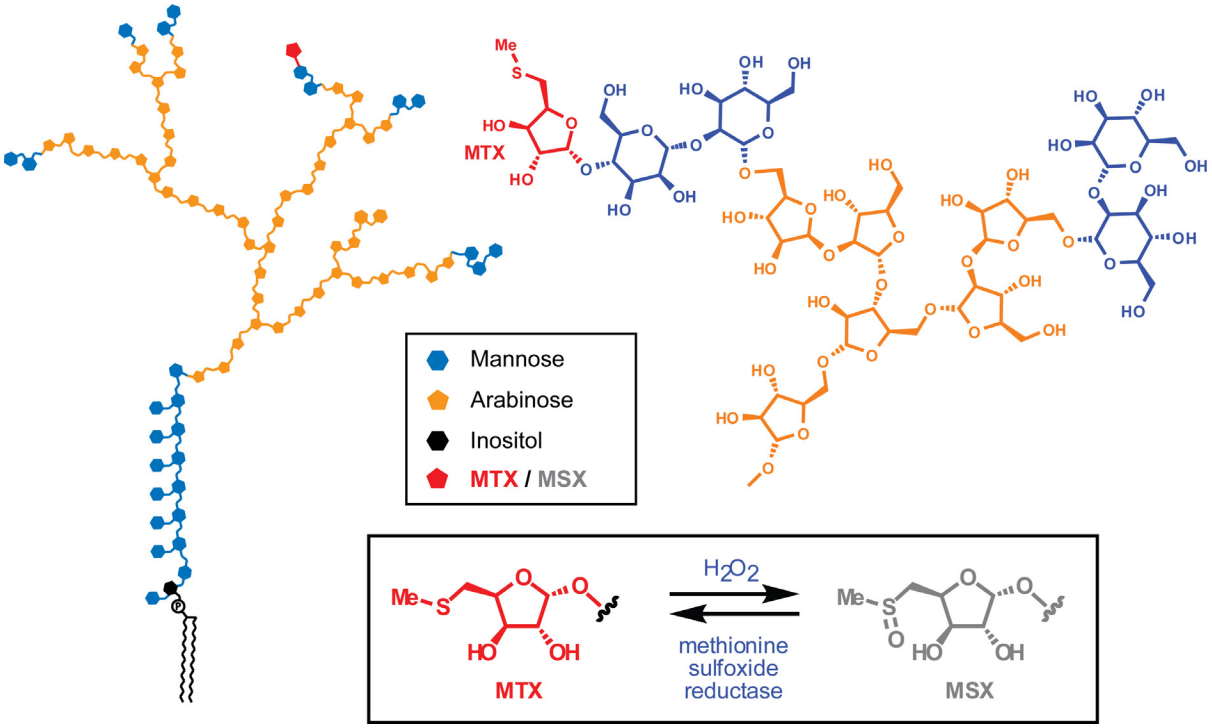

Figure 1. Schematic representation of LAM showing the structures of the MTX and MSX substituents and their interconversion by chemical oxidation and enzymatic reduction.

Recently, we discovered an unusual methylthiopentosyl residue attached to the mannosyl caps of LAM, which we subsequently identified as having an α-xylo configuration. This unusual discovery constitutes the first report of a methylthio-sugar residue incorporated into a polysaccharide, and one of very few examples of a xylo-configured sugar outside the plant kingdom. Mtb invests significant biosynthetic effort into incorporating MTX into its cell wall, which implies that this sugar may provide some advantage to the bacterium. The concurrent discovery of an oxidised form of the sugar (methylsulfinylxylose, MSX, Fig. 1), implies that MTX may play a role in oxidative protection for Mtb.

We have demonstrated that exposure of LAM to the biological oxidant H_2O_2 results in oxidation of only the MTX substituent (Fig.2). We have also found that the *S*-configured MSX sulfoxide can be reduced by the mycobacterial methionine sulfoxide reductase enzyme (MsrA). While oxidation of MTX would almost certainly affect its biological function *in vivo*, this damage could

be repaired, in part, by MsrA which is present in the mycobacterial cell wall/membrane fraction. Alternatively, there exists the possibilty that MSX on the surface of *M. tuberculosis* may be reduced by host MsrA (and MsrB that reduces the *R*-sulfoxide) when the bacteria reside inside macrophages. If so, then MSX would be the first natural non-protein substrate for these enzymes. Furthermore, this redox cycle of chemical oxidation and enzymatic reduction could also provide a mechanism for more general anti-oxidative protection, as has been established previously for methionine oxidation. Indeed, as H_2O_2 is a direct precursor of hydroxyl radicals in vivo, sequestration of H_2O_2 by MTX/MsrA could also reduce the production of OH• in the mycobacterial cell wall. The MsrA-catalysed reduction of MSX-LAM has also allowed us to prove that the MSX/MTX sugars have the absolute D-configuration.

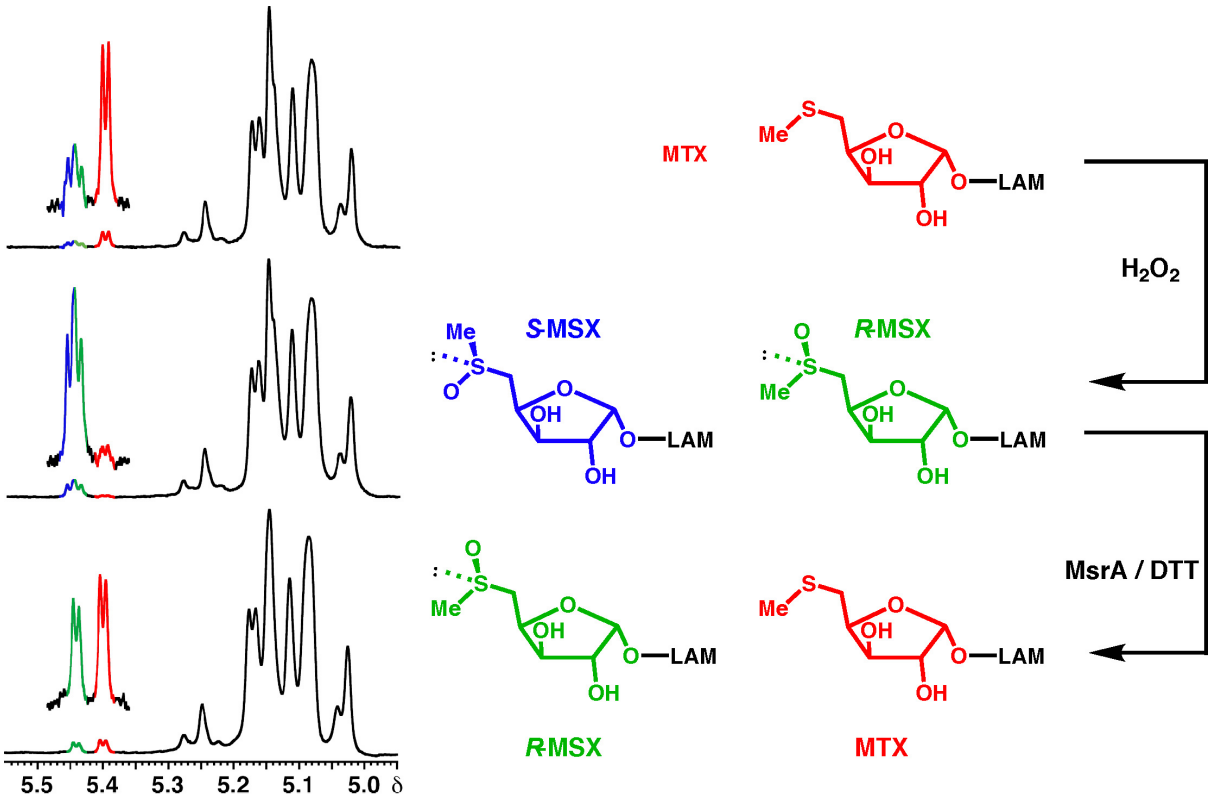

Figure 2. NMR spectra of *M. tuberculosis* LAM with the MTX and MSX anomeric protons inset. Oxidation of MTX leads to two diastereoisomers of MSX, one of which is reduced back to MTX using the MsrA enzyme.

Publications

Stalford, S.A., Fascione, M.A., Sasindran, S.J., Chatterjee, D., Dhandayuthapani, S. & Turnbull, W.B. (2009) A natural carbohydrate substrate for *Mycobacterium tuberculosis* methionine sulfoxide reductase A, *Chem. Commun.*, 110-112.

Collaborators

Delphi Chatterjee, Department of Microbiology, Immunology and Pathology, Colorado State University, USA.

Subramanian Dhandayuthapani, University of Texas Health Science Center at San Antonio, Edinburg, TX, USA.

Funding

This work is funded by the Royal Society, NIH and the University of Leeds.

Astbury Seminars 2008

17th January 2008
Prof Cees Dekker, Kavli Institute of NanoScience, Delft University of Technology
"Nanotechnology tools for biology, the power of single-molecule biophysics"

14th February 2008
Prof Thomas Kiefhaber, Department of Chemistry, Technical University of Munich
"Folding and stability of a trimeric assembly domain from phage T4 fibritin: What God has put asunder let no man join together"

13th March 2008
Prof Peter Leadlay FRS, Department of Biochemistry, University of Cambridge
"Engineering of multienzymes for antibiotic biosynthesis: from mechanisms to medicines"

27th March 2008
Prof Dagmar Klostermeier, Biophysical Chemistry, University of Basel
"Illuminating ATP-driven conformational changes in DEAD box helicases and their role for RNA unwinding"

3rd April 2008
Dr Paul Ko Ferrigno, Leeds Institute of Molecular Medicine
"Engineering a peptide aptamer toolkit for biological and clinical discovery"

8th May 2008
Prof Jack Johnson, Department of Molecular Biology, The Scripps Research Institute
"Biophysical Studies of Virus Particles and their Maturation: the Science and Technology of Programmed Nano-machines"

16th May 2008
Prof Sara Linse, Biophysical Chemistry, Centre for Molecular Protein Science, Lund University
"Protein association and fibrillation - the effects of nanoparticles"

22nd May 2008
Dr Jonathan Heddle, Tokyo Institute of Technology, Japan
"A ring-shaped protein as a novel component of nanodevices"

5th June 2008
Prof Gert Vriend, Centre for Molecular and Biomolecular Informatics, Radboud University Nijmegen Medical Centre
"Genetic disorders, bioinformatics, and protein structure"

3rd July 2008 The Astbury Annual Lecture
Prof Ulrich Hartl, Max Planck Institute of Biochemistry
"Chaperone-assisted protein folding in health and disease"

11th September 2008
Dr Ehmke Pohl, Wolfson Research Institute, University of Durham
"Spectroscopic and structural studies of the metal-dependent regulator proteins FurA and FurB from M. tuberculosis*"*

15th September 2008
Dr Karen Fleming, Thomas C Jenkins Department of Biophysics, Johns Hopkins University
"Membrane Protein Folding"

9th October 2008
Dr Paul Bates, Cancer Research UK
"Protein-Protein Interactions in Their Social Context"

23rd October 2008
Prof Peter Henderson, Astbury Centre for Structural Molecular Biology, The University of Leeds
"Insights into the molecular mechanism of membrane transport from the novel structure of Mhp1"

7th November 2008
Prof James McNamara, Department of Internal Medicine, University of Iowa
"RNA Aptamer Based Therapeutic Approaches"

27th November 2008 ***Joint seminar with Ion channels@Leeds***
Prof Raimund Dutzler, Department of Biochemistry, University of Zurich
"Structural basis for ion conduction and gating in prokaryotic pentameric ligand gated ion channels"

11th December 2008
Dr Liming Ying, National Heart and Lung Institute, Imperial College London
"Single Molecule Approaches to Biology"

Publications by Astbury Centre Members 2008

Agarwal, A.K., Johnson, A.P. and Fishwick, C.W.G. (2008) Synthesis of *de novo* designed small-molecule inhibitors of bacterial RNA polymerase. *Tetrahedron*, 64, 10049-10054.

Ananieva, O., Macdonald, A., Wang, X., McCoy, C., McIlrath, J., Tournier, C. and Arthur, J.S.C. (2008) Identification of novel phosphorylation sites in Msk1 by precursor ion scanning mass spectrometry. *Biochem. J.*, 402, 491-501.

Barfoot, R.J., Sheikh, K.H., Johnson, B.R.G., Colyer, J., Miles, R.E., Jeuken, L.J.C., Bushby, R.J. and Evans, S.D. (2008) Minimal F-actin cytoskeletal system for planar supported phospholipid bilayers. *Langmuir*, 24, 6827-6836.

Bartlett, N.W., Walton, R.P., Edwards, M.R., Aniscenko, J., Caramori, G., Zhu, J., Glanville, N., Choy, K.J., Jourdan, P., Burnet, J., Tuthill, T.J., Pedrick, M.S., Hurle, M.J., Plumpton, C., Sharp, N.A., Bussell, J.N., Swallow, D.M., Schwarze, J., Guy, B., Walmond, J., Jeffery, P.K., Lloyd, C.M., Papi, A., Killington, R.A., Rowlands, D.J., Blair, E.D., Clarke, N.J. and Johnston, S.L. (2008) Mouse models of rhinovirus-induced disease and exacerbation of allergic airway inflammation. *Nat. Med.*, 14, 199-204.

Besong, G., Billen, D., Dager, I., Kocienski, P., Sliwinski, E., Tai, L.R. and Boyle, F.T. (2008) A synthesis of (aR,7S)-(-)-N-acetylcolchinol and its conjugate with a cyclic RGD peptide. *Tetrahedron*, 64, 4700-4710.

Best, R.B., Paci, E., Hummer, G. and Dudko, O.K. (2008) Pulling direction as a reaction coordinate for the mechanical unfolding of single molecules. *Journal Of Physical Chemistry B*, 112, 5968-5976.

Bhavin, K., Byrne, K., Kawakami, M., Brockwell, D.J., Smith, D.A., Radford, S.E. and McLeish, T.C.B. (2008) Internal friction of single polypeptide chains at high stretch. *Faraday Discuss.*, 139, 35-51.

Bolt, A., Berry, A. and Nelson, A. (2008) Directed evolution of aldolases for exploitation in synthetic organic chemistry. *Arch. Biochem. Biophys.*, 474, 318-330.

Boyne, J.R., Colgan, K.J. and Whitehouse, A. (2008) Recruitment of the complete hTREX complex is required for Kaposi's Sarcoma-Associated herpesvirus intronless mRNA nuclear export and virus replication. *PLloS Pathogens*, 4.

Boyne, J.R., Colgan, K.J. and Whitehouse, A. (2008) Herpesvirus saimiri ORF57: A post-transcriptional regulatory protein. *Front. Biosci.*, 13, 2928-2938.

Breton, J., Gage, M.C., Hay, A.W., Keen, J.N., Wild, C.P., Donnellan, C., Findlay, J.B.C. and Hardie, L.J. (2008) Proteomic screening of a cell line model of esophageal carcinogenesis identifies cathepsin D and aldo-keto reductase 1C2 and 1B10 dysregulation in Barrett's esophagus and esophageal adenocarcinoma. *J. Proteome Res.*, 7, 1953-1962.

Burrows, P.C., Wigneshweraraj, S., Bose, D., Joly, N., Schumacher, J., Rappas, M., Pape, T., Stockley, P.G., Zhang, X.D. and Buck, M. (2008) Visualizing the organization and reorganization of transcription complexes for gene expression. *Biochem. Soc. Trans.*, 36, 776-779.

Carter, A.M., Rice, G.I., Standeven, K.F., Scott, D.J., Turner, A.J., Hooper, N.M. and Grant, P.J. (2008) Circulating neprilysin and cardiovascular risk: Associations with insulin resistance and the metabolic syndrome. *Heart*, 94, A58-A58.

Chambon, P., Fernyhough, C.M., Im, K., Chang, T.Y., Das, C., Embery, J., McLeish, T.C.B. and Read, D.J. (2008) Synthesis, temperature gradient interaction chromatography, and rheology of entangled styrene comb polymers. *Macromolecules*, 41, 5869-5875.

Chimienti, F., Wheeler, M.B., Nicholson, T.J., Bellomo, E.A., Wijesekara, N., Tarasov, A.I., Taneja, T., Sladek, R., Baldwin, S.A., Baldwin, J. and Rutter, G.A. (2008) Single nucleotide polymorphism rs13266634 modifies the zinc transport activity of SLC30A8/ZnT-8 in clonal pancreatic beta cells. *Diabetologia*, 51, 101.

Clarke, O.J. and Parker, M.J. (2008) Time-averaged predictions of folded and misfolded peptides using a reduced physicochemical model. *J. Comput. Chem.*, 29, 1177-1185.

Cordier, C., Morton, D., Leach, S., Woodhall, T., O'Leary-Steele, C., Warriner, S. and Nelson, A. (2008) An efficient method for synthesising unsymmetrical silaketals: Substrates for ring-closing, including macrocycle-closing, metathesis. *Org. Biomol. Chem.*, 6, 1734-1737.

Cordier, C., Morton, D., Murrison, S., Nelson, A. and O'Leary-Steele, C. (2008) Natural products as an inspiration in the diversity-oriented synthesis of bioactive compound libraries. *Nat. Prod. Rep.*, 25, 719-737.

Davis, M.P., Bottley, G., Beales, L.P., Killington, R.A., Rowlands, D.J. and Tuthill, T.J. (2008) Recombinant VP4 of human rhinovirus induces permeability in model membranes. *J. Virol.*, 82, 4169-4174.

Deacon, S.E., Roach, P.C.J., Postis, V.L.G., Wright, G.S.A., Xia, X.B., Phillips, S.E.V., Knox, J.P., Henderson, P.J.F., McPherson, M.J. and Baldwin, S.A. (2008) Reliable scale-up of membrane protein over-expression by bacterial auto-induction: From microwell plates to pilot scale fermentations. *Mol. Membr. Biol.*, 25, 588-598.

Dixon, N., Pali, T., Kee, T.P., Ball, S., Harrison, M.A., Findlay, J.B.C., Nyman, J., Vaananen, K., Finbow, M.E. and Marsh, D. (2008) Interaction of spin-labeled inhibitors of the vacuolar H^+-ATPase with the transmembrane V-o-sector. *Biophys. J.*, 94, 506-514.

Dodd, C.E., Johnson, B.R.G., Jeuken, L.J.C., Bugg, T.D.H., Bushby, R.J. and Evans, S.D. (2008) Native *E.coli* inner membrane incorporation in solid supported lipid bilayer membranes. *Biointerphases*, 3, FA59-FA67.

Duchesne, L., Wells, G., Ferning, D.G., Harris, S.A. and Levy, R. (2008) Supramolecular domains in mixed peptide self-assembled monolayers on gold nanoparticles. *Chembiochem*, 9, 2127-2134.

Dugan, G.E. and Hewitt, E.W. (2008) Structural and functional dissection of the human cytomegalovirus immune evasion protein US6. *J. Virol.*, 82, 3271-3282.

Dunn, S., Vohra, R.S., Murphy, J.E., Homer-Vanniasinkam, S., Walker, J.H. and Ponnambalam, S. (2008) The lectin-like oxidized low-density-lipoprotein receptor: A pro-inflammatory factor in vascular disease. *Biochem. J.*, 409, 349-355.

Dunsmore, C.J., Miller, K., Blake, K.L., Patching, S.G., Henderson, P.J.F., Garnett, J.A., Stubbings, W.J., Phillips, S.E.V., Palestrant, D.J., Angeles, J.D.L., Leeds, J.A., Chopra, I. and Fishwick, C.W.G. (2008) 2-aminotetralones: Novel inhibitors of MurA and MurZ. *Bioorg. Med. Chem. Lett.*, 18, 1730-1734.

Dupiereux, I., Falisse-Poirrier, N., Zorzi, W., Watt, N.T., Thellin, O., Zorzi, D., Pierard, O., Hooper, N.M., Heinen, E. and Elmoualij, B. (2008) Protective effect of prion protein via the N-terminal region in mediating a protective effect on paraquat-induced oxidative injury in neuronal cells. *J. Neurosci. Res.*, 86, 653-659.

Emmott, E., Dove, B.K., Howell, G., Chappell, L.A., Reed, M.L., Boyne, J.R., You, J.H., Brooks, G., Whitehouse, A. and Hiscox, J.A. (2008) Viral nucleolar localisation signals determine dynamic trafficking within the nucleolus. *Virology*, 380, 191-202.

Estrela, P., Paul, D., Li, P., Keighley, S.D., Migliorato, P., Laurenson, S. and Ferrigno, P.K. (2008) Label-free detection of protein interactions with peptide aptamers by open circuit potential measurement. *Electrochim. Acta*, 53, 6489-6496.

Feige, M.J., Groscurth, S., Marcinowski, M., Yew, Z.T., Truffault, V., Paci, E., Kessler, H. and Buchner, J. (2008) The structure of a folding intermediate provides insight into differences in immunoglobulin amyloidogenicity. *Proc. Natl. Acad. Sci. U. S. A.*, 105, 13373-13378.

Feige, M.J. and Paci, E. (2008) Rate of loop formation in peptides: A simulation study. *J. Mol. Biol.*, 382, 556-565.

Garner, A.E., Smith, D.A. and Hooper, N.M. (2008) Visualization of detergent solubilization of membranes: Implications for the isolation of rafts. *Biophys. J.*, 94, 1326-1340.

Garnett, J.A., Marincs, F., Baumberg, S., Stockley, P.G. and Phillips, S.E.V. (2008) Structure and function of the arginine repressor-operator complex from B*acillus subtilis*. *J. Mol. Biol.*, 379, 284-298.

Gell, C., Sabir, T., Westwood, J., Rashid, A., Smith, D.A.M., Harris, S.A. and Stockley, P.G. (2008) Single-molecule fluorescence resonance energy transfer assays reveal heterogeneous folding ensembles in a simple RNA stem-loop. *J. Mol. Biol.*, 384, 264-278.

Gorzny, M.L., Walton, A.S., Wnek, M., Stockley, P.G. and Evans, S.D. (2008) Four-probe electrical characterization of Pt-coated TMV-based nanostructures. *Nanotechnology*, 19.

Graham, R.S. and McLeish, T.C.B. (2008) Emerging applications for models of molecular rheology. *J. Non-Newtonian Fl. Mechan.*, 150, 11-18.

Grant, C.A., Brockwell, D.J., Radford, S.E. and Thomson, N.H. (2008) Effects of hydration on the mechanical response of individual collagen fibrils. *Appl. Phys. Lett.*, 92.

Griffin, S., StGelais, C., Owsianka, A.M., Patel, A.H., Rowlands, D. and Harris, M. (2008) Genotype-dependent sensitivity of hepatitis C virus to inhibitors of the p7 ion channel. *Hepatology*, 48, 1779-1790.

Griffin, S., Trowbridge, R., Thommes, P., Parry, N., Rowlands, D.J., Harris, M. and Bright, H. (2008) Chimeric GB virus BRNAas containing hepatitis c virus p7 are infectious *in vivo*. *J. Hepatol.*, 49, 908-915.

Griffiths, H.H., Morten, I.J. and Hooper, N.M. (2008) Emerging and potential therapies for Alzheimer's disease. *Expert Opin. Therapeutic Targets*, 12, 693-704.

Griffiths, R., Harrison, S.M., Macnab, S. and Whitehouse, A. (2008) Mapping the minimal regions within the ORF73 protein required for herpesvirus saimiri episomal persistence. *J. Gen. Virol.*, 89, 2843-2850.

Harris, S.A., Laughton, C.A. and Liverpool, T.B. (2008) Mapping the phase diagram of the writhe of DNA nanocircles using atomistic molecular dynamics simulations. *Nucleic Acids Res.*, 36, 21-29.

Harrison, S.M. and Whitehouse, A. (2008) Kaposi's sarcoma-associated herpesvirus (KSHV) RTa and cellular HMGB1 proteins synergistically transactivate the KSHVORF50 promoter. *FEBS Lett.*, 582, 3080-3084.

Hassell, D.G., Auhl, D., McLeish, T.C.B. and Mackley, M.R. (2008) The effect of viscoelasticity on stress fields within polyethylene melt flow for a cross-slot and contraction-expansion slit geometry. *Rheologica Acta*, 47, 821-834.

Hassell, D.G., Mackley, M.R., Sahin, M., Wilson, H.J., Harlen, O.G. and McLeish, T.C.B. (2008) Molecular physics of a polymer engineering instability: Experiments and computation. *Physical Review E*, 77.

Hooper, N.M. and Turner, A.J. (2008) A new take on prions: Preventing Alzheimer's disease. *Trends Biochem. Sci.*, 33, 151-155.

Horn, J., Marsden, S.P., Nelson, A., House, D. and Weingarten, G.G. (2008) Convergent, regiospecific synthesis of quinolines from o-aminophenylboronates. *Org. Lett.*, 10, 4117-4120.

Houmeida, A., Baron, A., Keen, J., Khan, G.N., Knight, P.J., Stafford, W.F., Thirumurugan, K., Thompson, B., Tskhovrebova, L. and Trinick, J. (2008) Evidence for the oligomeric state of 'elastic' titin in muscle sarcomeres. *J. Mol. Biol.*, 384, 299-312.

Jahn, T.R. and Radford, S.E. (2008) Folding versus aggregation: Polypeptide conformations on competing pathways. *Arch. Biochem. Biophys.*, 469, 100-117.

Jahn, T.R., Tennent, G.A. and Radford, S.E. (2008) A common beta-sheet architecture underlies *in vitro* and *in vivo* beta(2)-microglobulin amyloid fibrils. *J. Biol. Chem.*, 283, 17279-17286.

Jarowicki, K., Kilner, C., Kocienski, P.J., Komsta, Z., Milne, J.E., Wojtasiewicz, A. and Coombs, V. (2008) A synthesis of 1-lithiated glycals and 1-tributylstannyl glycals from 1-phenylsulfinyl glycals via sulfoxide-lithium ligand exchange. *Synthesis-Stuttgart*, 2747-2763.

Jeuken, L.J.C. (2008) AFM study on the electric-field effects on supported bilayer lipid membranes. *Biophys. J.*, 94, 4711-4717.

Jeuken, L.J.C., Weiss, S.A., Henderson, P.J.F., Evans, S.D. and Bushby, R.J. (2008) Impedance spectroscopy of bacterial membranes: Coenzyme-Q diffusion in a finite diffusion layer. *Anal. Chem.*, 80, 9084-9090.

Jeuken, L.J.C., Weiss, S.A., Henderson, P.J.F., Evans, S.D. and Bushby, R.J. (2008) Impendance spectroscopy of bacterial membranes: Coenzyme q diffusion in a finite diffusion layer. *Anal. Chem.*, 80, 9084-9090.

Johnson, S., Evans, D., Laurenson, S., Paul, D., Davies, A.G., Ferrigno, P.K. and Walti, C. (2008) Surface-immobilized peptide aptamers as probe molecules for protein detection. *Anal. Chem.*, 80, 978-983.

Jourdan, S.S. and McDowall, K.J. (2008) Sensing of 5 ' monophosphate by *Escherichia coli* RNAse G can significantly enhance association with RNA and stimulate the decay of functional mRNA transcripts *in vivo*. *Mol. Microbiol.*, 67, 102-115.

Jung, H.S., Burgess, S.A., Billington, N., Colegrave, M., Patel, H., Chalovich, J.M., Chantler, P.D. and Knight, P.J. (2008) Conservation of the regulated structure of folded myosin 2 in species separated by at least 600 million years of independent evolution. *Proc. Natl. Acad. Sci. U. S. A.*, 105, 6022-6026.

Kainov, D.E., Mancini, E.J., Telenius, J., Lisai, J., Grimes, J.M., Bamford, D.H., Stuart, D.I. and Tuma, R. (2008) Structural basis of mechanochemical coupling in a hexameric molecular motor. *J. Biol. Chem.*, 283, 3607-3617.

Khatri, B.S., Byrne, K., Kawakami, M., Brockwell, D.J., Smith, D.A., Radford, S.E. and McLeish, T.C.B. (2008) Internal friction of single polypeptide chains at high stretch. *Faraday Discuss.*, 139, 35-51.

Kime, L., Jourdan, S.S. and McDowall, K.J. (2008) Identifying and characterising substrates of the rnase e/g family of enzymes. *Methods Enzymol.*, 447, 215-241.

Knapman, T.W., Aggeli, A. and Ashcroft, A.E. (2008) Critical concentrations of beta-sheet peptide self-assembly quantified directly by nanoelectrospray ionization mass spectrometry. *Rapid Commun. Mass Spectrom.*, 22, 1611-1614.

Kocabas, D.S., Bakir, U., Phillips, S.E.V., McPherson, M.J. and Ogel, Z.B. (2008) Purification, characterization, and identification of a novel bifunctional catalase-phenol oxidase from *Scytalidium thermophilum*. *Appl. Microbiol. Biotechnol.*, 79, 407-415.

Kota, Z., Pali, T., Dixon, N., Kee, T.P., Harrison, M.A., Findlay, J.B.C., Finbow, M.E. and Marsh, D. (2008) Incorporation of transmembrane peptides from the vacuolar H^+-ATPase in phospholipid membranes: Spin-label electron paramagnetic resonance and polarized infrared spectroscopy. *Biochemistry*, 47, 3937-3949.

Kulharia, M., Goody, R.S. and Jackson, R.M. (2008) Information theory-based scoring function for the structure-based prediction of protein-ligand binding affinity. *J. Chem. Inf. Model.*, 48, 1990-1998.

Kyle, S., Riley, J.M., Aggeli, A., Ingham, E. and McPherson, M.J. (2008) Self-assembling peptides for scaffolds in regenerative medicine: Production using recombinant DNA technology. *Tissue Engineering Part A*, 14, OP247.

Lambert, D.W., Clarke, N.E., Hooper, N.M. and Turner, A.J. (2008) Calmodulin interacts with angiotensin-converting enzyme-2 (ACE2) and inhibits shedding of its ectodomain. *FEBS Lett.*, 582, 385-390.

Lambert, D.W., Hooper, N.M. and Turner, A.J. (2008) Angiotensin-converting enzyme 2 and new insights into the renin-angiotensin system. *Biochem. Pharmacol.*, 75, 781-786.

Leach, S.G., Cordier, C.J., Morton, D., McKiernan, G.J., Warriner, S. and Nelson, A. (2008) A fluorous-tagged linker from which small molecules are released by ring-closing metathesis. *J. Org. Chem.*, 73, 2753-2759.

Liverpool, T.B., Harris, S.A. and Laughton, C.A. (2008) Supercoiling and denaturation of DNA loops. *Phys. Rev. Lett.*, 100.

Lukoyanova, N., Baldwin, S.A. and Trinick, J. (2008) 3D reconstruction of mammalian septin filaments. *J. Mol. Biol.*, 376, 1-7.

Ma, P.K., Yuille, H.M., Blessie, V., Gohring, N., Igloi, Z., Nishiguchi, K., Nakayama, J., Henderson, P.J.F. and Phillips-Jones, M.K. (2008) Expression, purification and activities of the entire family of intact membrane sensor kinases from E*nterococcus faecalis*. *Mol. Membr. Biol.*, 25, 449-473.

Macnab, S., White, R., Hiscox, J. and Whitehouse, A. (2008) Production of an infectious herpesvirus saimiri-based episomally maintained amplicon system. *J. Biotechnol.*, 134, 287-296.

Madine, J., Jack, E., Stockley, P.G., Radford, S.E., Serpell, L.C. and Middleton, D.A. (2008) Structural insights into the polymorphism of amyloid-like fibrils formed by region 20-29 of amylin revealed by solid-state NMR and X-ray fiber diffraction. *J. Am. Chem. Soc.*, 130, 14990-15001.

Mankouri, J., Griffin, S. and Harris, M. (2008) The hepatitis C virus non-structural protein NS5A alters the trafficking profile of the epidermal growth factor receptor. *Traffic*, 9, 1497-1509.

Mankouri, J., Milward, A., Pryde, K.R., Warter, L., Martin, A. and Harris, M. (2008) A comparative cell biological analysis reveals only limited functional homology between the NS5A proteins of hepatitis C virus and GB virus b. *J. Gen. Virol.*, 89, 1911-1920.

McDowall, K.J., *The chemistry, measurement and modulation of RNA stability*, in *Wiley enclyclopedia of chemical biology*, T.P. Begley, Editor. 2008.

McGhee, A.M., Kilner, C. and Wilson, A.J. (2008) Conformer independent heterodimerisation of linear arrays using three hydrogen bonds. *Chem. Commun.*, 344-346.

Middleton, D.A., Baldwin, S.A., Herbert, R.B., Henderson, P.J.F. and Patching, S.G. (2008) Exploiting isotope labelling for solid-state NMR studies of drugs and their targets. *J. Labelled Compd. Radiopharm.*, 51, 249-249.

Morton, V.L., Stockley, P.G., Stonehouse, N.J. and Ashcroft, A.E. (2008) Insights into virus capsid assembly from non-covalent mass spectrometry. *Mass Spectrom. Rev.*, 27, 575-595.

Murphy, J.E., Vohra, R.S., Dunn, S., Holloway, Z.G., Monaco, A.P., Homer-Vanniasinkam, S., Walker, J.H. and Ponnambalam, S. (2008) Oxidised LDL internalisation by the LOX-1 scavenger receptor is dependent on a novel cytoplasmic motif and is regulated by dynamin-2. *J. Cell Sci.*, 121, 2136-2147.

Ndieyira, J.W., Watari, M., Barrera, A.D., Zhou, D., Vogtli, M., Batchelor, M., Cooper, M.A., Strunz, T., Horton, M.A., Abell, C., Rayment, T., Aeppli, G. and McKendry, R.A. (2008) Nanomechanical detection of antibiotic mucopeptide binding in a model for superbug drug resistance. *Nature Nanotechnology*, 3, 691-696.

Norcross, N.R., Melbardis, J.P., Solera, M.F., Sephton, M.A., Kilner, C., Zakharov, L.N., Astles, P.C., Warriner, S.L. and Blakemore, P.R. (2008) Total synthesis of (+/-)-alpha-isosparteine, (+/-)-beta-isosparteine, and (+/-)-sparteine from a common tetraoxobispidine intermediate. *J. Org. Chem.*, 73, 7939-7951.

Nyola, A. and Hunte, C. (2008) A structural analysis of the transient interaction between cytochrome bc_1 complex and its substrate cytochrome *c*. *Biochem. Soc. Trans.*, 36, 981-985.

Paproski, R.J., Visser, F., Zhang, J., Tackaberry, T., Damaraju, V., Baldwin, S.A., Young, J.D. and Cass, C.E. (2008) Mutation of Trp(29) of human equilibrative nucleoside transporter 1 alters affinity for coronary vasodilator drugs and nucleoside selectivity. *Biochem. J.*, 414, 291-300.

Parat, S., Pelotier, B., Fournier, L., Rajzmann, M., Kocienski, P.J. and Pons, J.M. (2008) Aldolisation and carboxylation reactions from alpha-silyl-beta-lactams: A combined theoretical and experimental study. *Heterocycles*, 75, 2429-2441.

Patching, S.G., Henderson, P.J.F., Herbert, R.B. and Middleton, D.A. (2008) Solid-state NMR spectroscopy detects interactions between tryptophan residues of the *E.coli* sugar transporter GaiP and the alpha-anomer of the D-glucose substrate. *J. Am. Chem. Soc.*, 130, 1236-1244.

Patching, S.G., Psakis, G., Baldwin, S.A., Baldwin, J., Henderson, P.J.F. and Middleton, D.A. (2008) Relative substrate affinities of wild-type and mutant forms of the *Escherichia coli* sugar transporter GalP determined by solid-state NMR. *Mol. Membr. Biol.*, 25, 474-484.

Pellecchia, M., Bertini, I., Cowburn, D., Dalvit, C., Giralt, E., Jahnke, W., James, T.L., Homans, S.W., Kessler, H., Luchinat, C., Meyer, B., Oschkinat, H., Peng, J., Schwalbe, H. and Siegal, G. (2008) Perspectives on NMR in drug discovery: A technique comes of age. *Nature Reviews Drug Discovery*, 7, 738-745.

Pirrat, P., Smith, M.A., Pearson, A.R., McPherson, M.J. and Phillips, S.E.V. (2008) Structure of a xenon derivative of *Escherichia coli* copper amine oxidase: Confirmation of the proposed oxygen-entry pathway. *Acta Cryst F*, 64, 1105-1109.

Plante, J., Campbell, F., Malkova, B., Kilner, C., Warriner, S.L. and Wilson, A.J. (2008) Synthesis of functionalised aromatic oligamide rods. *Organic & Biomolecular Chemistry*, 6, 138-146.

Platt, G.W., Routledge, K.E., Homans, S.W. and Radford, S.E. (2008) Fibril growth kinetics reveal a region of beta(2)-microglobulin important for nucleation and elongation of aggregation. *J. Mol. Biol.*, 378, 251-263.

Postis, V.L.G., Deacon, S.E., Roach, P.C.J., Wright, G.S.A., Xia, X., Ingram, J.C., Hadden, J.M., Henderson, P.J.F., Phillips, S.E.V., McPherson, M.J. and Baldwin, S.A. (2008) A high-throughput assay of membrane protein stability. *Mol. Membr. Biol.*, 25, 617-624.

Rahman, M., Patching, S.G., Ismat, F., Henderson, P.J.F., Herbert, R.B., Baldwin, S.A. and McPherson, M.J. (2008) Probing metal ion substrate-binding to the E. *coli Z*itB exporter in native membranes by solid state NMR. *Mol. Membr. Biol.*, 25, 683-690.

Redondo, C., Vouropoulou, M., Evans, J. and Findlay, J.B.C. (2008) Identification of the retinol-binding protein (RBP) interaction site and functional state of RBPs for the membrane receptor. *FASEB J.*, 22, 1043-1054.

Reha, D., Barford, W. and Harris, S. (2008) A multi-scale method for the calculation of charge transfer rates through the Pi-stack of DNA: Application to DNA dynamics. *Physical Chemistry Chemical Physics*, 10, 5436-5444.

Resch, A., Afonyushkin, T., Lombo, T.B., McDowall, K.J., Blasi, U. and Kaberdin, V.R. (2008) Translational activation by the noncoding RNA DsrA involves alternative RNase III processing in the rpoS 5 '-leader. *RNA*, 14, 454-459.

Roach, P.C.J., Postis, V.L.G., Deacon, S.E., Wright, G.S.A., Ingram, J.C., Xia, X.B., McPherson, M.J. and Baldwin, S.A. (2008) Large-scale preparation of bacterial cell membranes by tangential flow filtration. *Mol. Membr. Biol.*, 25, 609-616.

Roberts, A.J., Numata, N., Walker, M.L., Malkova, B., Kon, T., Ohkura, R., Arisaka, F., Knight, P.J., Sutoh, K. and Burgess, S.A. (2008) Aaa+ ring and linker swing mechanism in the dynein motor. *Cell*.

Rogers, M.S., Hurtado-Guerrero, R., Firbank, S.J., Halcrow, M.A., Dooley, D.M., Phillips, S.E.V., Knowles, P.F. and McPherson, M.J. (2008) Cross-link formation of the cysteine 228-tyrosine 272 catalytic cofactor of galactose oxidase does not require dioxygen. *Biochemistry*, 47, 10428-10439.

Rolfsson, O., Toropova, K., Morton, V., Francese, S., Basnak, G., Thompson, G.S., Homans, S.W., Ashcroft, A.E., Stonehouse, N.J., Ranson, N.A. and Stockley, P.G. (2008) RNA packing specificity and folding during assembly of the bacteriophage MS2.. *Comp. Math. Method. Medicine*, 9, 339-349.

Rose, R.J., Verger, D., Daviter, T., Remaut, H., Paci, E., Waksman, G., Ashcroft, A.E. and Radford, S.E. (2008) Unraveling the molecular basis of subunit specificity in P pilus assembly by mass spectrometry. *Proc. Natl. Acad. Sci. U. S. A.*, 105, 12873-12878.

Rose, R.J., Welsh, T.S., Waksman, G., Ashcroft, A.E., Radford, S.E. and Paci, E. (2008) Donor-strand exchange in chaperone-assisted pilus assembly revealed in atomic detail by molecular dynamics. *J. Mol. Biol.*, 375, 908-919.

Sellers, J.R., Thirumurugan, K., Sakamoto, T., Hammer, J.A. and Knight, P.J. (2008) Calcium and cargoes as regulators of myosin 5a activity. *Biochem. Biophys. Res. Commun.*, 369, 176-181.

Shelton, H. and Harris, M. (2008) Hepatitis C virus NS5A protein binds the SH3 domain of the Fyn tyrosine kinase with high affinity: Mutagenic analysis of residues within the SH3 domain that contribute to the interaction. *Virol. J.*, 5.

Shimamura, T., Yajima, S., Suzuki, S., Rutherford, N.G., O'Reilly, J., Henderson, P.J.F. and Iwata, S. (2008) Crystallization of the hydantoin transporter Mhp1 from *Microbacterium liquefaciens*. *Acta Cryst F*, 64, 1172-1174.

Slugoski, M.D., Ng, A.M.L., Yao, S.Y.M., Smith, K.M., Lin, C.C., Zhang, J., Karpinski, E., Cass, C.E., Baldwin, S.A. and Young, J.D. (2008) A proton-mediated conformational shift identifies a mobile pore-lining cysteine residue (Cys-561) in human concentrative nucleoside transporter 3. *J. Biol. Chem.*, 283, 8496-8507.

Slugoski, M.D., Smith, K.M., Mulinta, R., Ng, A.M.L., Yao, S.Y.M., Morrison, E.L., Lee, Q.O.T., Zhang, J., Karpinski, E., Cass, C.E., Baldwin, S.A. and Young, J.D. (2008) A conformationally mobile cysteine residue (Cys-561) modulates Na^+ and H^+ activation of human CNT3. *J. Biol. Chem.*, 283, 24922-24934.

Smith, D.P., Anderson, J., Plante, J., Ashcroft, A.E., Radford, S.E., Wilson, A.J. and Parker, M.J. (2008) Trifluoromethyldiazirine: An effective photo-induced cross-linking probe for exploring amyloid formation. *Chem. Commun.*, 5728-5730.

Solmaz, S.R. and Hunte, C. (2008) Structure of complex III with bound cytochrome *c* in reduced state and definition of a minimal core interface for electron transfer. *J. Biol. Chem.*, 283, 17542-17549.

Spencer, K.A., Dee, M., Britton, P. and Hiscox, J.A. (2008) Role of phosphorylation clusters in the biology of the coronavirus infectious bronchitis virus nucleocapsid protein. *Virology*, 370, 373-381.

Stockmann, H., Bronowska, A., Syme, N.R., Thompson, G.S., Kalverda, A.P., Warriner, S.L. and Homans, S.W. (2008) Residual ligand entropy in the binding of p-substituted benzenesulfonamide ligands to bovine carbonic anhydrase II. *J. Am. Chem. Soc.*, 130, 12420-12426.

Suchanova, B. and Tuma, R. (2008) Folding and assembly of large macromolecular complexes monitored by hydrogen-deuterium exchange and mass spectrometry. *Microbial Cell Factories*, 7.

Taniguchi, Y., Brockwell, D.J. and Kawakami, M. (2008) The effect of temperature on mechanical resistance of the native and intermediate states of I27. *Biophys. J.*, 95, 5296-5305.

Tarasov, A.I., Nicolson, T.J., Riveline, J.P., Taneja, T.K., Baldwin, S.A., Baldwin, J.M., Charpentier, G., Gautier, J.F., Froguel, P., Vaxillaire, M. and Rutter, G.A. (2008) A rare mutation in ABCC8/SUR1 leading to altered ATP-sensitive K^+ channel activity and beta-cell glucose sensing is associated with type 2 diabetes in adults. *Diabetes*, 57, 1595-1604.

Tassieri, M., Evans, R.M.L., Barbu-Tudoran, L., Khaname, G.N., Trinick, J. and Waigh, T.A. (2008) Dynamics of semiflexible polymer solutions in the highly entangled regime. *Phys. Rev. Lett.*, 101.

Tassieri, M., Evans, R.M.L., Barbu-Tudoran, L., Trinick, J. and Waigh, T.A. (2008) The self-assembly, elasticity, and dynamics of cardiac thin filaments. *Biophys. J.*, 94, 2170-2178.

Telenius, J., Wallin, A.E., Straka, M., Zhang, H.B., Mancini, E.J. and Tuma, R. (2008) RNA packaging motor: From structure to quantum mechanical modelling and sequential-stochastic mechanism. *Comput. Mathemat. Method Medicine*, 9, 351-369.

Tolley, A.C. and Stonehouse, N.J. (2008) Conformational changes in the connector protein complex of the bacteriophage phi 29 DNA packaging motor. *Comput. Mathemat. Method Medicine*, 9, 327-337.

Toropova, K., Basnak, G., Twarock, R., Stockley, P.G. and Ranson, N.A. (2008) The three-dimensional structure of genomic RNA in bacteriophage MS2: Implications for assembly. *J. Mol. Biol.*, 375, 824-836.

Trinh, C.H., Hunter, T., Stewart, E.E., Phillips, S.E.V. and Hunter, G.J. (2008) Purification, crystallization and X-ray structures of the two manganese superoxide dismutases from *Caenorhabditis elegans*. *Acta Cryst F*, 64, 1110-1114.

Tuma, R., Tsuruta, H., French, K.H. and Prevelige, P.E. (2008) Detection of intermediates and kinetic control during assembly of bacteriophage P22 procapsid. *J. Mol. Biol.*, 381, 1395-1406.

Uppal, S., Diggle, C.P., Carr, I.M., Fishwick, C.W.G., Ahmed, M., Ibrahim, G.H., Helliwell, P.S., Latos-Bielenska, A., Phillips, S.E.V., Markham, A.F., Bennett, C.P. and Bonthron, D.T. (2008) Mutations in 15-hydroxyprostaglandin dehydrogenase cause primary hypertrophic osteoarthropathy. *Nat. Genet.*, 40, 789-793.

Verger, D., Rose, R.J., Paci, E., Costakes, G., Daviter, T., Hultgren, S., Remaut, H., Ashcroft, A.E., Radford, S.E. and Waksman, G. (2008) Structural determinants of polymerization reactivity of the P pilus adaptor subunit PapF. *Structure*, 16, 1724-1731.

Vohra, R.S., Dunn, S., Howell, G.J., Walker, J.H., Ponnambalam, S. and Homer-Vanniasinkam, S. (2008) A novel mechanism for cellular recognition and endocytosis of pro-atherogenic oxidized low-density lipoproteins (oxLDL) by the lectin-like oxidized low-density lipoprotein scavenger receptor-1 (LOX-1). *Br. J. Surg.*, 95, 016.

Wallin, A.E., Ojala, H., Haeggstrom, E. and Tuma, R. (2008) Stiffer optical tweezers through real-time feedback control. *Appl. Phys. Lett.*, 92.

Weyand, S., Shimamura, T., Yajima, S., Suzuki, S., Mirza, O., Krusong, K., Carpenter, E.P., Rutherford, N.G., Hadden, J.M., O'Reilly, J., Ma, P., Saidijam, M., Patching, S.G., Hope, R.J., Norbertczak, H.T., Roach, P.C.J., Iwata, S., Henderson, P.J.F. and Cameron, A.D. (2008) Structure and molecular mechanism of a nucleobase-cation-symport-1 family transporter. *Science*, 322, 709-713.

Wilkinson, D.K., Turner, E.J., Parkin, E.T., Garner, A.E., Penny, J.H., Crawford, M., Stewart, G.W. and Hooper, N.M. (2008) Membrane raft actin deficiency and altered Ca^{2+}-induced vesiculation in stomatin-deficient overhydrated hereditary stomatocytosis. *Biochim. Biophys Acta-Biomembranes*, 1778, 125-132.

Xia, X.B., Postis, V.L.G., Rahman, M., Wright, G.S.A., Roach, P.C.J., Deacon, S.E., Ingram, J.C., Henderson, P.J.F., Findlay, J.B.C., Phillips, S.E.V., McPherson, M.J. and Baldwin, S.A. (2008) Investigation of the structure and function of a S*hewanella oneidensis* arsenical-resistance family transporter. *Mol. Membr. Biol.*, 25, 691-705.

Xu, Y., Ye, J., Liu, H., Cheng, E., Yang, Y., Wang, W.X., Zhao, M., Zhou, D., Liu, D.S. and Fang, R.X. (2008) DNA-templated CMV viral capsid proteins assemble into nanotubes. *Chem. Commun.*, 49-51.

Xue, W.F., Homans, S.W. and Radford, S.E. (2008) Systematic analysis of nucleation-dependent polymerization reveals new insights into the mechanism of amyloid self-assembly. *Proc. Natl. Acad. Sci. U. S. A.*, 105, 8926-8931.

Yew, Z.T., Krivov, S. and Paci, E. (2008) Free-energy lanscapes of proteins in the presence and absence of force. *J. Phys. Chem. B.*, 112, 16902-16907.

You, J.H., Howell, G., Pattnaik, A.K., Osorio, F.A. and Hiscox, J.A. (2008) A model for the dynamic nuclear/nucleolar/cytoplasmic trafficking of the porcine reproductive and respiratory syndrome virus (PRRSV) nucleocapsid protein based on live cell imaging. *Virology*, 378, 34-47.

Young, J.D., Yao, S.Y.M., Sun, L., Cass, C.E. and Baldwin, S.A. (2008) Human equilibrative nucleoside transporter (ENT) family of nucleoside and nucleobase transporter proteins. *Xenobiotica*, 38, 995-1021.

UNIVERSITY OF LEEDS

Leeds, United Kingdom
LS2 9JT
Tel. 0113 243 1751
www.leeds.ac.uk